



Figure 6.25. Individual Instrumented Dowel Bars Prior to being Welded to Dowel Bar Cage.

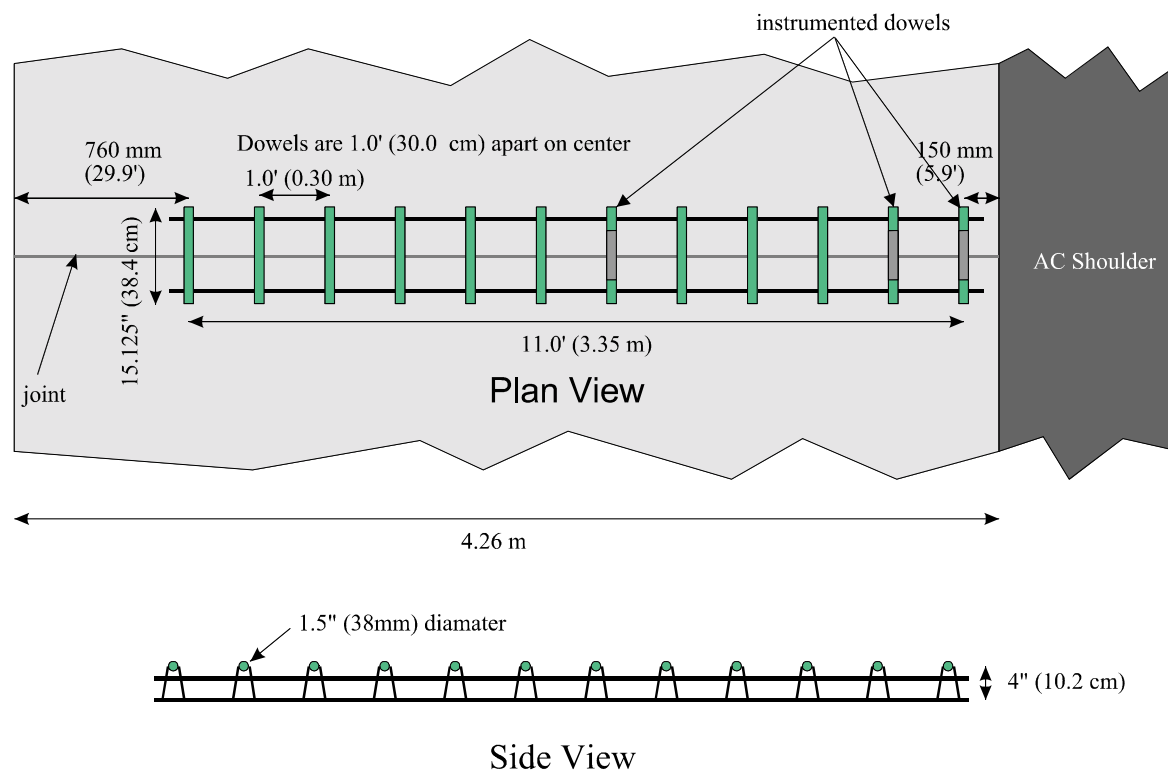


Figure 6.26. Instrumented Dowel Locations and Orientation at Joint 7, North Tangent.

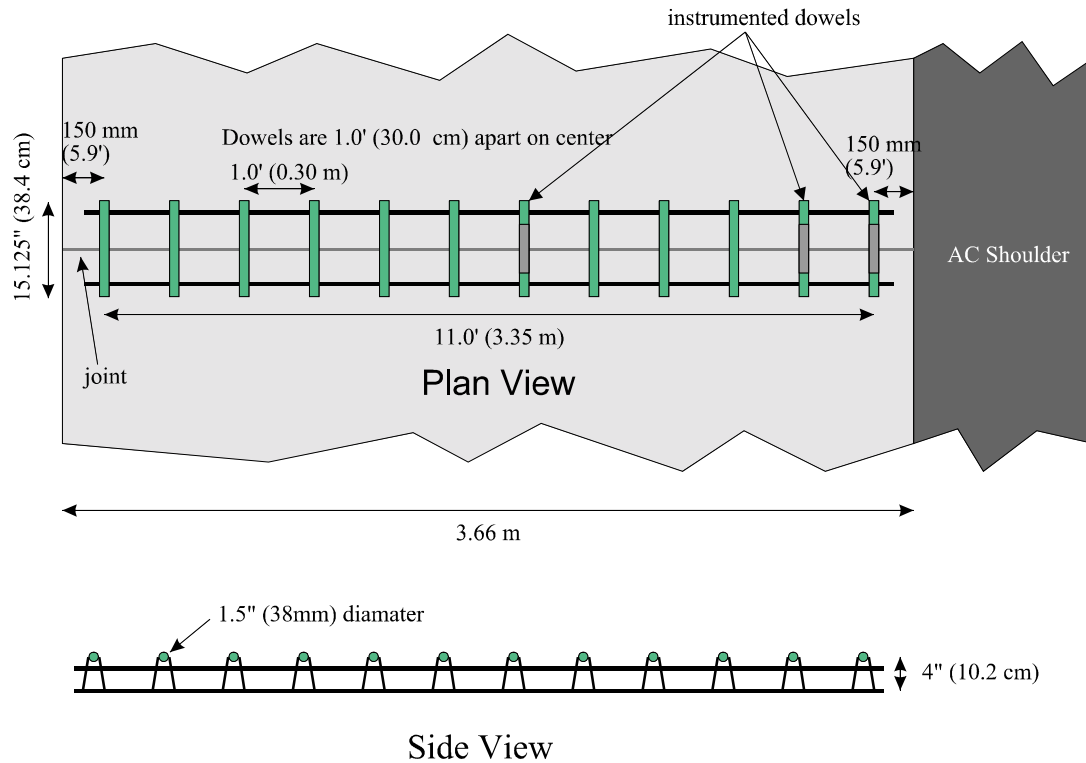


Figure 6.27. Instrumented Dowel Locations and Orientation at Joint 20, North Tangent.

attached to them and the dimensions of the dowels and pavement for the instrumented dowels at Joints 7 and 20 on the North Tangent, respectively. Appendix A shows additional details of the location of Joints 7 and 20 on the North Tangent.

6.12 Weather Station

Because environmental factors affect pavement performance, a weather station was installed above the HVS caravan to record weather data. The weather station was manufactured by Davis Instruments of Hayward, California. The biggest advantage of using a Davis weather station is it included the option of selecting only components that had relevance to the study of pavements. Several components were installed at the Palmdale test site to monitor and store the

following data: air temperature, solar radiation, rainfall, wind speed and direction, and humidity, as shown in Table 6.1.

All components are connected to a display and weather link/data logger. The weather link/data logger monitors and stores the data for download to a PC. Currently, weather data is being collected every two hours.

Table 6.1 Instrumentation Included in the Davis Weather Station in use at the Palmdale Test Site.

Component	Weather Data
External temperature sensor	Air temperature
Solar radiation sensor	Solar Radiation
Rain collector	Rainfall
Anemometer	Wind speed and direction
Humidity sensor	Humidity

7.0 CONCRETE PAVEMENT CONSTRUCTION

The principal contractor for the Palmdale pavement construction was Coffman Specialties, Inc. of San Diego, California. Caltrans personnel were in charge of the construction management and material sampling during construction of the Palmdale test site. The University of California, Berkeley Pavement Research Center, and its sub-contracted agencies Dynatest Consulting, Inc., of Ojai, California and the Council of Scientific and Industrial Research, of South Africa, (CSIR), were responsible for pavement instrumentation and independent material sampling.

7.1 Concrete Batch Plant

The fast-setting hydraulic cement concrete (FSHCC) was produced by Coffman Specialties using a portable 50 cu. yd./hr. dry-mix plant. The plant was located approximately 1 km from the construction site just south of the North Tangent.

The batch plant attempted to place the constituents in the ready mix truck as continuously as possible to avoid uneven distribution of material in the ready mix drum. The aggregate and cement were weighed in a hopper before placement into the ready mix trucks. The water and admixtures were added to the trucks in the right amount by flow meters. Typical load times for the batch plant were between 10 and 15 minutes.

7.2 Concrete Supply Trucks

Ready mix trucks were supplied by Western Rock Co. of Upland, California. The trucks carried approximately 7.5 cubic yard loads of FSHCC. The ready mix trucks were used to mix

the FSHCC and transport it from the batch plant to the construction site. The trucks mixed the concrete for approximately 80 revolutions in the drum prior to placing the concrete at the site. At times, the ready mix trucks were observed adding water to the mix at the site to increase the workability of the mix.

Transport of the concrete from the batch plant to the North Tangent took only about five minutes. However, the South Tangent required trucks to go past the construction site and turn around at the next freeway exit, thereby making the trip time from the batch plant to the South Tangent range from 10 to 25 minutes, depending on traffic.

The consistency of the FSHCC supplied by the trucks was typically good for the first few trucks of the day. After 4 to 5 trucks had offloaded, the consistency became more variable — one truck would be dry and the next truck would be too wet. Most trucks had several hardened clumps of cement exiting the drum along with the workable mix. These cement clumps ranged from 150 to 300 mm in diameter.

The rate of slump loss was also very high. It was frequently observed that a good consistency mix would be coming out of the chute and then within a couple of minutes it began to become difficult to offload from the truck. When this condition occurred, the contractor would add water to the drum to increase workability and help remove the FSHCC from the drum. This resulted in mixes with higher than targeted water-to-cement ratios, as seen in Tables 4.3 and 4.4 in Section 4.3.

It was also observed that almost every night after paving, the contractor crew spent time chipping hardened concrete out of the ready mix truck drums.

7.3 Concrete Paving Type

Initially, a slip-form paver was going to be used to pave the instrumented test sections. However, the contractor and Caltrans ultimately decided to hand pour and hand screed the test section to protect the instrumentation from potential damage.

The distribution of labor was as follows: One laborer directed the trucks, operated the concrete chute, and managed the initial placement of the concrete. Another laborer manually consolidated the concrete pavement with a hand vibrator. Two laborers operated the rotating screed while three laborers continuously shoveled concrete into areas requiring more concrete. Several laborers were behind the screed finishing the pavement, bull-floating, and finish-troweling the slab edges.

A tining rig followed the finishing crew. The tining rig first dragged burlap over the concrete. The concrete surface was then tined longitudinally and finally sprayed with a white polymer-based curing compound. The curing compound was used to seal the concrete surface to prevent evaporation of water from the hardening concrete.

7.4 Sampling of the FSHCC for Strength Testing

Test beams and cylinders were collected from the site by the UCB Pavement Research Center, Caltrans, and Coffman Specialties, Inc. UCB needed a sufficient quantity of specimens to test beams and cylinders at 8 hours, 7 days, and 90 days. Both the North and South Tangents were divided into three pavement sections, each with its own pavement structure, as described in Section 4. Each section required approximately 10 truckloads of concrete. For each section, two of these trucks were selected at random by the UCB personnel. From each of the selected

truckloads, six beams and six cylinders were cast, for a total of 72 beam and 72 cylinder specimens.

The concrete sampled for beam specimens was taken from the ready mix truck chute and transported a short distance (< 5 m) to the test specimen molds. The concrete was then placed in beam molds in a single lift and consolidated with an electric vibrator. The beam dimensions utilized for flexural strength testing were 152 × 152 × 533 mm per ASTM C 78. For each test section (six sections total), twelve beams were sampled for a total of 72 beams. The wheelbarrow was cleaned between samples. Table 7.1 shows the beam sampling plan.

Table 7.1 Beam Strength Testing Sampling Plan—Concrete Beams 152 mm × 152 mm × 533 mm.

Curing Time	Samples from First Truck	Samples from Second Truck	Number of Test Sections	Total Number of Samples
8 Hours	2	2	6	24
7 Days	2	2	6	24
90 Days	2	2	6	24
			Total Beams:	72

The concrete sampled for cylinder specimens was captured and transported using the same method as the beam specimens. The concrete for the specimens was placed in cylinder molds in two lifts and each lift was consolidated with an electric vibrator. The cylinder dimensions utilized for compressive strength testing were 152 mm diameter by 305 mm height. Table 7.2 shows the cylinder sampling plan for Palmdale construction.

Table 7.2 Cylinder Compressive Strength Testing Sampling Plan—Concrete Cylinders, 152 mm Diameter × 305 mm Height.

Curing Time	Samples from First Truck	Samples from Second Truck	Number of Sections	Total Number of Samples
8 Hours	2	2	6	24
7 Days	2	2	6	24
90 Days	2	2	6	24
			Total Cylinders:	72

8.0 FRESH CONCRETE PROPERTIES

The fast-setting hydraulic cement concrete (FSHCC) used for the Palmdale test site construction was an 80/20 blend of Ultimax® to PCC. The consistency of the concrete mix varied considerably from truck to truck. Some trucks arrived at the site with very wet mix and significant amounts of bleed water at the concrete surface, as shown in Figure 8.1. Other trucks arrived with mix that was close to setting inside the truck and required the addition of significant amounts of water to empty the FSHCC from the ready mix truck, as shown in Figure 8.2.

On at least one occasion, the concrete mix began to set inside the ready mix truck and the fins began to clog with concrete, as shown in Figure 8.3. On this same occasion, the contractor ordered the truck to roll off the site and dump its load away from the test sections because the mix had already set too much. A bag of citric acid retarder was then added to this truck to save it from having to be put out of service due to seizure of the mix inside.

When paving the North Tangent, the contractor was taking temperature readings of the mix as it was being placed and noted that the mix temperature was quite high, indicating that it was setting quickly. The contractor decided to pave the North Tangent sections early in the morning to avoid the hot temperatures of the late morning and early afternoon. This helped to eliminate some of the flash setting conditions experienced on the South Tangent.

Many of the mixes arriving at the site were fairly inconsistent and often required the addition of water. Twice during the three days of construction on the North Tangent and once during the construction of the South Tangent, the concrete set before an acceptable finish could be achieved and the paving had to cease. On one of these occasions, the unfinished concrete was removed with a jackhammer and a saw cut was made at the joint of the last acceptably finished



Figure 8.1. Wet Mix with Bleed Water on South Tangent.



Figure 8.2. Unworkable Mix on South Tangent.



Figure 8.3. Clogged Fins inside Ready Mix Truck, North Tangent.



Figure 8.4. Good Mix Quality and Finish, South Tangent.

slab. A cold joint was then constructed and paving continued the next day.

Many other trucks arrived with workable mix that was placed in time for a good finish, as shown in Figure 8.4.

Air entrainment tests were performed. The values ranged from 2 to 4 percent. Slump tests were also performed and the results range from 0 to greater than 6 inches, as presented in Table 8.1.

Table 8.1 Air Entrainment and Slump.

Tangent	Section	Slab	Date and Time Paved	Sampled Truck	Slump (in.)	Air Entrainment (Percent)
South	5C	41	6/10/1998, 1:50 PM	4	None	None
South	5B	31	6/11/1998, 8:00 AM	5	3.5	4
South	3D	20	6/11/1998, 9:20 AM	12	None	3.5
South	3A	17	6/11/1998, 9:35 AM	13	None	None
South	1D	13	6/11/1998, 10:00 AM	16	None	None
South	1A	5	6/11/1998, 10:45 AM	19	None	None
North	11A	3	6/16/1998, 6:30 AM	4	2.5	3
North	11C	10	6/16/1998, 7:10 AM	11	2	2.6
North	9B	18	6/17/1998, 6:40 AM	3	>6	2.6
North	9C	24	6/17/1998, 7:41 AM	7	4	3
North	7A	33	6/17/1998, 9:05 AM	13	>6	2
North	7C	41	6/18/1998, 7:20 AM	6	4	None

9.0 FAST-SETTING HYDRAULIC CEMENT CONCRETE STRENGTH TESTING

Strength testing was performed by Caltrans, the University of California, Berkeley Pavement Research Center (PRC), Kleinfelder of Pleasanton, CA, and Arrow Engineering of Lancaster, CA. Arrow Engineering performed all the 8-hour cylinder breaks while at the Palmdale construction project for UCB. Kleinfelder tested all the 7-day cylinders for UCB. The following sections are a summary of the strength test results.

9.1 Pavement Research Center Strength Tests

9.1.1 Pavement Research Center Flexural Strength Beam Testing

The UCB Pavement Research Center sampled, cured, and tested beams in accordance with ASTM C 78-94 with some minor alterations for curing in the field. ASTM C 78 is the standard test method for flexural strength of concrete using a third-point loading configuration. The test configuration had a loading span of 457 mm. Of the six beams sampled per truck, two beams were tested at 8 hours, two at 7 days, and two at 90 days. The beams tested at 8 hours were cured at the construction site prior to testing. The beams tested at 7 days and 90 days were de-molded after approximately 48 hours and were saturated with water and covered with wet burlap and plastic. All of the 8-hour, 90-day and most of the 7-day beams were tested with a Rainhardt manual hydraulic third-point beam tester. Tables 9.1 and 9.2 list the raw beam data for the 8-hour, 7-day, and 90-day tests for the South and North Tangents, respectively. The third-point loading configuration test from ASTM C 78 can be related to the Caltrans center point test CT 523 by multiplying the ASTM C 78 results by 1.05 (6).

Table 9.1 South Tangent Flexural Strengths—Beam Specimens.

Specimen Number	Section Location	Specimen Age	$M_R^{(1)}$ (psi)	Average $M_R^{(1)}$ (psi)	Average $M_R^{(1)}$ (MPa)
F1A1	1A	8 Hours	263	277	1.91
F1A2	1A	8 Hours	292		
F1A3	1A	7 Days	547	550	3.79
F1A4	1A	7 Days	554		
F1A5	1A	90 Days	700	673	4.64
F1A6	1A	90 Days	645		
F1D1	1D	8 Hours	281	264	1.82
F1D2	1D	8 Hours	247		
F1D3	1D	7 Days	450	460	3.17
F1D4	1D	7 Days	470		
F1D5	1D	90 Days	643	587	4.05
F1D6	1D	90 Days	530		
F3A1	3A	8 Hours	200	216	1.49
F3A2	3A	8 Hours	233		
F3A3	3A	7 Days	446	475	3.27
F3A4	3A	7 Days	503		
F3A5	3A	90 Days	577	577	3.98
<i>F3A6⁽²⁾</i>	<i>3A</i>	<i>90 Days</i>	<i>202</i>		
F3D1	3D	8 Hours	345	340	2.34
F3D2	3D	8 Hours	335		
F3D3	3D	7 Days	631	646	4.45
F3D4	3D	7 Days	662		
F3D5	3D	90 Days	818	849	5.85
F3D6	3D	90 Days	880		
F5B1	5B	8 Hours	366	372	2.56
F5B2	5B	8 Hours	377		
F5B3	5B	7 Days	725	711	4.90
F5B4	5B	7 Days	697		
F5B5	5B	90 Days	1078	965	6.65
F5B6	5B	90 Days	852		
F5C1	5C	8 Hours	327	339	2.34
F5C2	5C	8 Hours	351		
F5C3	5C	7 Days	595	590	4.07
F5C4	5C	7 Days	585		
F5C5	5C	90 Days	595	590	4.07
F5C6	5C	90 Days	585		

1) M_R is the concrete modulus of rupture for a third-point loading configuration

2) test result not included in average

Table 9.2 North Tangent Flexural Strengths—Beam Specimens.

Specimen Number	Section Location	Specimen Age	$M_R^{(1)}$ (psi)	Average $M_R^{(1)}$ (psi)	Average $M_R^{(1)}$ (MPa)
F7A1	7A	8 Hours	263	277	1.91
F7A2	7A	8 Hours	292		
F7A3	7A	7 Days	545	522	3.60
F7A4	7A	7 Days	500		
F7A5	7A	90 Days	813	713	4.92
F7A6	7A	90 Days	613		
F7C1	7C	8 Hours	271	276	1.90
F7C2	7C	8 Hours	282		
F7C3	7C	7 Days	538	540	3.72
F7C4	7C	7 Days	543		
F7C5	7C	90 Days	808	795	5.48
F7C6	7C	90 Days	782		
F9B1	9B	8 Hours	340	328	2.26
F9B2	9B	8 Hours	317		
F9B3	9B	7 Days	672	648	4.47
F9B4	9B	7 Days	623		
F9B5	9B	90 Days	980	881	6.07
F9B6	9B	90 Days	782		
F9C1	9C	8 Hours	261	265	1.83
F9C2	9C	8 Hours	270		
F9C3	9C	7 Days	590	641	4.42
F9C4	9C	7 Days	691		
F9C5	9C	90 Days	775	743	5.12
F9C6	9C	90 Days	711		
F11A1	11A	8 Hours	320	333	2.30
F11A2	11A	8 Hours	345		
F11A3	11A	7 Days	558	598	4.12
F11A4	11A	7 Days	637		
F11A5	11A	90 Days	833	821	5.66
F11A6	11A	90 Days	808		
F11C1	11C	8 Hours	345	345	2.38
F11C2	11C	8 Hours	346		
F11C3	11C	7 Days	620	627	4.32
F11C4	11C	7 Days	633		
F11C5	11C	90 Days	821	775	5.34
F11C6	11C	90 Days	729		

1) M_R is the concrete modulus of rupture for a third-point loading configuration

Tables 9.3, 9.4, and 9.5 list the average flexural strengths for 8 hours, 7 days, and 90 days for the South Tangent, North Tangent, and both tangents combined, respectively.

Table 9.3 South Tangent Average Flexural Strengths—Beam Specimens.

Section Number	Specimen Age	$M_R^{(1)}$ (psi)	$M_R^{(1)}$ (MPa)	Standard Deviation (psi)	Standard Deviation (MPa)	C.O.V. (Percent)
1,3,5	8 Hours	301	2.08	57	0.39	19
1,3,5	7 Days	572	3.94	94	0.65	17
1,3,5	90 Days	730	5.03	161	1.11	22

1) M_R is the concrete modulus of rupture for a third-point loading configuration
C.O.V. is the coefficient of variation.

Table 9.4 North Tangent Average Flexural Strengths—Beam Specimens.

Section Number	Specimen Age	$M_R^{(1)}$ (psi)	$M_R^{(1)}$ (MPa)	Standard Deviation (psi)	Standard Deviation (MPa)	C.O.V. (Percent)
7,9,11	8 Hours	304	2.1	35	0.24	11
7,9,11	7 Days	596	4.11	59	0.41	10
7,9,11	90 Days	788	5.43	86	0.59	11

M_R is the concrete modulus of rupture for a third-point loading configuration
C.O.V. is the coefficient of variation.

Table 9.5 Both Tangents Combined Average Flexural Strengths—Beam Specimens.

Section Number	Specimen Age	$M_R^{(1)}$ (psi)	$M_R^{(1)}$ (MPa)	Standard Deviation (psi)	Standard Deviation (MPa)	C.O.V. (Percent)
1,3,5,7,9,11	8 Hours	303	2.09	46	0.32	15
1,3,5,7,9,11	7 Days	584	4.03	78	0.54	13
1,3,5,7,9,11	90 Days	753	5.19	130	0.90	17

M_R is the concrete modulus of rupture for a third-point loading configuration
C.O.V. is the coefficient of variation.

The average flexural strength for the FSHCC increased over 90 percent from the 8 hour to 7-day test. The 7-day to 90-day average flexural strength gain was 30 percent. Table 9.6 presents the average flexural strength for each test section.

Table 9.6 Average Flexural Strengths by Section—Beam Specimens.

Section Number	Section Thickness (Inches)	8 Hours			7 Days			90 Days		
		$M_R^{(1)}$, psi (MPa)	Standard Deviation, psi (MPa)	C.O.V. (%)	$M_R^{(1)}$, psi (MPa)	Standard Deviation, psi (MPa)	C.O.V. (%)	$M_R^{(1)}$, psi (MPa)	Standard Deviation, psi (MPa)	C.O.V. (%)
1, South Tangent	4	271 (1.87)	20 (0.14)	7	505 (3.48)	53 (0.37)	10	630 (4.34)	72 (0.5)	11
3, South Tangent	6	278 (1.92)	73 (0.50)	26	560 (3.86)	103 (0.71)	18	758 (5.23)	160 (1.1)	21
5, South Tangent	8	355 (2.45)	22 (0.15)	6	650 (4.48)	71 (0.49)	11	770 (5.31)	141 (0.97)	18
7, North Tangent	8	277 (1.91)	13 (0.09)	5	531 (3.66)	21 (0.14)	4	754 (5.20)	95 (0.65)	13
9, North Tangent	8	297 (2.05)	38 (0.26)	13	644 (4.40)	46 (0.32)	7	812 (5.60)	117 (0.81)	14
11, North Tangent	8	339 (2.34)	9 (0.06)	3	612 (4.22)	37 (0.26)	6	798 (5.50)	47 (0.32)	6

1) M_R is the concrete modulus of rupture for a third-point loading configuration
C.O.V. is the coefficient of variation.

The overall variability in the flexural strength data was less than 15 percent except for Section 3, which had an average coefficient of variation of 22 percent. A closer look at the raw data presented in Tables 9.1 and 9.2 shows that much of the variation in test sections was due to the variation in strength between beams taken from two separate trucks. For example, Figure 9.1 shows a plot of strength gain for the South Tangent test sections. Two different ready mix trucks were sampled for each section. Figure 9.1 demonstrates that some of the variability in the data is a result of the variability in the supplied concrete, even for the same test section (i.e., Section 7A and Section 7C). A plot of the strength gain for the North Tangent sections, shown in Figure 9.2, reinforces the results shown in Figure 9.1.

Tables 9.6, 9.1, and 9.2 demonstrate that no section met the 8-hour specification of 400 psi (2.76 MPa) flexural strength and only half of the sections met the 7-day specification of 600 psi (4.14 MPa) flexural strength. This is assuming Caltrans center-point testing and ASTM third-

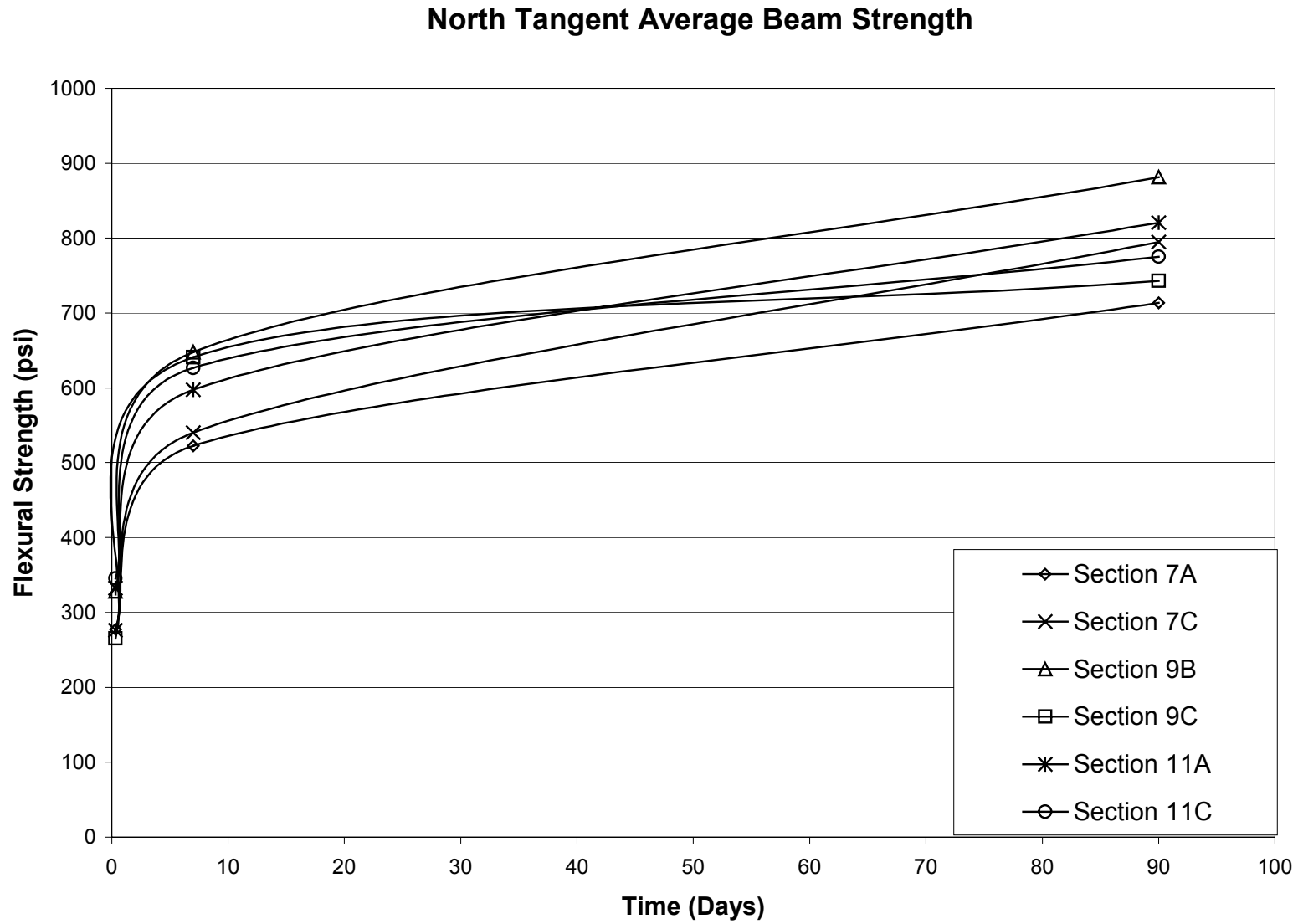


Figure 9.1. Average Beam Flexural Strength, North Tangent

South Tangent Average Beam Strength

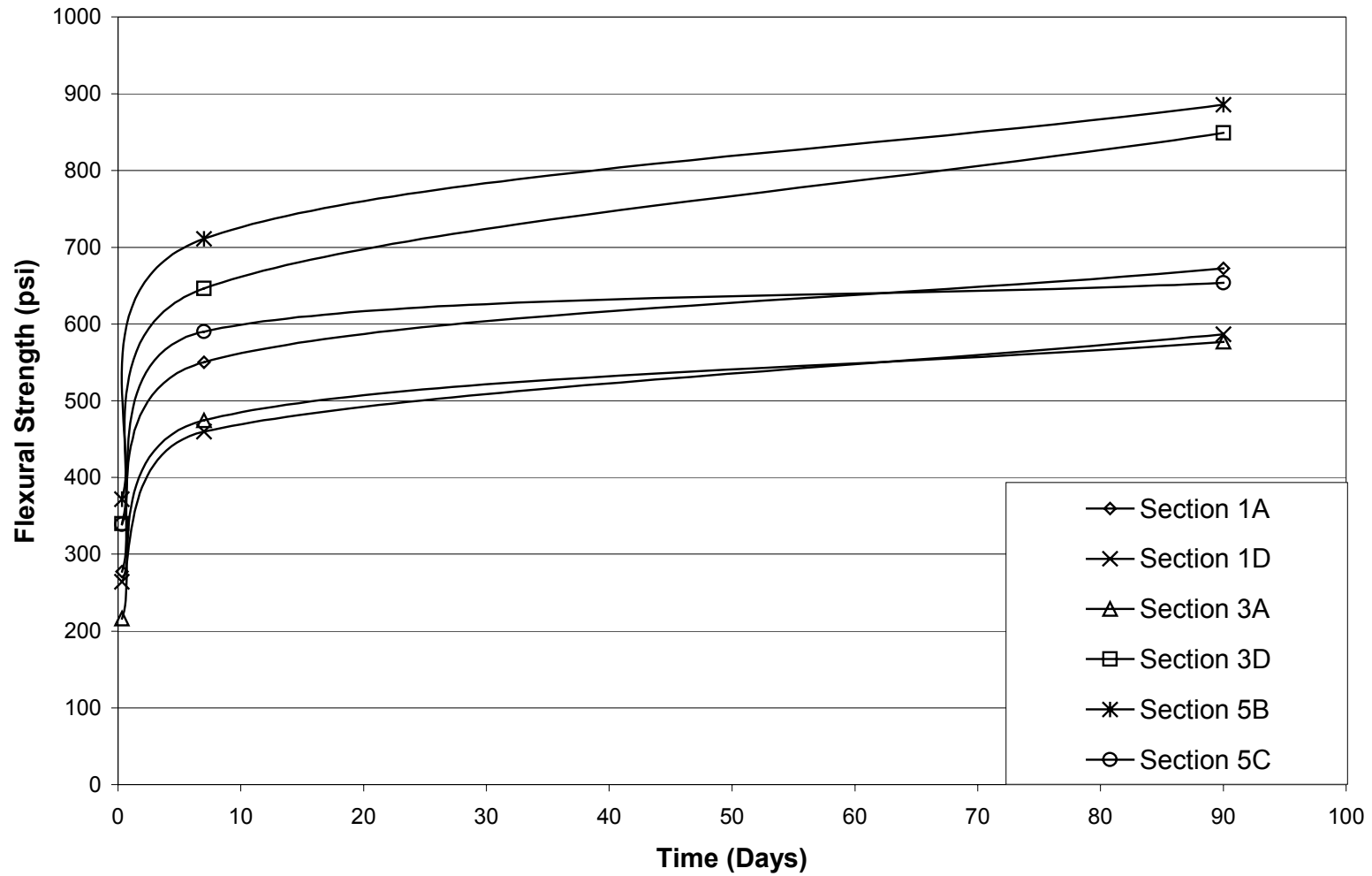


Figure 9.2. Average Beam Flexural Strength, South Tangent.

point testing would give similar results. The 90-day data show all sections had an average flexural strength greater than 600 psi (4.14 MPa) with five out of six sections having an average flexural strength greater than 700 psi (4.83 MPa). The main reason the 90-day flexural strength was so high was that 20 percent of the cement content was Portland cement. The Portland cement gave an added long-term strength gain to the concrete mix, while the Ultimax cement gave the concrete its high early strength characteristics.

Figure 9.3 shows the average beam strength gain for each Palmdale test section. This plot demonstrates again the variability in strength found between test sections. It also shows that the strength gain rate after 7 days is similar for all mixes.

9.1.2 Pavement Research Center Compressive Strength Cylinder Testing

The UCB Pavement Research Center sampled, cured, and tested cylinders in accordance with ASTM C 39 with some minor alterations for curing in the field. ASTM C 39 is the standard test method for compressive strength of concrete.

For each test section, twelve cylinders were sampled. Six cylinders were sampled from two random trucks per section. Of the six cylinders sampled per truck, two cylinders were tested at eight hours, two at seven days, and two were tested at 90 days. The 8-hour cylinders were cured at the construction site prior to testing. The 7-day cylinders were demolded after approximately 48 hours and were saturated with water and covered with wet burlap and plastic. All the 8-hour and 7-day beams were tested at a certified materials testing laboratory. Tables 9.7 and 9.8 below list the raw cylinder data for the 8-hour, 7-day, and 90-day tests for the South and North Tangents, respectively.

Average Beam Strength versus Time (North and South Tangents)

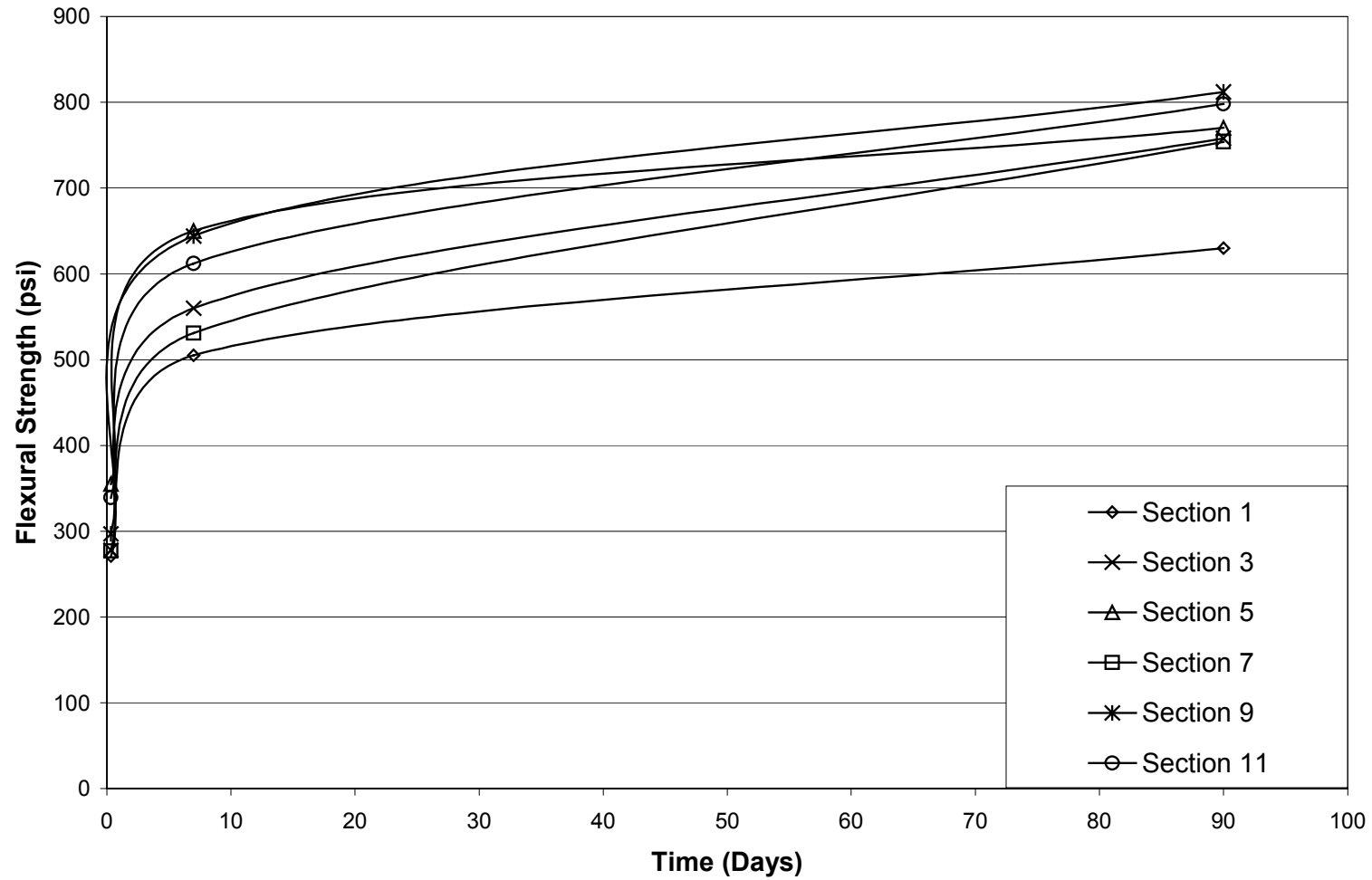


Figure 9.3. Average Beam Strength Gain for Palmdale Test Sections.

Table 9.7 South Tangent Compressive Strengths—Cylinder Specimens.

Specimen Number	Section Location	Specimen Age	F'_c⁽¹⁾ (psi)	Average F'_c⁽¹⁾ (psi)	Average F'_c⁽¹⁾ (MPa)
1A1	1A	8 Hours	1740	1725	11.89
1A2	1A	8 Hours	1710		
1A3	1A	7 Days	3860	3665	25.27
1A4	1A	7 Days	3470		
1A5	1A	90 Days	7040	6555	45.20
1A6	1A	90 Days	6070		
1D1	1D	8 Hours	1480	1470	10.14
1D2	1D	8 Hours	1460		
1D3	1D	7 Days	3260	3240	22.34
1D4	1D	7 Days	3220		
1D5	1D	90 Days	6760	5425	37.42
1D6	1D	90 Days	4090		
3A1	3A	8 Hours	1130	1145	7.89
3A2	3A	8 Hours	1160		
3A3	3A	7 Days	2490	2565	17.68
3A4	3A	7 Days	2640		
3A5	3A	90 Days	5800	5835	40.23
3A6	3A	90 Days	5880		
3D1	3D	8 Hours	2290	2240	15.44
3D2	3D	8 Hours	2190		
3D3	3D	7 Days	4430	4460	30.75
3D4	3D	7 Days	4490		
3D5	3D	90 Days	5640	6585	45.41
3D6	3D	90 Days	7530		
5B1	5B	8 Hours	2520	2520	17.37
5B2	5B	8 Hours	2520		
5B3	5B	7 Days	4750	4735	32.65
5B4	5B	7 Days	4720		
5B5	5B	90 Days	7570	7695	53.03
5B6	5B	90 Days	7820		
5C1	5C	8 Hours	2150	2170	14.96
5C2	5C	8 Hours	2190		
5C3	5C	7 Days	4110	4155	28.65
5C4	5C	7 Days	4200		
5C5	5C	90 Days	7710	7930	54.65
5C6	5C	90 Days	8150		

1) F'_c is the concrete compressive strength.

Table 9.8 North Tangent Compressive Strengths—Cylinder Specimens.

Specimen Number	Section Location	Specimen Age	F'_c⁽¹⁾ (psi)	Average F'_c⁽¹⁾ (psi)	Average F'_c⁽¹⁾ (MPa)
7A1	7A	8 Hours	1730	1710	11.79
7A2	7A	8 Hours	1690		
7A3	7A	7 Days	3450	3705	25.54
7A4	7A	7 Days	3960		
7A5	7A	90 Days	7240	6950	47.90
7A6	7A	90 Days	6660		
7C1	7C	8 Hours	1890	1890	13.03
7C2	7C	8 Hours	1890		
7C3	7C	7 Days	4480	4425	30.51
7C4	7C	7 Days	4370		
7C5	7C	90 Days	7290	7070	48.72
7C6	7C	90 Days	6850		
9B1	9B	8 Hours	2240	2215	15.27
9B2	9B	8 Hours	2190		
9B3	9B	7 Days	4770	4610	31.78
9B4	9B	7 Days	4450		
9B5	9B	90 Days	6530	6610	45.59
9B6	9B	90 Days	6690		
9C1	9C	8 Hours	2290	2240	15.44
9C2	9C	8 Hours	2190		
9C3	9C	7 Days	4250	4290	29.58
9C4	9C	7 Days	4330		
9C5	9C	90 Days	4950	4640	31.99
9C6	9C	90 Days	4330		
11A1	11A	8 Hours	2040	2035	14.03
11A2	11A	8 Hours	2030		
11A3	11A	7 Days	4680	4810	33.16
11A4	11A	7 Days	4940		
11A5	11A	90 Days	7620	7010	48.35
11A6	11A	90 Days	6400		
11C1	11C	8 Hours	2240	2255	15.55
11C2	11C	8 Hours	2270		
11C3	11C	7 Days	5500	5265	36.30
11C4	11C	7 Days	5030		
11C5	11C	90 Days	5640	6895	47.54
11C6	11C	90 Days	8150		

1) F'_c is the concrete compressive strength.

Tables 9.9, 9.10, and 9.11 list the average compressive strengths for 8-hour, 7-day, and 90-day tests on cylinder specimens for the South Tangent, North Tangent, and both tangents combined, respectively. The average compressive strengths on the North and South Tangent for 8-hour, 7-day, and 90-day tests were similar. The South Tangent average compressive strength data was more variable than the North Tangent strengths at 8 hours and 7 days.

Table 9.9 South Tangent Average Compressive Strengths—Cylinder Specimens.

Section Number	Specimen Age	F' _c ⁽¹⁾ (psi)	F' _c ⁽¹⁾ (MPa)	Standard Deviation (psi)	Standard Deviation (MPa)	C.O.V. (Percent)
1,3,5	8 Hours	1880	13.0	497	3.43	26
1,3,5	7 Days	3800	26.2	779	5.37	20
1,3,5	90 Days	6670	46.0	1195	8.24	15

1) F'_c is the concrete compressive strength.

Table 9.10 North Tangent Average Compressive Strengths—Cylinder Specimens.

Section Number	Specimen Age	F' _c ⁽¹⁾ (psi)	F' _c ⁽¹⁾ (MPa)	Standard Deviation (psi)	Standard Deviation (MPa)	C.O.V. (Percent)
7,9,11	8 Hours	2060	14.2	213	1.47	10
7,9,11	7 Days	4520	31.2	529	3.65	12
7,9,11	90 Days	6530	45.0	1094	7.54	17

1) F'_c is the concrete compressive strength

Table 9.11 Both Tangents Combined Average Compressive Strengths—Cylinder Specimens.

Section Number	Specimen Age	F' _c ⁽¹⁾ (psi)	F' _c ⁽¹⁾ (MPa)	Standard Deviation (psi)	Standard Deviation (MPa)	C.O.V. (Percent)
1,3,5,7,9,11	8 Hours	1970	13.6	385	2.65	20
1,3,5,7,9,11	7 Days	4160	28.7	747	5.15	18
1,3,5,7,9,11	90 Days	6600	45.5	1123	7.74	17

1) F'_c is the concrete compressive strength.

Table 9.12 presents the average compressive strength for each test section.

Table 9.12 Average Compressive Strengths by Section—Cylinder Specimens.

Section	Section Thickness (in. [mm])	8 Hours			7 Days			90 Days		
		F' _C ⁽¹⁾ (psi [MPa])	Standard Deviation (psi [MPa])	C.O.V. (%)	F' _C ⁽¹⁾ (psi [MPa])	Standard Deviation (psi [MPa])	C.O.V. (%)	F' _C ⁽¹⁾ (psi [MPa])	Standard Deviation (psi [MPa])	C.O.V. (%)
1, South Tangent	4 (101.6)	1598 (11.02)	148 (1.02)	9	3453 (23.81)	293 (2.02)	8	5992 (41.31)	1330 (9.17)	22
3, South Tangent	6 (152.4)	1693 (11.67)	634 (4.37)	37	3513 (24.22)	1096 (7.56)	31	6211 (42.82)	887 (6.12)	14
5, South Tangent	8 (203.2)	2345 (16.17)	203 (1.4)	9	4445 (30.65)	337 (2.32)	8	7808 (53.83)	247 (1.7)	3
7, North Tangent	8 (203.2)	1800 (12.41)	105 (0.72)	6	4065 (28.03)	467 (3.22)	11	7007 (48.31)	304 (2.1)	4
9, North Tangent	8 (203.2)	2228 (15.36)	48 (0.33)	2	4450 (30.68)	229 (1.58)	5	5627 (38.8)	1169 (8.06)	21
11, North Tangent	8 (203.2)	2145 (14.79)	128 (0.88)	6	5038 (34.74)	342 (2.36)	7	6954 (47.95)	1139 (7.85)	16

1) F'_C is the concrete compressive strength.

The average variability in the compressive strength data was less than 15 percent for each test section except for Section 3. This demonstrates that the material sampled from each section was representative of the concrete placed in the section as determined by the compressive strength test procedure. The variability in the compressive strength was similar to the variability in the flexural strength testing. Figures 9.4 and 9.5 show the average compressive strength gain for each set of specimens (sampled from a single truck) for the South and North Tangent, respectively. The variability between samples demonstrates that the variability was a result of the concrete mix rather than test procedure.

The average compressive strength of the FSHCC shows a 100 percent increase from its 8-hour to 7-day strength. The concrete's 7-day to 90-day average compressive strength gain was almost 60 percent. This large increase in strength from 7 days to 90 days was probably due to the Portland cement in the mix. Figure 9.6 shows the average compressive strength gain for each test

Average Cylinder Strength versus Time (South Tangent)

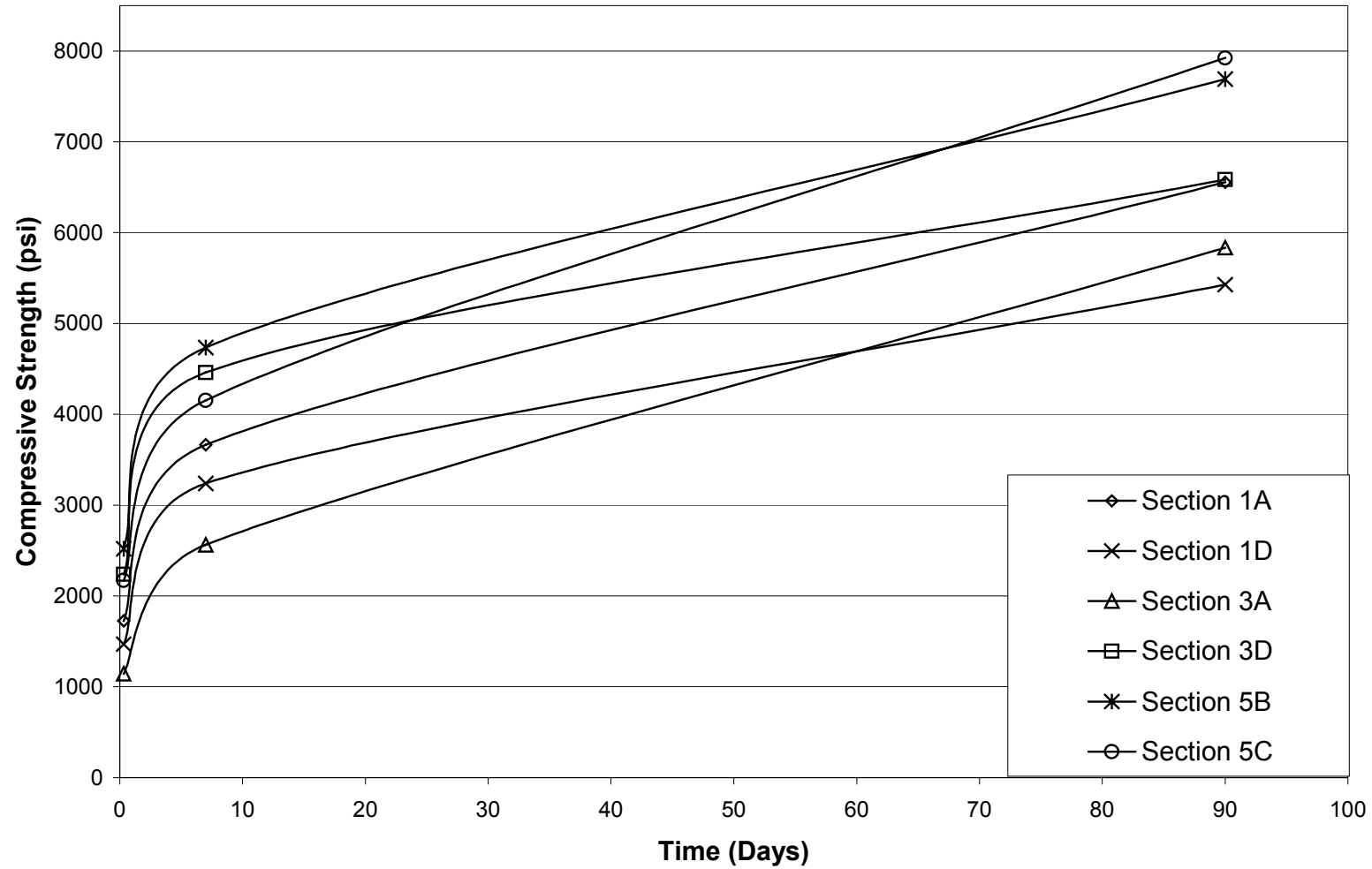


Figure 9.4. Average Cylinder Compressive Strength versus Time (South Tangent).

Average Cylinder Strength versus Time (North Tangent)

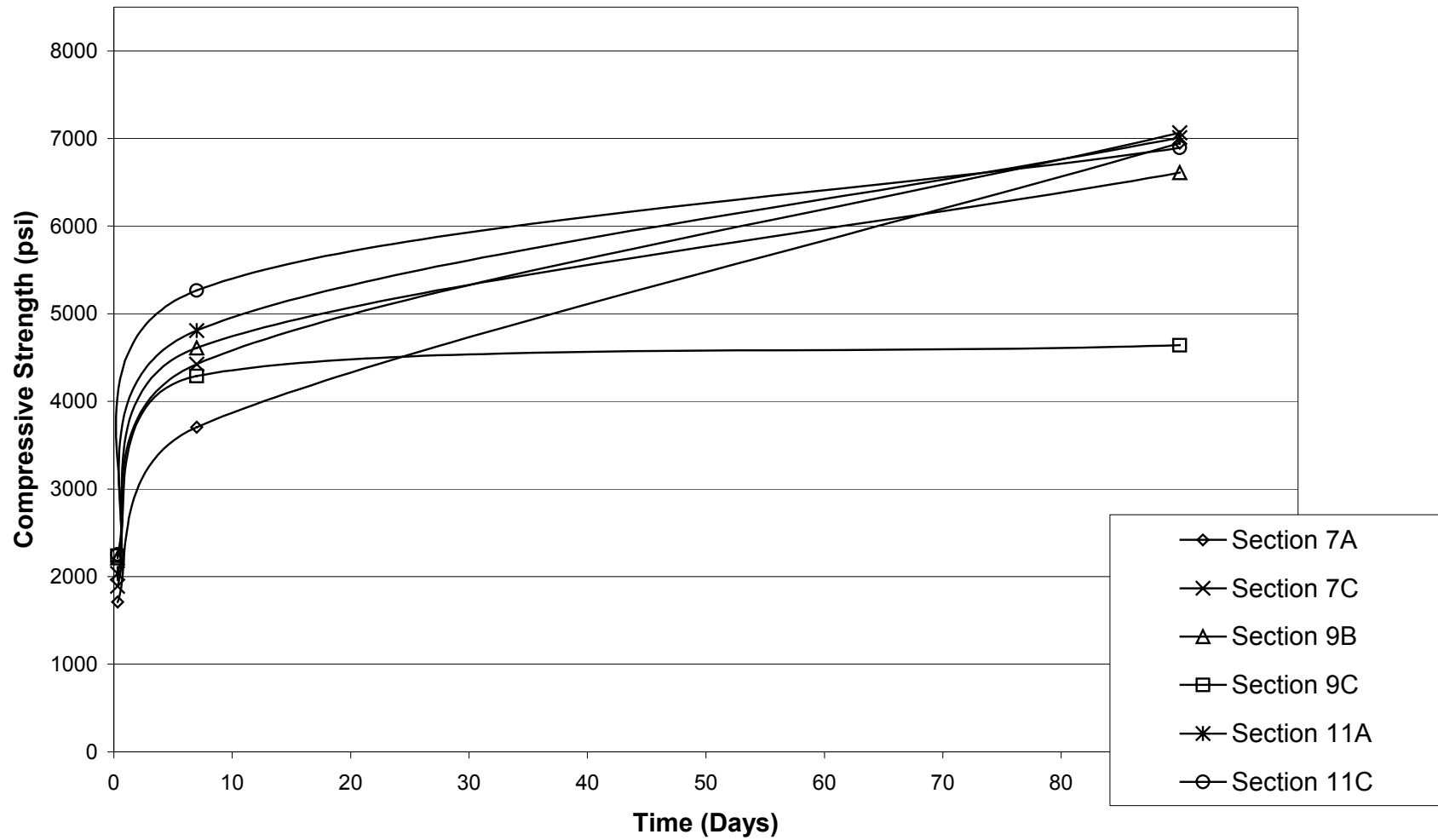


Figure 9.5. Average Cylinder Compressive Strength versus Time (North Tangent).

Average Cylinder Strength versus Time (North and South Tangents)

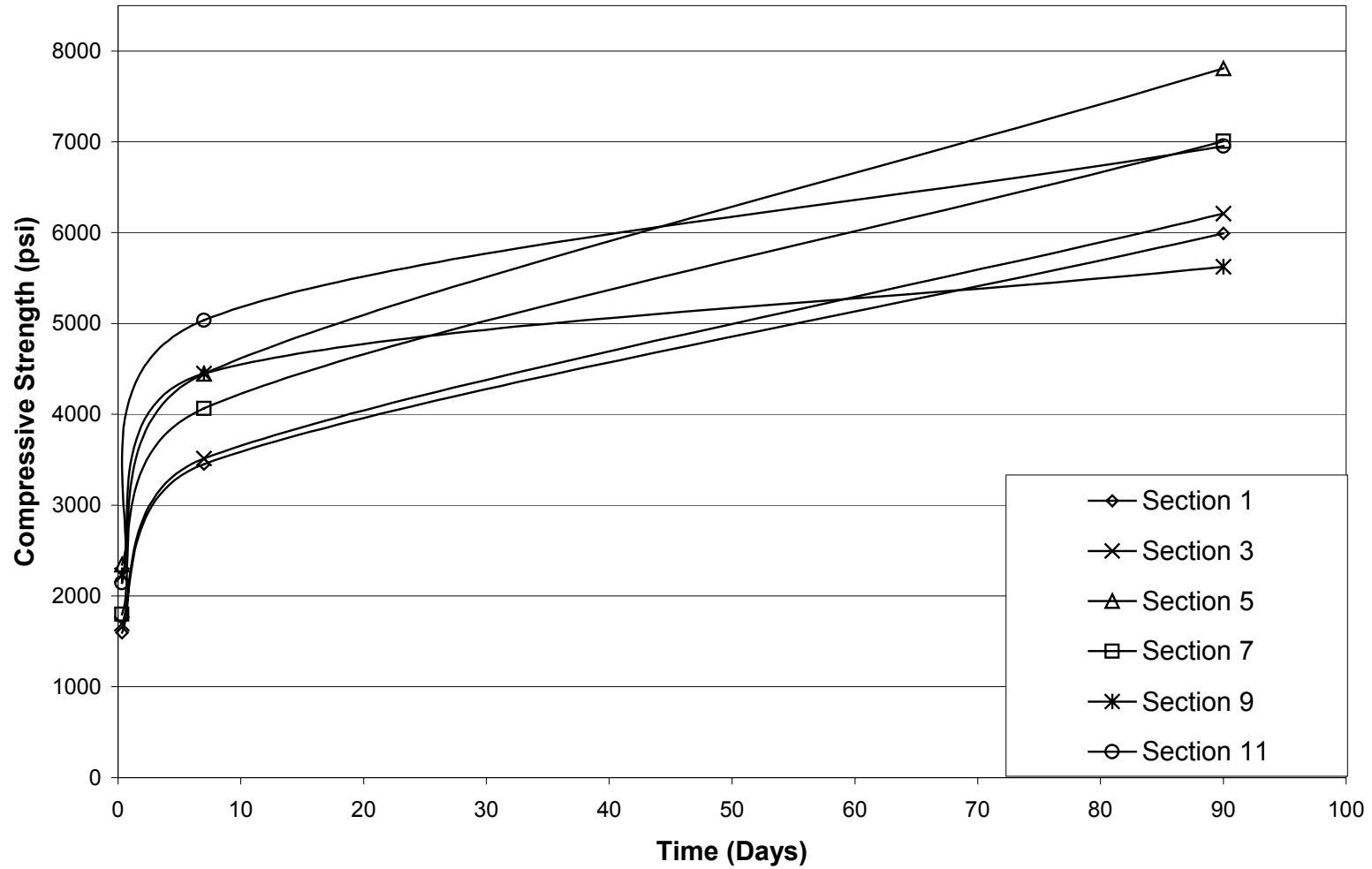


Figure 9.6. Average Cylinder Compressive Strength versus Time (North and South Tangents).

section at Palmdale. As with the beam strength results, the cylinder strength results varied from section to section. The cylinder results did not have the same strength gain rate after 7 days as seen with the beam results.

9.1.3 Cylinder versus Beam Strength Relationship for Palmdale FSHCC

To determine if a correlation exists between beam (flexural) and cylinder (compressive) strength data taken from the Palmdale site, a plot with the raw cylinder and beam data is shown in Figure 9.7. Figure 9.7 shows that a reasonable correlation exists between beam (flexural) and cylinder (compressive) strength for the UCB samples taken at Palmdale. The correlation appears to be stronger at lower strengths (less than 600 psi [4.14 MPa]).

In order to identify where the most scatter exists in the data, a plot of beam (flexural) and cylinder (compressive) strength at each specimen age was made. Figure 9.8 shows that the scatter for the tests at 8 hours and 7 days is much less than for the tests at 90 days. At 90 days, there appears to be little correlation between flexural and compressive strength. Further laboratory testing needs to be completed to verify or dismiss the trend observed for the tests at 90 days.

The relationship shown in Figure 9.7 can be used to relate beam (flexural) and cylinder (compressive) strength data as long as the data is not extrapolated beyond the original data points. Furthermore, the curve shown in Figure 9.7 is only valid for the exact mix used at Palmdale, including the aggregate and cement type.

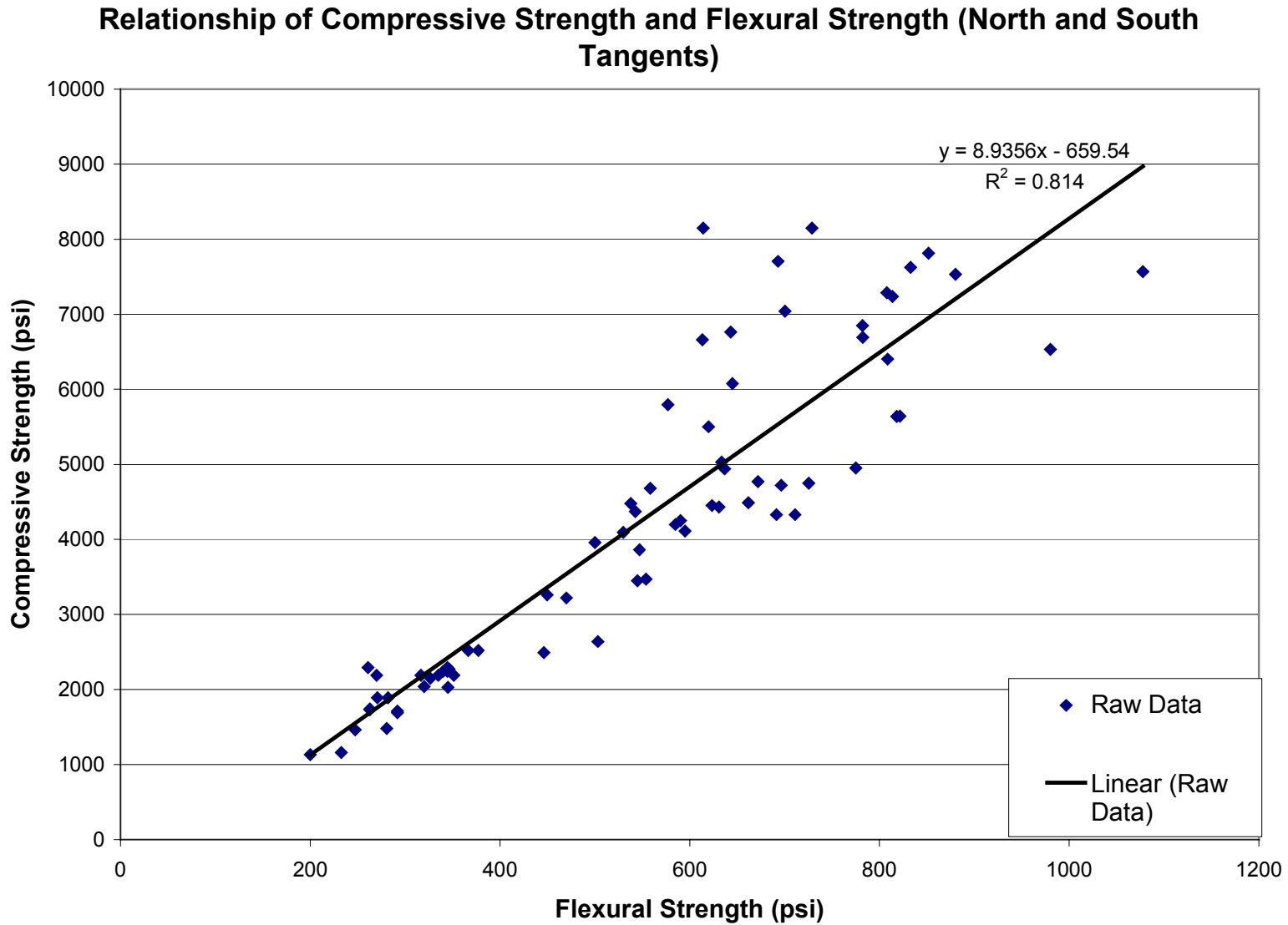


Figure 9.7. Relationship of Compressive Strength and Flexural Strength for Palmdale Test Sections.

Relationship of Compressive Strength and Flexural Strength at Different Specimen Ages

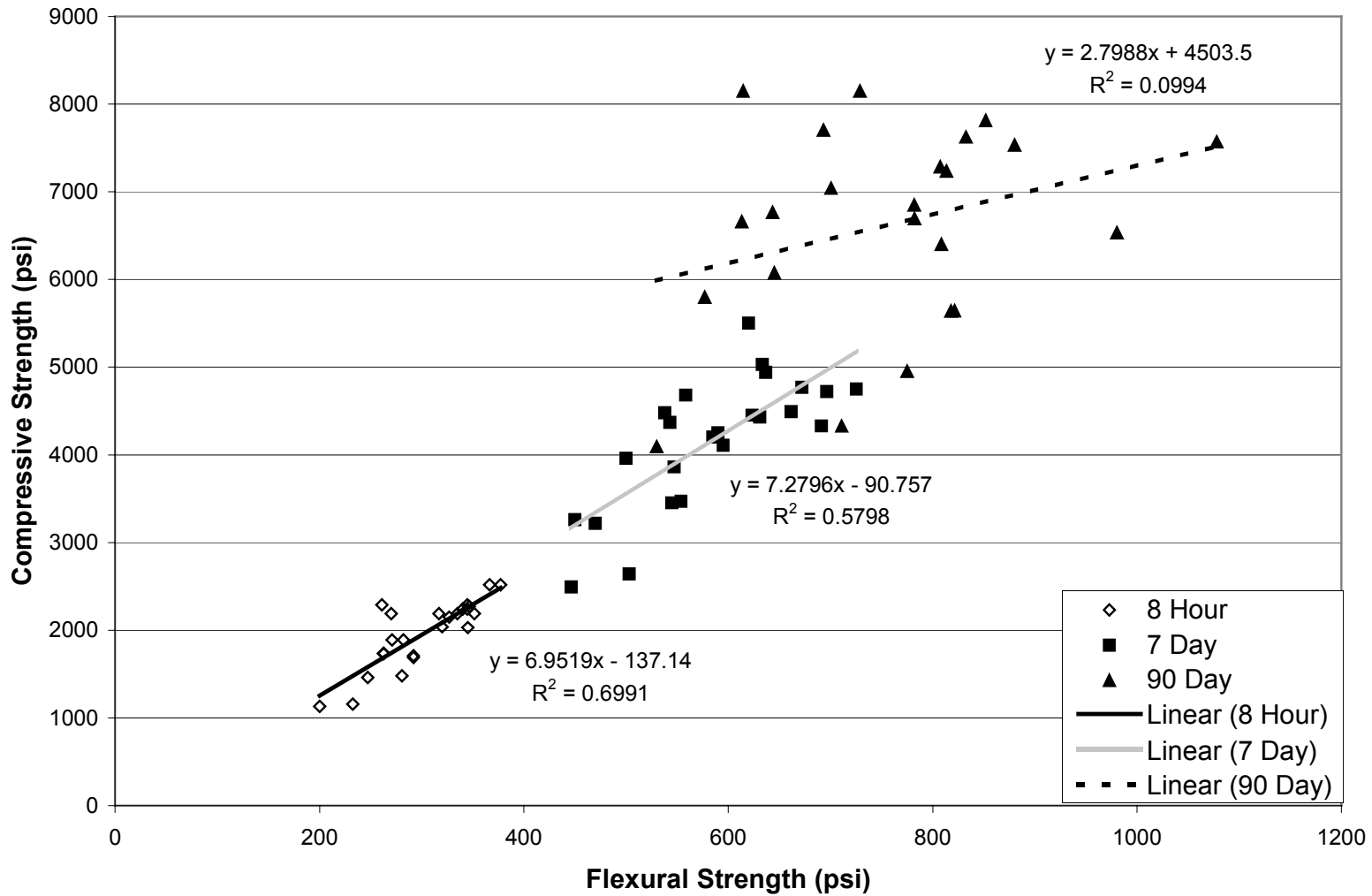


Figure 9.8. Relationship of Compressive Strength and Flexural Strength at Different Specimen Ages.

9.2 Caltrans Strength Testing

Caltrans personnel sampled, cured, and tested beams in accordance with California Test (CT) 523. The beam dimensions were $152 \times 152 \times 914$ mm long with a loading span of 762 mm. CT 523 is the test method used by Caltrans for flexural strength of concrete. The test uses a center-point loading configuration.

As per the Caltrans test method, the concrete mix was placed in the beam molds in two lifts. Each lift was tamped 70 times in an evenly distributed pattern with a steel rod to consolidate the mix. Caltrans personnel sampled beams for 8-hour and 7-day tests. Caltrans did not cast beams for any 90-day tests. The beams to be tested at 8 hours were cured at the construction site prior to testing. The beams to be tested at 7 days were demolded after 24 hours and placed in a moist sand pit until the time of the test. All of the 8-hour and 7-day beams were tested with a manual hydraulic center-point beam tester as per test CT 523.

The 8-hour and 7-day test results were obtained from Gary Laurent, Caltrans resident engineer for the Palmdale project. Table 9.13 lists the flexural beam test data for the 8-hour and 7-day tests for the North and South Tangents. Table 9.13 only contains strength data taken from the HVS test section areas.

Tables 9.14 and 9.15 present flexural beam data for the 8-hour and 7-day center-point flexural beam tests for the 100 percent Ultimax test sections and CTS test section, respectively. The 100 percent Ultimax and CTS test section data was included in this report in order to present all the strength data available from the Palmdale construction. The 100 percent Ultimax and CTS strength data was not placed on the HVS test sections. The CTS placement was completed on the slabs located north of the test sections on the North Tangent. The 100 percent Ultimax was

placed on several of the slabs at the north end of the South Tangent, just north of the test sections.

In Tables 9.13–9.15, the Station column indicates the point along the section at which the concrete sample was taken and refers to the site plan, shown in Appendix B.

Table 9.13 Flexural Strengths for Caltrans Center-Point Beam Tests on 80/20 (Ultimax/PCC) Concrete.

Caltrans Beam	Age	$M_R^{(1)}$ (psi)	$M_R^{(1)}$ (MPa)	Location	Station
1	8 Hours	375	2.59	South Tangent	887+63 – 888+46
2	6 Days	749	5.16	South Tangent	887+63 – 888+46
3	8 Hours	338	2.33	South Tangent	887+63 – 888+46
4	7 Days	540	3.72	South Tangent	887+63 – 888+46
5	7 Days	708	4.88	South Tangent	887+63 – 888+46
6	8 Hours	396	2.73	South Tangent	887+63 – 888+46
14	8 Hours	405	2.79	South Tangent	884+ 82 – 885+50
15	8 Hours	364	2.51	South Tangent	884+ 82 – 885+50
16	8 Hours	375	2.59	South Tangent	884+ 82 – 885+50
17	7 Days	562	3.87	South Tangent	884+ 82 – 885+50
18	7 Days	604	4.16	South Tangent	884+ 82 – 885+50
21	8 Hours	427	2.94	North Tangent	890+40 – 891+40
22	8 Days	624	4.30	North Tangent	890+40 – 891+40
23	8 Hours	499	3.44	North Tangent	890+40 – 891+40
24	7 Days	832	5.74	North Tangent	890+40 – 891+40
25	8 Days	666	4.59	North Tangent	890+40 – 891+40
26	9 Days	583	4.02	North Tangent	890+40 – 891+40
30	8 Hours	479	3.30	North Tangent	893+50 – 894+10
31	7 Days	541	3.73	North Tangent	893+50 – 894+10
33	8 Hours	357	2.46	North Tangent	893+50 – 894+10
43	8 Hours	333	2.30	South Tangent	887+60 – 886+40
44	8 Hours	344	2.37	South Tangent	887+60 – 886+40
45	7 Days	541	3.73	South Tangent	887+60 – 886+40
46	7 Days	625	4.31	South Tangent	887+60 – 886+40
47	8 Hours	286	1.97	South Tangent	886+90 – 886+20
48	8 Hours	354	2.44	South Tangent	886+90 – 886+20
49	8 Hours	283	1.95	South Tangent	886+90 – 886+20
50	24 Hours	340	2.34	South Tangent	886+90 – 886+20
51	7 Days	479	3.30	South Tangent	886+90 – 886+20
52	7 Days	520	3.59	South Tangent	886+90 – 886+20
53	8 Hours	275	1.90	South Tangent	886+20 – 885+50
54	8 Hours	250	1.72	South Tangent	886+20 – 885+50

continued

Caltrans Beam	Age	M_R⁽¹⁾ (psi)	M_R⁽¹⁾ (MPa)	Location	Station
55	7 Days	479	3.30	South Tangent	886+20 – 885+50
56	7 Days	562	3.87	South Tangent	886+20 – 885+50
57	7 Days	520	3.59	South Tangent	886+20 – 885+50
59	8 Hours	198	1.37	North Tangent	891+40 – 892+10
60	8 Hours	250	1.72	North Tangent	891+40 – 892+10
61	8 Hours	260	1.79	North Tangent	891+40 – 892+10
62	7 Days	656	4.52	North Tangent	891+40 – 892+10
63	24 Hours	312	2.15	North Tangent	891+40 – 892+10
64	7 Days	513	3.54	North Tangent	891+40 – 892+10
65	7 Days	531	3.66	North Tangent	891+40 – 892+10
66	8 Hours	104	0.72	North Tangent	892+10 – 892+80
67	8 Hours	104	0.72	North Tangent	892+10 – 892+80
69	24 Hours	380	2.62	North Tangent	892+10 – 892+80
70	7 Days	541	3.73	North Tangent	892+10 – 892+80
71	7 Days	541	3.73	North Tangent	892+10 – 892+80
72	7 Days	583	4.02	North Tangent	892+10 – 892+80
73	8 Hours	104	0.72	North Tangent	892+80 – 893+50
74	7 Days	604	4.16	North Tangent	892+80 – 893+50
76	7 Days	520	3.59	North Tangent	892+80 – 893+50
77	10 Hours	198	1.37	North Tangent	892+80 – 893+50
78	24 Hours	312	2.15	North Tangent	892+80 – 893+50

1) M_R is the concrete modulus of rupture.

From Table 9.13, it can be seen that only 15 percent of the beams made the 8-hour strength specification of 400 psi (2.76 MPa) while only 35 percent of the 7-day beam strengths made the 600 psi (4.14 MPa) specification.

Table 9.14 shows that the 100 percent Ultimix mixes were able to make the 8-hour 400 psi (2.76 MPa) strength specification, but only one 25 percent of the beams were able to make the 600 psi (4.14 MPa) strength at 7 days.

Table 9.14 Flexural Strengths for Caltrans Center-Point Beam Tests on 100 Percent Ultimax Concrete.

Caltrans Beam	Age	$M_R^{(1)}$ (psi)	$M_R^{(1)}$ (MPa)	Location	Station
7	8 Hours	416	2.87	South Tangent	884+63 – 885+27
8	7 Days	583	4.02	South Tangent	884+63 – 885+27
9	8 Hours	406	2.80	South Tangent	884+63 – 885+27
10	8 Hours	395	2.72	South Tangent	884+63 – 885+27
11	7 Days	541	3.73	South Tangent	884+63 – 885+27
12	7 Days	458	3.16	South Tangent	884+63 – 885+27
40	8 Hours	437	3.01	South Tangent	884+55 – 884+82
41	8 Hours	416	2.87	South Tangent	884+55 – 884+82
42	7 Days	604	4.16	South Tangent	884+55 – 884+82

1) M_R is the concrete modulus of rupture.

Table 9.15 Flexural Strengths for Caltrans Center-Point Beam Tests on 100 Percent CTS Concrete.

Caltrans Beam	Age	$M_R^{(1)}$ (psi)	$M_R^{(1)}$ (MPa)	Location	Station
34	3 Hours	104	0.72	North Tangent	894+10 – 894+50
35	8 Hours	229	1.58	North Tangent	894+10 – 894+50
36	8 Hours	291	2.01	North Tangent	894+10 – 894+50
37	7 Days	104	0.72	North Tangent	894+10 – 894+50
38	7 Days	296	2.04	North Tangent	894+10 – 894+50

1) M_R is the concrete modulus of rupture.

The flexural strength data for the CTS test slabs was very low for the 8 hour and 7 day tests. One reason for the low strengths was probably the high water-to-cement ratio used to slip-form pave the CTS test slabs.

Table 9.16 summarizes the 8-hour and 7-day flexural strength test results for the uninstrumented Palmdale sections. The sections were constructed with an 80/20 blend of Ultimax to Portland cement concrete (PCC). The uninstrumented sections were any sections in which UCB did not install instruments and which the HVS will not be testing in the future. The

uninstrumented sections were located at either end of the HVS test sections (instrumented sections). The North Tangent flexural strength results had a very high variability compared to the South Tangent.

Table 9.16 Summary of Flexural Strength Results from Caltrans Center-Point Beam Tests on 80/20 (Ultimax/PCC) Concrete, Non-HVS/Instrumented Sections.

Location	Specimen Age	Average $M_R^{(1)}$ (psi)	Average $M_R^{(1)}$ (MPa)	Standard Deviation (psi [MPa])	C.O.V. (Percent)
South Tangent	8 Hours	393	2.71	28 (0.19)	7
South Tangent	7 Days	575	3.96	71 (0.49)	12
North Tangent	8 Hours	452	3.12	107 (0.74)	24
North Tangent	7 Days	443	3.05	315 (2.17)	71

1) M_R is the concrete modulus of rupture.

Table 9.17 summarizes flexural beam test data for the 8-hour and 7-day tests for the instrumented Palmdale sections (HVS test sections). As described in Section 4.3, the concrete was an 80/20 blend of Ultimax to PCC. The instrumented sections represented in Table 9.17 are the same ones from which UCB Pavement Research Center took and tested samples, as described in Section 9.1.

Table 9.17 Summary of Average Flexural Strength Results from Caltrans Center-Point Beam Tests on 80/20 (Ultimax/PCC) Concrete, Instrumented Sections.

Location	Specimen Age	Average $M_R^{(1)}$ (psi)	Average $M_R^{(1)}$ (MPa)	Standard Deviation (psi [MPa])	C.O.V. (Percent)
South Tangent	8 Hours	304	2.10	40 (0.28)	13
South Tangent	7 Days	520	3.59	51 (0.35)	10
North Tangent	8 Hours	170	1.17	75 (0.52)	44
North Tangent	7 Days	561	3.87	49 (0.34)	9

1) M_R is the concrete modulus of rupture.

It should be noted that a high coefficient of variation (C.O.V.) was observed for the 8-hour flexural beam tests from the North Tangent. A comparison of Tables 9.16 and 9.17 shows that the strengths results obtained from the 8-hour beam tests on concrete from the uninstrumented sections were considerably higher than those obtained from the instrumented sections. The 7-day strengths were similar for both the instrumented and uninstrumented test sections. The discussion of results in Section 9.3 speculates on some of the potential reasons for these low and variable strength results.

Tables 9.18 and 9.19 summarize the modulus of rupture for the 8-hour and 7-day flexural strength tests for the CTS and 100 percent Ultimix supplied cement, respectively.

Table 9.18 Summary of Flexural Strength Results from Caltrans Center-Point Beam Tests on CTS Sections.

Location	Specimen Age	Average $M_R^{(1)}$ (psi)	Average $M_R^{(1)}$ (MPa)	Standard Deviation (psi [MPa])	C.O.V. (Percent)
North Tangent	8 Hours	260	1.79	44 (0.3)	17
North Tangent	7 Days	200	1.38	136 (0.94)	68

1) M_R is the concrete modulus of rupture.

Table 9.19 Summary of Flexural Strength Results from Caltrans Center-Point Beam Tests on 100 Percent Ultimix Sections.

Location	Specimen Age	Average $M_R^{(1)}$ (psi)	Average $M_R^{(1)}$ (MPa)	Standard Deviation (psi [MPa])	C.O.V. (Percent)
North Tangent	8 Hours	414	2.85	16 (0.11)	4
North Tangent	7 Days	547	3.77	65 (0.45)	12

1) M_R is the concrete modulus of rupture.

9.3 Discussion of Beam Results

The special provisions for the FSHCC placed on test sections in Palmdale required that the beam samples reach an average flexural strength of 400 psi (2.76 MPa) in 8 hours and 600

psi (4.14 MPa) average flexural strength in 7 days as determined by CT 523. Only the Caltrans FSHCC testing data is applicable to this specification because the UCB Pavement Research Center utilized a different testing method.

Because the UCB Pavement Research Center (PRC) used different sampling, curing, and testing techniques, PRC results should be expected to differ from the results obtained by Caltrans. Prior research has shown that different beam dimensions and loading configurations give different flexural strength values (7-10). The PRC beam and cylinder results have shown more than 50 percent strength gain after 7 days, and that more variability exists in cylinders than in beams. Laboratory testing at Caltrans indicates that test CT 523 yields results approximately 5 percent higher than those obtained from test ASTM C 78-94 (6). Results presented in this report do not exactly follow this trend, most likely due to a high variability in the concrete used to construct the Palmdale test sections and the high variability in the Caltrans beam results.

A number of factors may influence the rate of strength gain, among them: the amount and type of retarders (Delvo and citric acid) used, the percent Portland Cement content, and water content. The average water-to-cement ratio was higher than the target value.

Some of the variables identified by the PRC that may potentially affect FSHCC strength are:

- The compaction method used to prepare the test specimens (rodding used in CT 523 versus vibrating used in ASTM C 78-94)
- Variation in admixtures
- Variation in cement composition

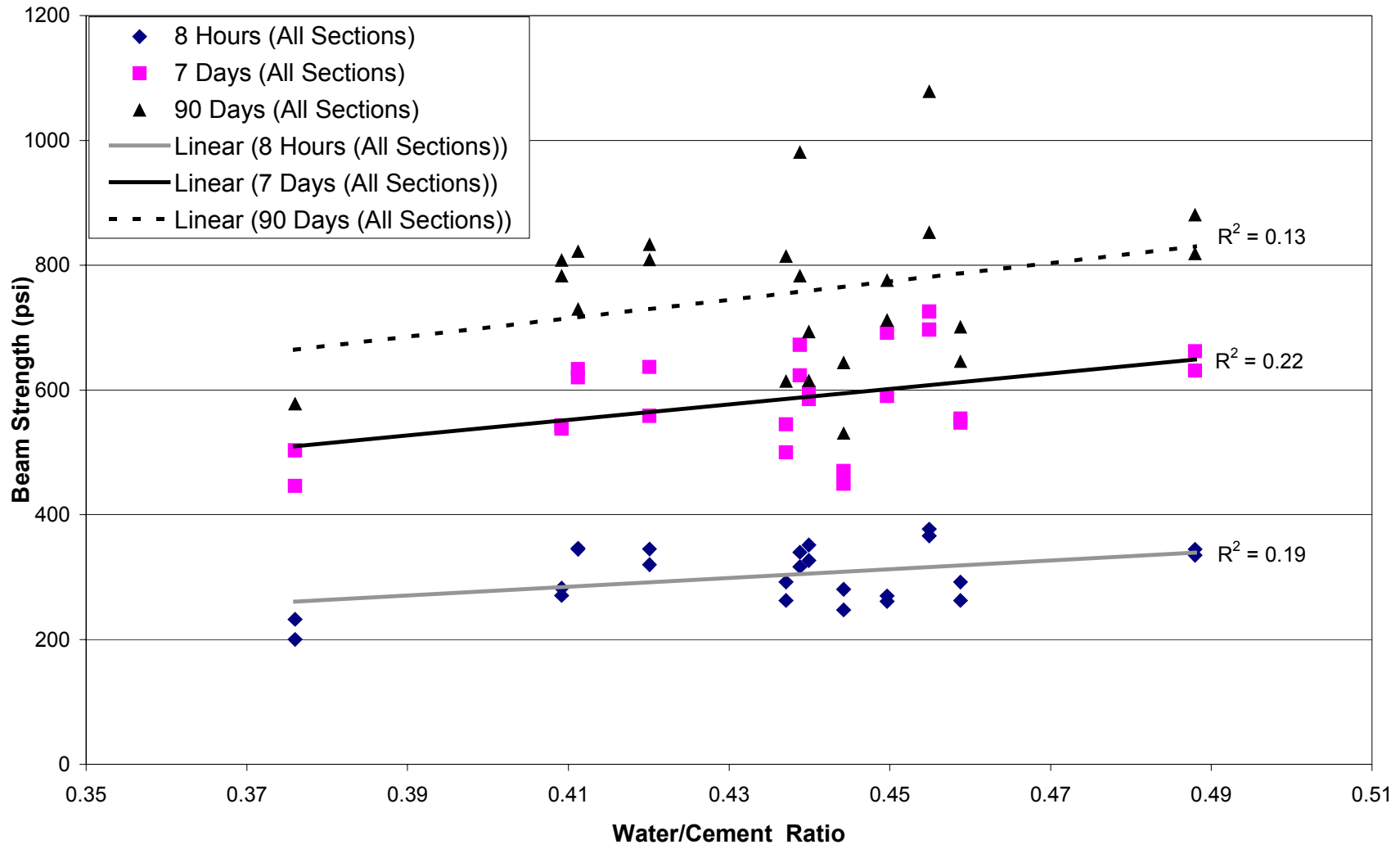
- Variation in the water/cement ratio between batches
- Variation in the dry batching process
- Sampling and curing time variation
- Ambient temperature variation
- FSHCC buildup in the transit trucks

Caltrans may have already addressed some of the variables listed, while other potential variables must be confirmed or dismissed with further investigation. The most significant variable contributing to the high variability in strength results is likely the water-to-cement ratio. Figure 9.9 shows that there is almost no relationship between calculated water-to-cement ratio and beam strength at various times. The main reason for there not being any correlation is that the water-to-cement ratio was estimated from batch weights and the amount of water added at the job site. The estimated water added at the job site is likely the most significant contributor to variability in the calculated water-to-cement ratio. The water-to-cement ratio does not include any water that was used to clean the mixer drum and which may have remained in the mixer drum prior to batching.

9.4 Fast-setting Hydraulic Cement Analysis

X-ray diffraction was carried out by Erlin, Hime Associates on two cement samples taken from the contractor's supply. The chemical analysis was done to determine if the cement supplied to the contractor was consistent and whether it was the cause of variance in the strength results. From the expert opinion of the cement laboratory (11), the two cement samples appeared to be of the same chemical composition. According to the cement laboratory, X-ray diffraction could not

Water/Cement Ratio versus Raw Beam Strength



accurately predict phase composition of the cement if less than 3 percent of a constituent was present (especially if amorphous).

9.5 Deflection Analysis of FSHCC Pavement using the Heavy Weight Deflectometer (HWD)

During the spring and summer of 1998, nondestructive load-deflection tests were performed on the fast-setting hydraulic cement concrete (FSHCC) test sections, near Palmdale, California, as part of the research for CAL/APT Long Life Pavement Rehabilitation Strategies (LLPRS-Rigid). The test sections were constructed during July 1998 and all test data presented were for the old State Route 14 PCC slabs, as well as the new FSHCC slabs at 1, 7, 50 and 90 days. The purpose of this analysis was to determine the pavement's bearing capacity and calculate certain material characteristics of each pavement layer.

The Dynatest Model 8082 Heavy Weight Deflectometer (HWD) Test System was used to generate the NDT load-deflection data analyzed for this report. The HWD generates a transient, impulse-type load of 25-30 millisecond duration, at any desired (peak) load level between 27 and 245 kN (6,000 and 55,000 lbf.), thereby approximating the effect of a 50-80 kph (30-50 mph) moving wheel load. For this project, test loads ranged from 27 to 111 kN (6,000 to 25,000 lbf.) and were normalized to 40kN and 80 kN (9 and 18 kip).

The HWD generated load-deflection data was analyzed using the Dynatest ELMOD computer program. ELMOD is an acronym for Evaluation of Layer Moduli and Overlay Design, and the program is used primarily for analysis of AC and CRCP pavement types. The ELMOD program backcalculates the material properties of a uni-axial, semi-infinite pavement system (i.e., the elastic moduli or "E"-values of each structural layer in the pavement) using the

Odemark-Boussinesq transformed section approach. ELCON is ELMOD for concrete, and provides joint and edge analysis capabilities using the new Westergaard equations for evaluating jointed concrete pavements. For the purposes of this analysis, ELCON was primarily used.

9.5.1 HWD Analysis Approach

Both the South and the North Tangents were tested between 10:00 a.m. and 1:00 p.m.

The North Tangent (Sections 7, 9, and 11) was tested along the center and left edge of each slab.

The South Tangent (Sections 1,3, and 5) was tested along the center of each slab.

The stationing for this project was carried out in units of meters (feet). The starting point (0) on both the North and South Tangents is located at the southern end of each test section, with stationing increasing northward. HWD testing was performed on each concrete slab constructed. Figure 9.10 shows the HWD drop locations for both the North and South Tangents.

The pavement thicknesses for analysis purposes are the same as those reported in Sections 4.2.1 and 4.2.2. For comparison purposes, the old PCC slab material properties are presented with the FSHCC slab properties. The old PCC slab was removed to place the new FSHCC test sections. The old PCC slab thickness was 200 mm.

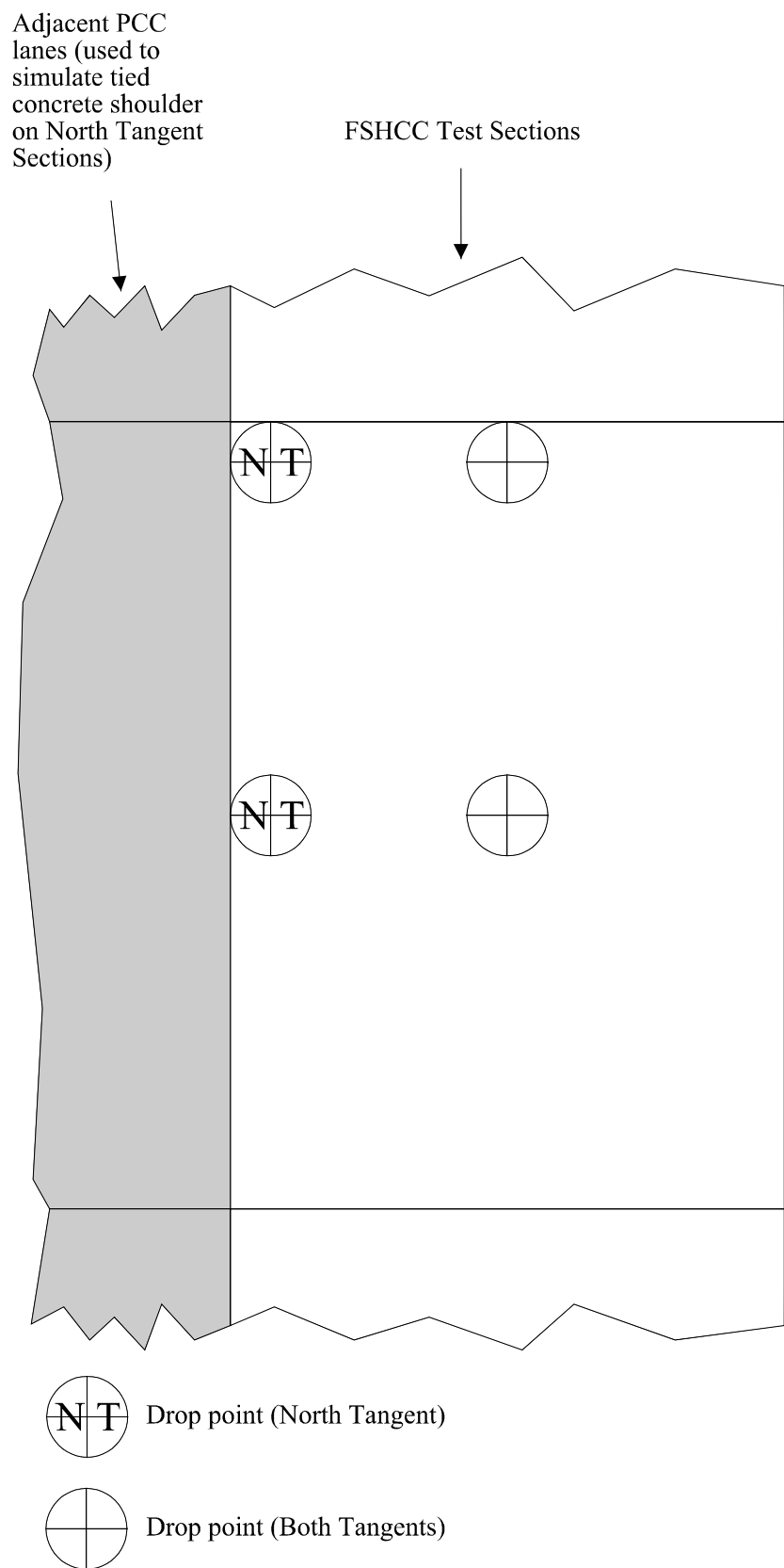


Figure 9.10. HWD Drop Locations, North and South Tangents.

9.5.1.1 North Tangent

9.5.1.1.1 Deflections

Normalized center deflections for both 40 kN and 80kN (9,000 lbf. and 18,000 lbf.) wheel loads and are plotted in Figures 9.11 and 9.12. The deflections are summarized in Table 9.20

Table 9.20 Summary of North Tangent HWD Deflections.

Material	Age	Test Load, kN (kip)	Normalized Deflections, μ (mils)			
			Average	Standard Deviation	84th Percentile	C.O.V., (Percent)
Old PCC	~30 years	40 (9)	94 (3.71)	16 (0.62)	110 (4.33)	17.0
FSHCC	1 Day	40 (9)	61 (2.39)	8 (0.33)	69 (2.72)	13.1
FSHCC	7 Days	40 (9)	56 (2.22)	12 (0.47)	68 (2.70)	21.4
FSHCC	50 Days	40 (9)	72 (2.85)	30 (1.19)	102 (4.03)	41.7
FSHCC	90 Days	40 (9)	76 (2.99)	27 (1.08)	103 (4.07)	35.5
Old PCC	~30 years	80 (18)	187 (7.38)	30 (1.17)	217 (8.56)	16.0
FSHCC	1 Day	80 (18)	120 (4.73)	17 (0.66)	137 (5.39)	14.2
FSHCC	7 Days	80 (18)	111 (4.38)	22 (0.87)	133 (5.25)	19.8
FSHCC	50 Days	80 (18)	138 (5.44)	57 (2.25)	195 (7.69)	41.3
FSHCC	90 Days	80 (18)	144 (5.66)	50 (1.96)	194 (7.62)	34.7

Inspection of Figures 9.11-9.12 and Table 9.20 shows that the measured deflections for all days are fairly variable, and are consistent with the measured deflections on the 30-year old Portland cement concrete (PCC) slabs (i.e., existing PCC) up to 7 days. Tests on the FSHCC at 50 and 90 days appear to exhibit significantly higher variability as shown by the coefficient of variation (C.O.V.) increasing to 35-40 percent from 15-20 percent. The trend of increased deflection with age for the FSHCC is contrary to the expected decrease in deflection one would associate with increasing strength. This may, however, be associated with subgrade variation,

North Tangent - 40 kN Deflections

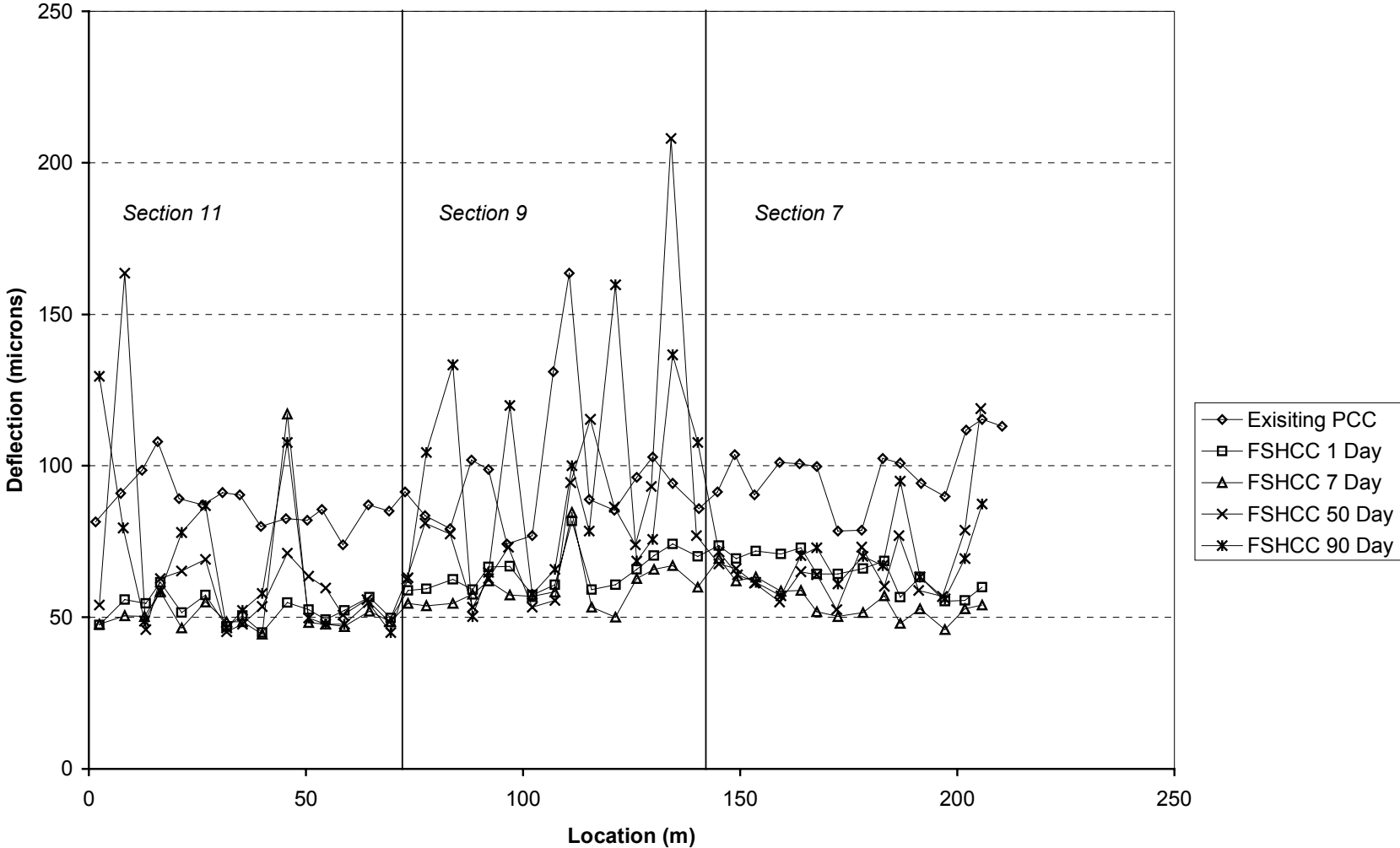


Figure 9.11. HWD Deflections, 40kN Load, North Tangent.

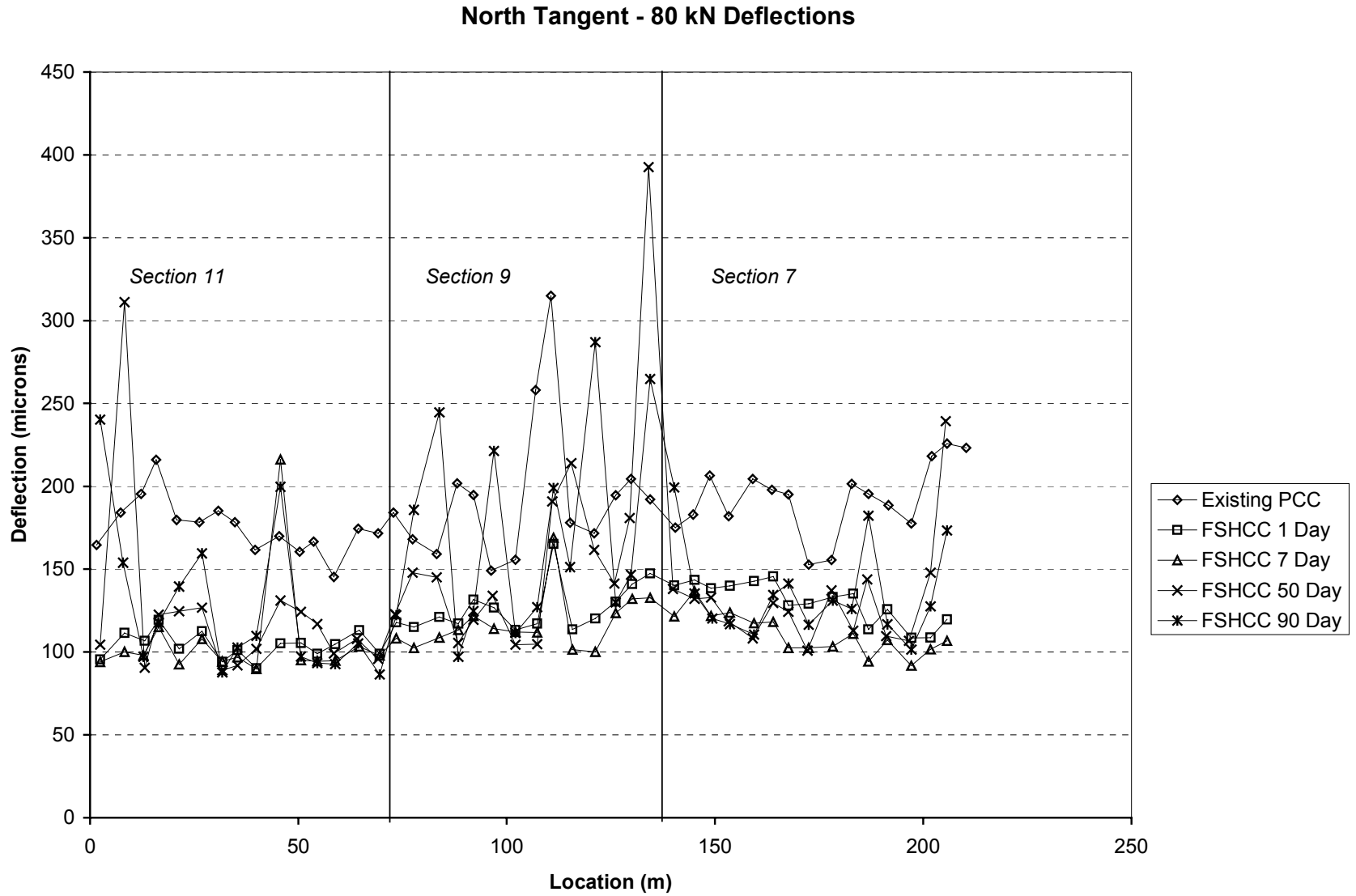


Figure 9.12. HWD Deflections, 80kN Load, North Tangent.

variability in the concrete stiffness, variability in the cement treated base, and variability in concrete thickness. Longitudinal variations in deflection response appear to be fairly consistent across all sections for a given testing day.

9.5.1.1.2 Layer Moduli

PCC, FSHCC, and subgrade moduli were backcalculated for each test point using ELCON. The base moduli for CTB were fixed at 1,380 MPa (200 ksi) for all tests performed on the North Tangent. This value was based on backcalculated CTB moduli from HWD data measured directly on the CTB layer. PCC and FSHCC moduli are plotted in Figure 9.13 and are somewhat consistent, averaging approximately 42,500 MPa (6,000 ksi). North Tangent layer moduli calculated from the deflection data are presented in Table 9.21.

Table 9.21 North Tangent Layer Moduli Calculated from the HWD Deflection Data.

Material	Age	PCC and FSHCC Modulus, MPa (ksi)			
		Average	Standard Deviation	84th Percentile	C.O.V. (Percent)
Old PCC	~30 Years	41144 (5966)	5110 (741)	36034 (5225)	12.4
Section 11					
FSHCC	1 Day	43752 (6344)	9641 (1398)	34110 (4946)	22.0
FSHCC	7 Days	44131 (6399)	14110 (2046)	30013 (4352)	32.0
FSHCC	50 Days	56634 (8212)	36365 (5273)	20268 (2939)	64.2
FSHCC	90 Days	49952 (7243)	14917 (2163)	35034 (5080)	29.9
Section 9					
FSHCC	1 Day	40593 (5886)	5510 (799)	35083 (5087)	13.6
FSHCC	7 Days	43283 (6276)	5414 (785)	37862 (5490)	12.5
FSHCC	50 Days	38979 (5652)	19897 (2885)	19083 (2767)	51.0
FSHCC	90 Days	33717 (4889)	14407 (2089)	19303 (2799)	42.7
Section 7					
FSHCC	1 Day	36083 (5232)	6310 (915)	29772 (4317)	17.5
FSHCC	7 Day	43566 (6317)	8952 (1298)	34614 (5019)	20.5
FSHCC	50 Days	37103 (5380)	12241 (1775)	24862 (3605)	33.0
FSHCC	90 Days	42262 (6128)	14952 (2168)	27310 (3960)	35.4

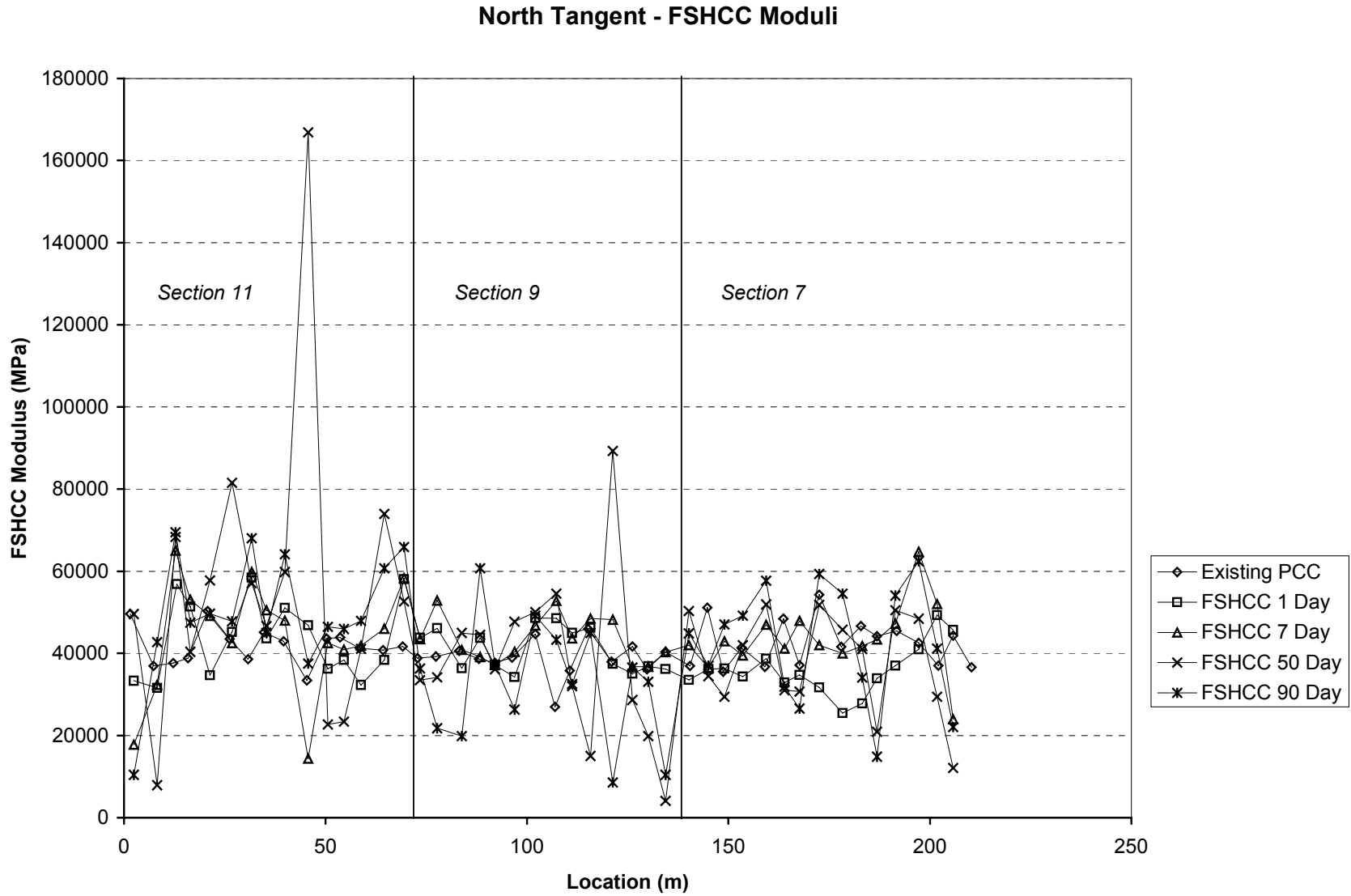


Figure 9.13. Surface Moduli (Backcalculated) for North Tangent.

As would be expected, the variability trend observed in the deflection data is evident in the backcalculated moduli. The trend of consistently increasing average deflection with time, however, is not reflected in the calculated FSHCC moduli. It is important to note that the FSHCC mix, as placed, varied between all sections based on the observed consistency of the material during construction and the measured concrete strength results. The calculated moduli, however, suggest reasonable similarity between sections, but this needs to be confirmed from QC measurements.

Backcalculated subgrade moduli are shown in Figure 9.14 and Table 9.22. Inspection of the figure and the table shows generally consistent subgrade response, with an average modulus of approximately 205 MPa (30 ksi). Comparison of the calculated PCC and FSHCC average subgrade moduli shows reasonable similarity between the two values for all sections. The subgrade moduli of the PCC and FSHCC should be similar given that the FSHCC was placed at the same location as the old PCC pavement.

Estimated subgrade moduli do not appear to reflect the trend of increasing variability with time shown by deflections, which is consistent with the expected response. However, there does generally appear to be a trend of decreased subgrade modulus over time, which would explain the increasing deflection observed with time. The most common cause of subgrade modulus variation with time is considered to be variation in moisture content. The observed trend would typically be expected to result from increasing moisture content, which does not appear reasonable for the time period over which the deflections were measured. Another possibility involves stress sensitivity of the subgrade, which would be expected to correlate with any trends observed in the surface (FSHCC) modulus, (i.e. as FSHCC modulus increased, stress

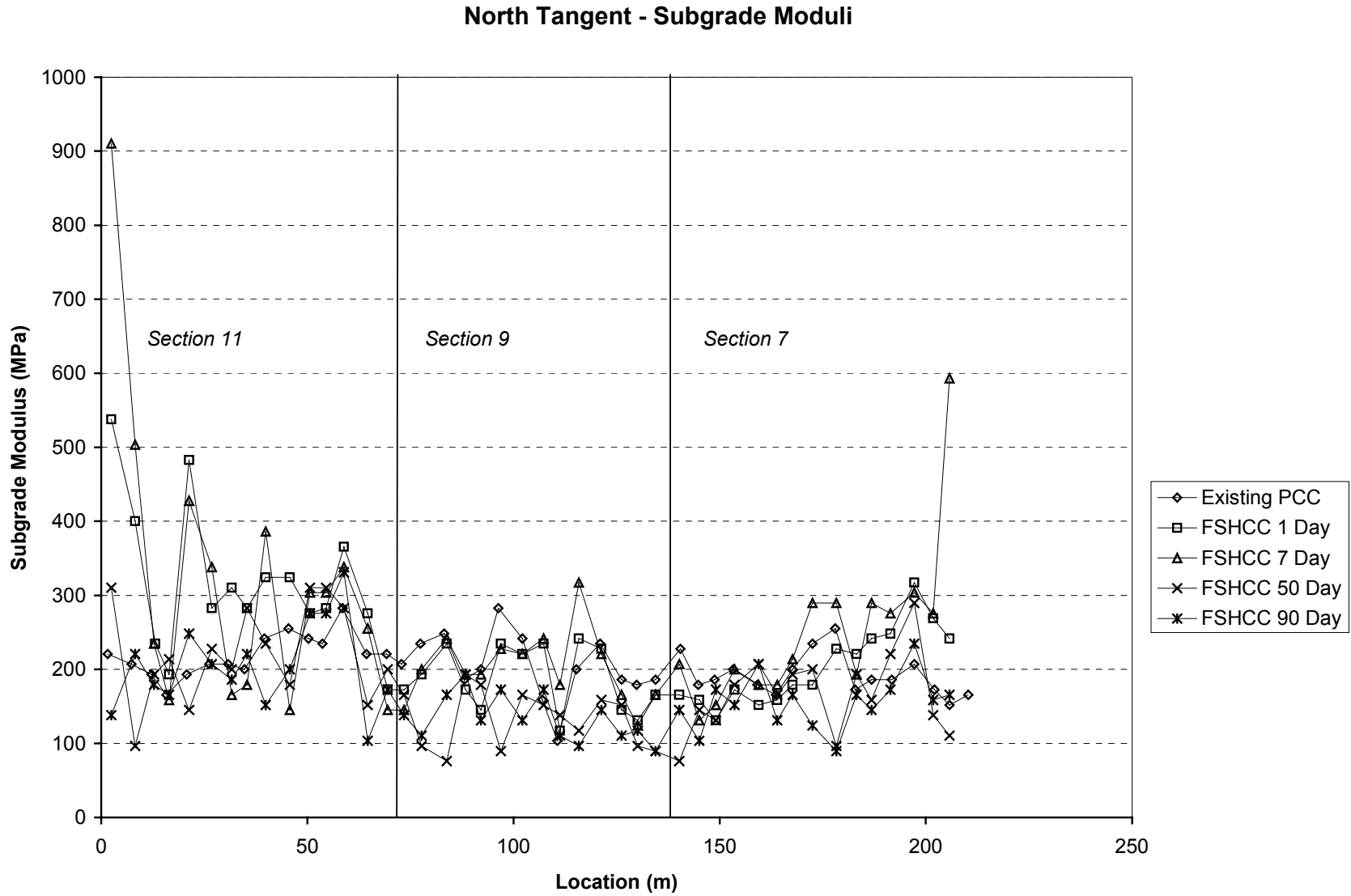


Figure 9.14. Subgrade Moduli (Backcalculated), North Tangent.

Table 9.22 North Tangent Subgrade Moduli Calculated from the FWD Deflection Data.

North Tangent	Subgrade Modulus, MPa (ksi)			
	Average	Standard Deviation	84th Percentile	C.O.V., (Percent)
Old SR14 PCC	207 (30)	34 (5)	172 (25)	16.7
Section 11				
1 Day	317 (46)	97 (14)	221 (32)	30.4
7 Days	317 (46)	200 (29)	124 (18)	63.0
50 Days	221 (32)	69 (10)	159 (23)	31.3
90 Days	207 (30)	62 (9)	145 (21)	30.0
Section 9				
1 Day	186 (27)	41 (6)	145 (21)	22.2
7 Days	200 (29)	48 (7)	159 (23)	24.1
50 Days	131 (19)	41 (6)	90 (13)	31.6
90 Days	138 (20)	28 (4)	103 (15)	20.0
Section 7				
1 Day	207 (30)	55 (8)	152 (22)	26.7
7 Days	255 (37)	110 (16)	138 (20)	43.2
50 Days	172 (25)	48 (7)	124 (18)	28.0
90 Days	159 (23)	34 (5)	117 (17)	21.7

induced on subgrade decreased for a given HWD load). Finally, the decrease in subgrade moduli could be an indication of micro- or macro-cracks occurring in the concrete surface layer.

9.5.1.1.3 Joint Evaluation

The FSHCC joint evaluation analyses provides information in terms of calculated modulus of subgrade reaction (k) at the center and joint load transfer efficiency (L.T.E.), for both transverse and longitudinal joints, based on measured deflections. Average values of calculated modulus of subgrade reaction are shown in Figure 9.15. The k-values are based on backcalculated subgrade moduli and therefore exhibit similar trends to those observed in the backcalculated layer moduli. It should be noted that joint evaluation analysis results are typically

highly dependent on the time of day at which the NDT was performed due to temperature effects. The L.T.E. information for the North Tangent is summarized in Table 9.23.

Table 9.23 North Tangent Joint Load Transfer Efficiencies.

Material	Age	Average Values of Joint Response				
		k_{center} , MN/m ³ (pci)	k_{edge} , MN/m ³ (pci)	L.T.E., Percent Transverse	L.T.E., Percent Longitudinal (Center Slab)	L.T.E., Percent Longitudinal (Corner Slab)
Old PCC ⁽¹⁾		101 (370)	No Test	No Test	No Test	No Test
Section 11 (plain longitudinal joints, doweled transverse joints)						
FSHCC	1 Day	189 (694)	181 (666)	89	89	96
FSHCC	7 Days	200 (737)	136 (502)	89	82	70
FSHCC	50 Days	119 (439)	67 (247)	93	94	86
FSHCC	90 Days	107 (394)	85 (312)	92	68	47
Section 9 (tied longitudinal joints, doweled transverse joints)						
FSHCC	1 Day	99 (365)	166 (610)	91	95	97
FSHCC	7 Days	107 (392)	110 (404)	89	87	86
FSHCC	50 Days	69 (255)	76 (278)	93	95	90
FSHCC	90 Days	75 (275)	91 (334)	93	77	66
Section 7 (plain joints)						
FSHCC	1 Day	118 (434)	208 (765)	88	95	99
FSHCC	7 Days	146 (538)	126 (465)	70	84	82
FSHCC	50 Days	95 (348)	74 (271)	73	95	90
FSHCC	90 Days	81 (298)	100 (367)	64	78	52

1) No joint tests were taken on Route 14 existing PCC slabs.

The k-value at the center of slab was compared to the backcalculated k-value at the edge of the slab in Table 9.23. The k-value at the edge was always different than k_{center} . This demonstrates that the k-value is not a unique material parameter, rather it is dependent on location and geometry of the pavement system.

As Table 9.23 shows, a lower L.T.E. was observed for the transverse joints in Section 7. This behavior is expected given that Sections 9 and 11 have doweled transverse joints, while Section 7 has plain joints. Figure 9.16 shows a plot of L.T.E. across the transverse joints on the North Tangent. It is clear from Figure 9.16 that the doweled joints have a consistently higher

North Tangent - Modulus of Subgrade Reaction

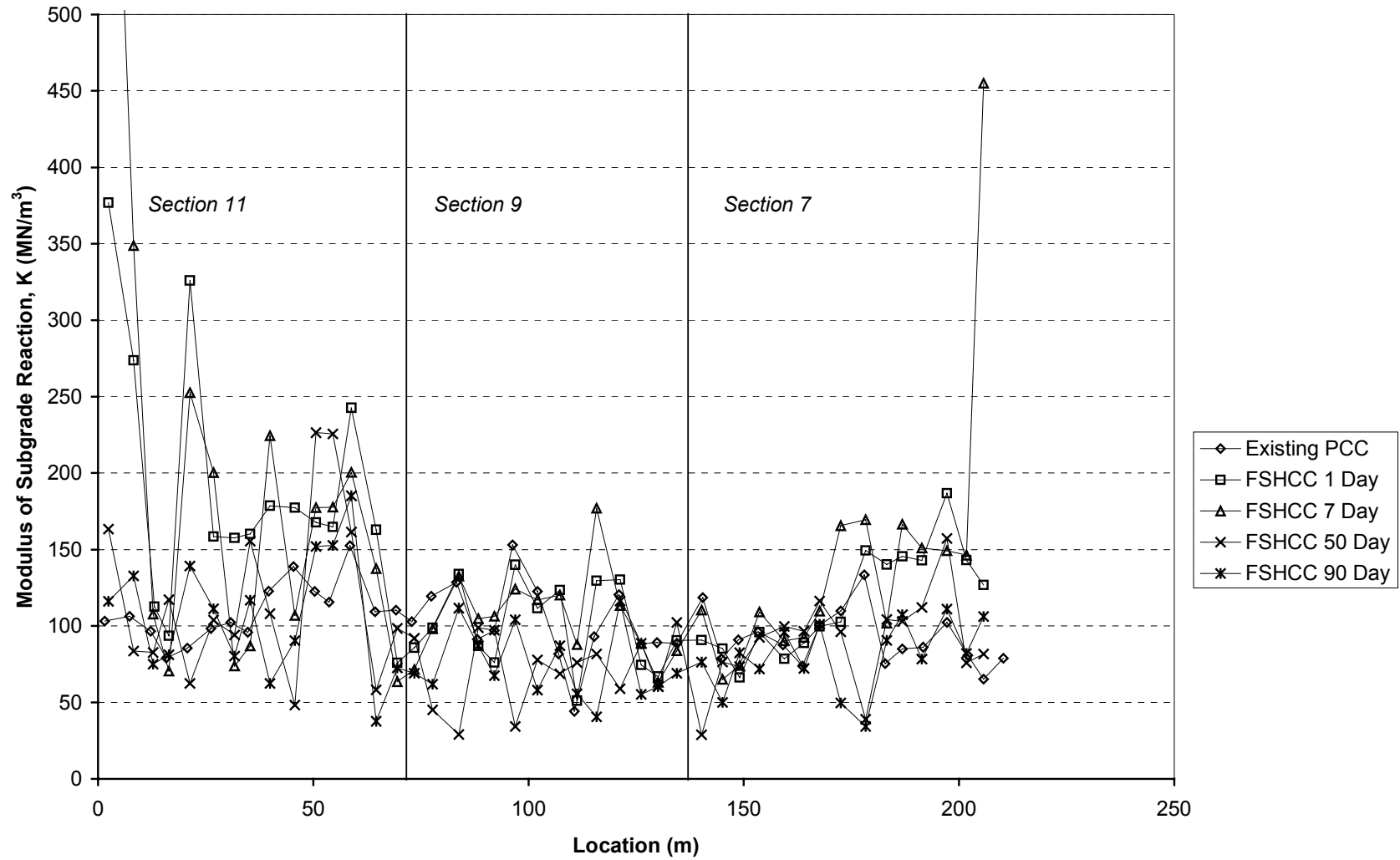


Figure 9.15. North Tangent Modulus of Subgrade Reaction.

L.T.E. over time. At 90 days, the doweled joints of Sections 9 and 11 average above 90 percent whereas the undoweled joints of Section 7 average 64 percent.

Section 9 longitudinal joints are tied with deformed rebar, while Section 7 and 11 longitudinal joints are not tied. Figures 9.17 and 9.18 show plots of L.T.E. across the longitudinal joint on the North Tangent. Figure 9.17 shows the L.T.E. across the longitudinal joint when the HWD drop is at the mid-slab edge while Figure 9.18 shows the L.T.E. when the HWD drop is at the corner of the slab. At the mid-slab edge, the L.T.E. across the tied longitudinal joint (Section 9) was not significantly greater than the longitudinal joints without tie bars (aggregate interlock only).

One reason for similar L.T.E. for tied and untied longitudinal joints was that the lane adjacent to the FSHCC slabs was not saw cut cleanly. This condition left an uneven surface with which the new FSHCC sections could bond and interlock, as shown in Figure 9.19. Another plausible reason for similar L.T.E. results of tied and untied joints is that tie bars do not give significantly greater L.T.E. than aggregate interlock early in the pavement life. HVS loading across the tied and untied longitudinal joint will determine the effects tied and untied joints have on fatigue life of the pavement. Figure 9.18 shows that there is a slight improvement with tie bars when the L.T.E. is measured at the corner of the slab. Given that the highest deflection in a slab occurs at the slab corner, tie bars probably help to decrease the relative deflection across adjacent slab corners as compared to aggregate interlock joints without tie bars.

The decrease of the L.T.E. across the longitudinal joints over time, as shown in Figures 9.17 and 9.18, was probably due to the drying shrinkage of the concrete. This shrinkage resulted

North Tangent Transverse Joint Load Transfer Efficiency

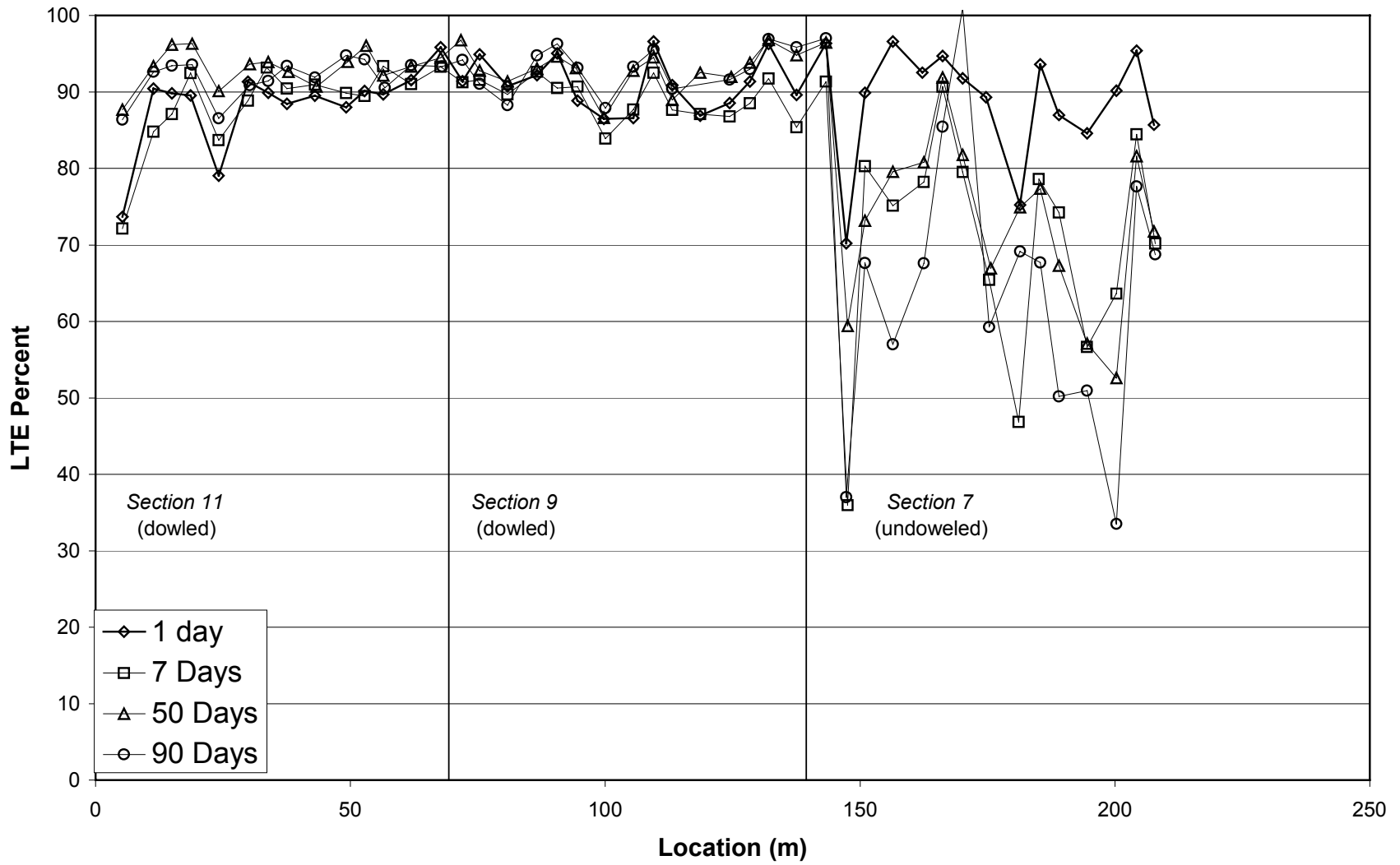


Figure 9.16. Transverse Joint Load Transfer Efficiency, North Tangent.

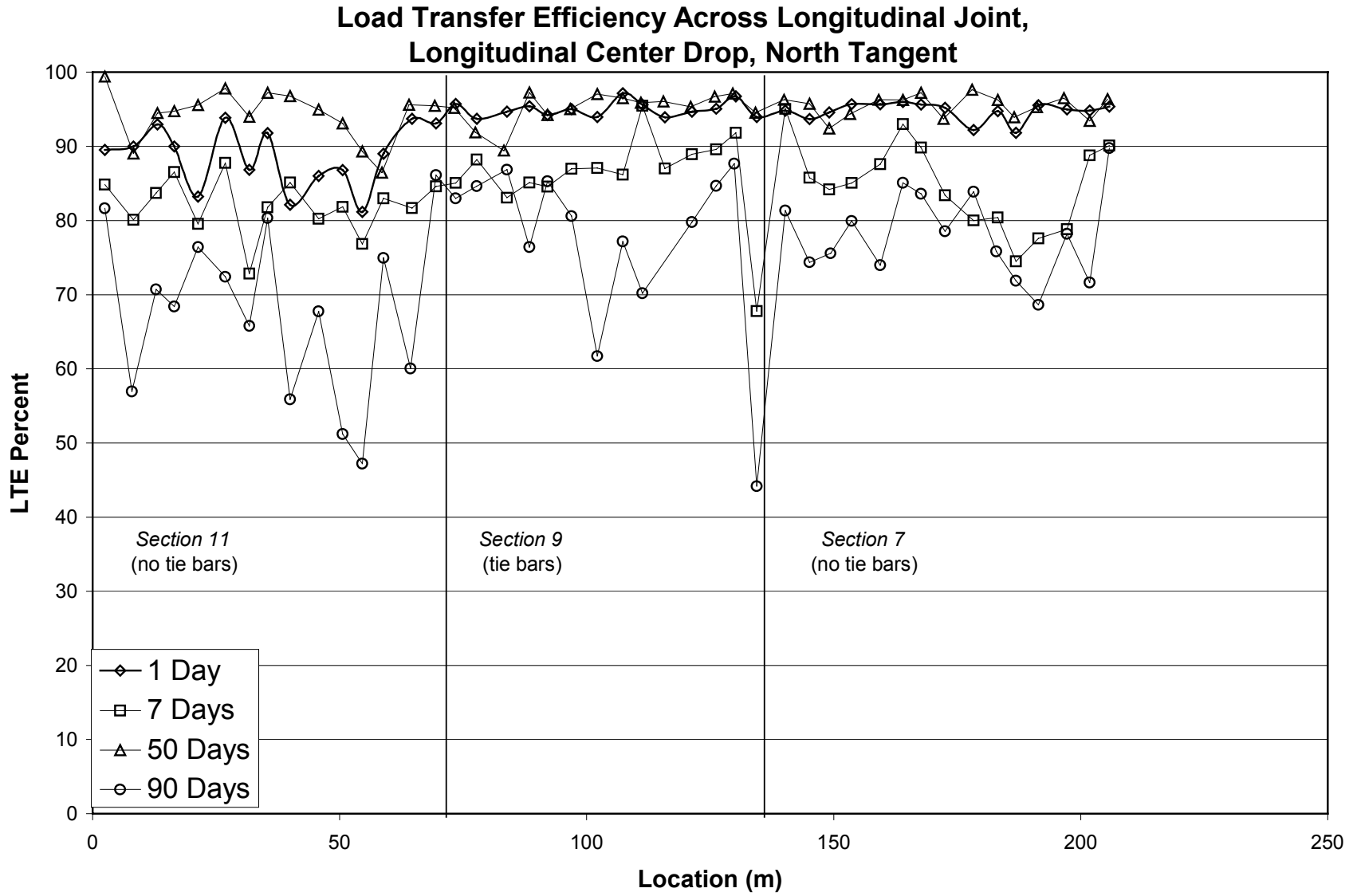


Figure 9.17. Longitudinal Joint Load Transfer Efficiency, Longitudinal Center Drop, North Tangent.

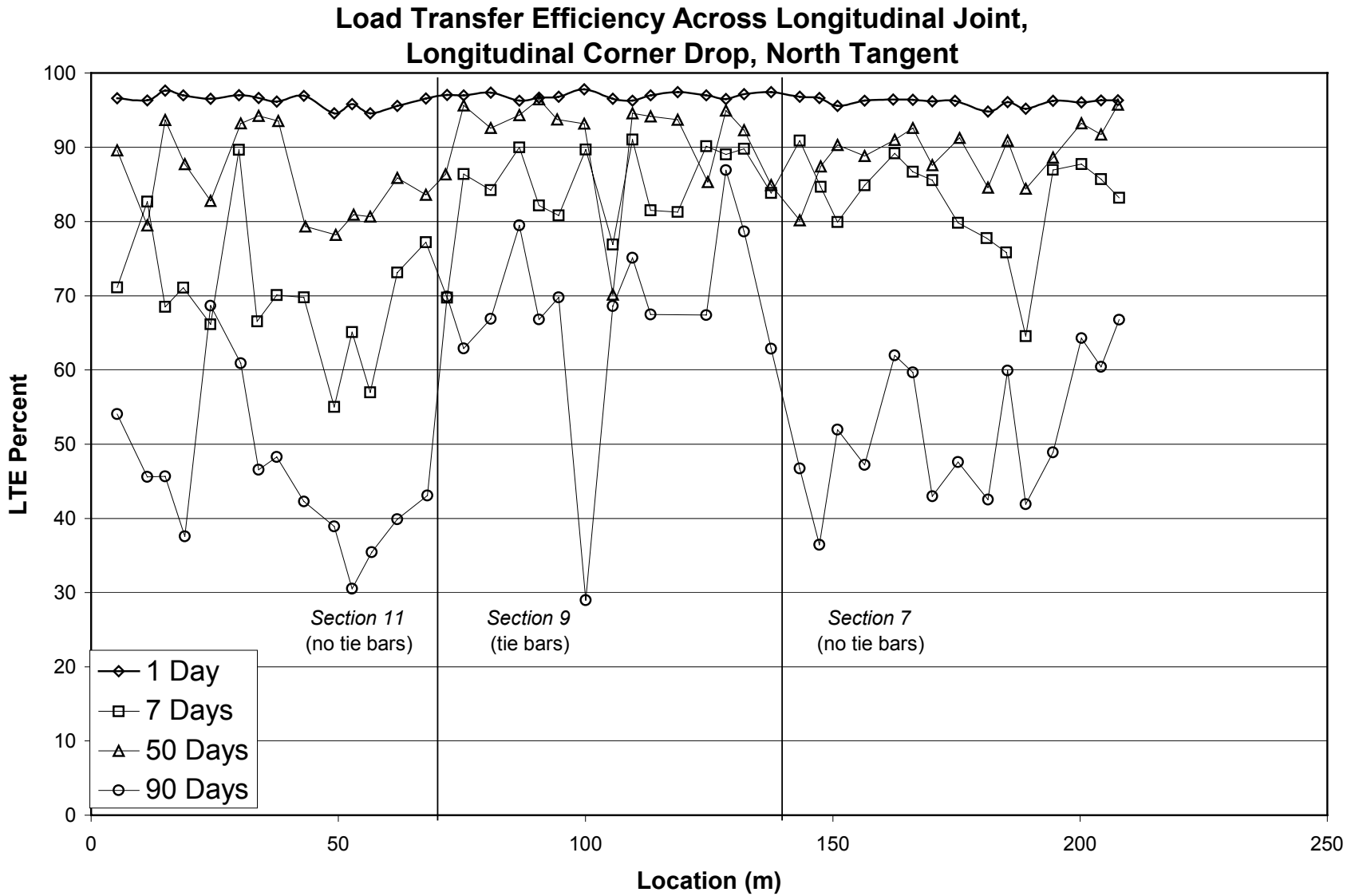


Figure 9.18. Longitudinal Joint Load Transfer Efficiency, Longitudinal Corner Drop, North Tangent.



Figure 9.19. Detail photo of Rough Longitudinal Surface of Existing PCC Slabs, South Tangent.

in the new FSHCC pavement moving away from the adjacent lane and thereby allowing more free movement of the joint.

The fact that Section 11 had a widened lane of 4.3 m (14 ft) instead of 3.7 m (12 ft) lane didn't seem to affect the load transfer results across the transverse or longitudinal joint.

9.5.1.2 South Tangent

9.5.1.2.1 Deflections

Normalized center deflections for both 40 kN and 80 kN (9,000 lbf. and 18,000 lbf.) wheel loads are plotted in Figures 9.20 and 9.21, respectively. The deflections for both the 40 kN and 80 kN loads are summarized in Tables 9.24 and 9.25, respectively.

Table 9.24 Summary of South Tangent HWD Deflections, 40 kN (9 kip).

Material	Age	Normalized 40 kN (9 kip) Deflections, μ (mils)			
		Average	Standard Deviation	84th Percentile	C.O.V., (Percent)
Old PCC		149 (5.87)	20 (0.77)	169 (6.64)	13.4
Section 1					
	1 Day	164 (6.45)	44 (1.73)	208 (8.18)	26.8
	7 Day	164 (6.45)	58 (2.30)	223 (8.76)	35.4
	50 Day	249 (9.82)	121 (4.78)	371 (14.6)	48.6
	90 Day	241 (9.49)	69 (2.73)	310 (12.2)	28.6
Section 3					
	1 Day	91 (3.58)	15 (0.59)	106 (4.17)	16.5
	7 Day	84 (3.31)	12 (0.46)	96 (3.77)	14.3
	50 Day	103 (4.06)	21 (0.83)	124 (4.89)	20.4
	90 Day	116 (4.56)	20 (0.80)	136 (5.36)	17.2
Section 5					
	1 Day	73 (2.87)	13 (0.52)	86 (3.39)	17.8
	7 Day	76 (3.00)	11 (0.45)	88 (3.45)	14.5
	50 Day	97 (3.83)	47 (1.85)	144 (5.68)	48.5
	90 Day	101 (3.97)	48 (1.88)	149 (5.85)	47.5

Inspection of Figures 9.20-9.21 and Tables 9.24-9.25 shows that the measured deflections for all days are somewhat variable, and are consistent with measured deflections of typical Portland cement concrete (PCC) slabs, including the existing PCC slabs near the Palmdale test sections. Longitudinal variations in deflection response appear to be fairly consistent for Section 5, but are increasingly variable for Sections 1 and 3. This may be due to the change in surface

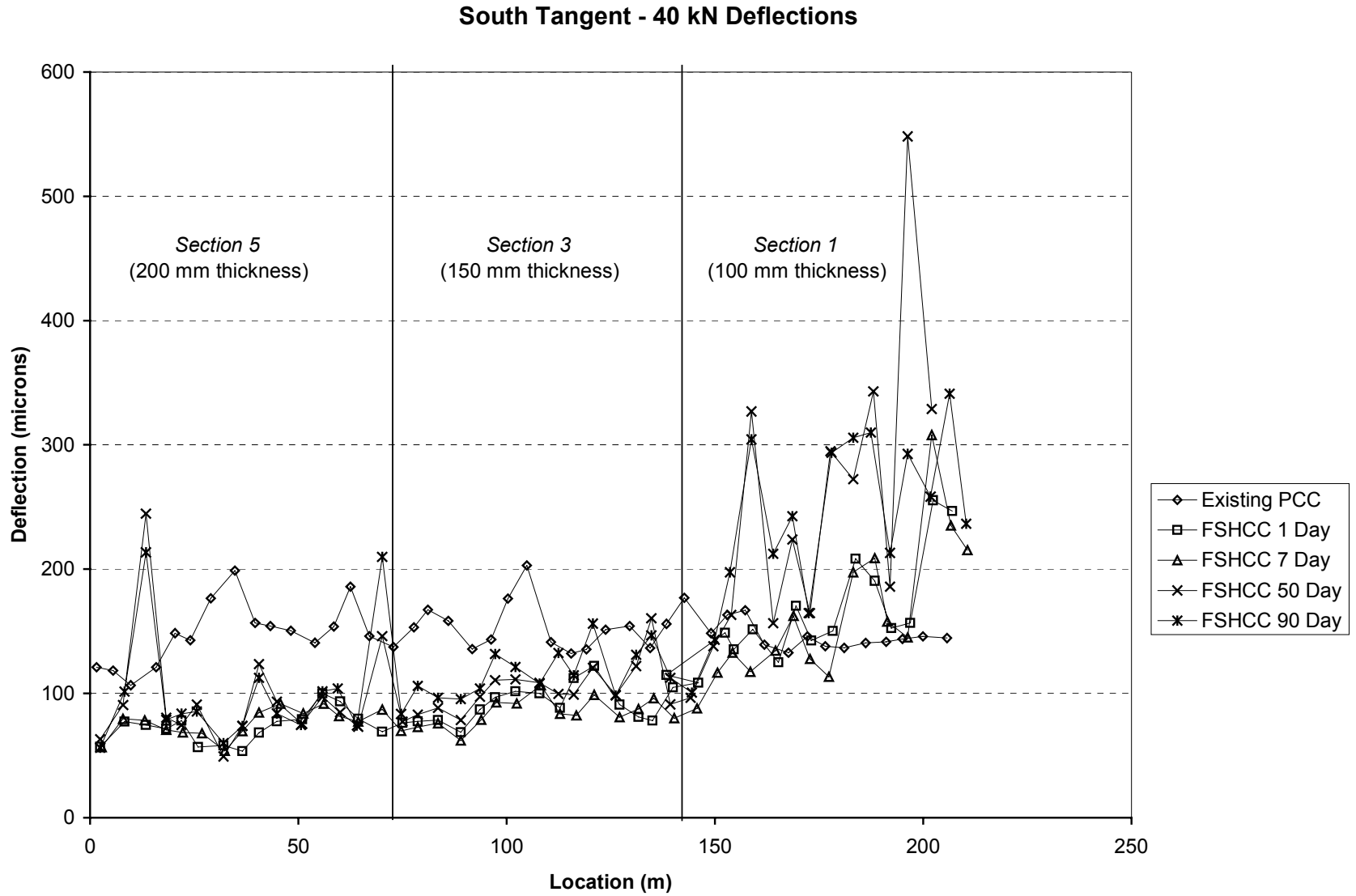


Figure 9.20. HWD Deflections, 40kN Load, South Tangent.

South Tangent - 80 kN Deflections

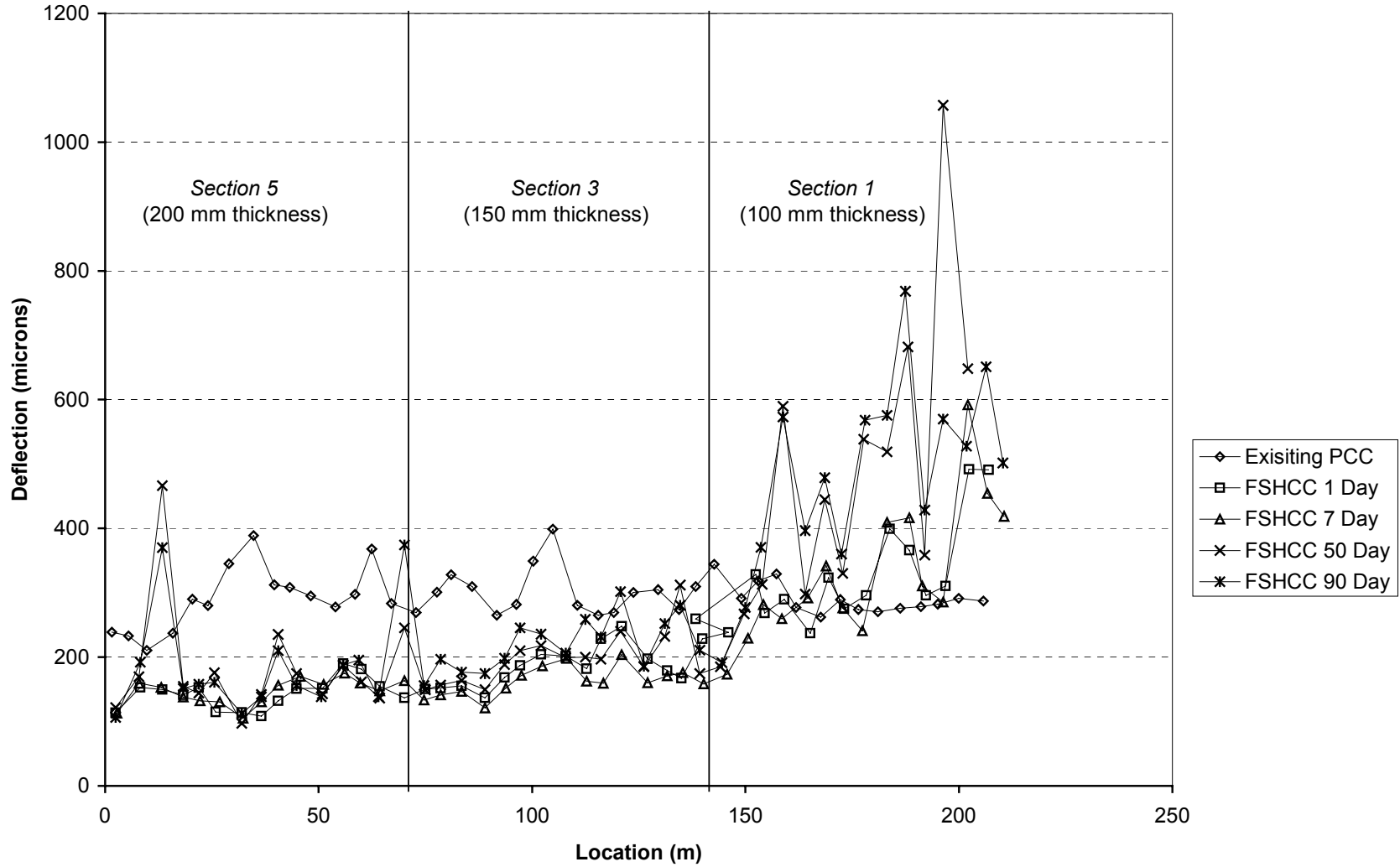


Figure 9.21. HWD Deflections, 80kN Load, South Tangent.

Table 9.25 Summary of South Tangent HWD Deflections, 80 kN (18 kip).

Material	Age	Normalized 80 kN (18 kip) Deflections, μ (mils)			
		Average	Standard Deviation	84th Percentile	C.O.V. (Percent)
Old PCC	~30 Years	295 (11.6)	38 (1.50)	333 (13.1)	12.9
Section 1					
FSHCC	1 Day	325 (12.8)	81 (3.17)	406 (16.0)	24.9
FSHCC	7 Day	333 (13.1)	108 (4.24)	439 (17.3)	32.4
FSHCC	50 Day	480 (18.9)	233 (9.17)	711 (28.0)	48.5
FSHCC	90 Day	483 (19.0)	149 (5.85)	632 (24.9)	30.8
Section 3					
FSHCC	1 Day	186 (7.31)	32 (1.27)	218 (8.58)	17.2
FSHCC	7 Day	163 (6.40)	23 (0.90)	185 (7.30)	14.2
FSHCC	50 Day	198 (7.80)	42 (1.66)	241 (9.47)	21.2
FSHCC	90 Day	220 (8.68)	42 (1.64)	262 (10.3)	19.1
Section 5					
FSHCC	1 Day	143 (5.62)	24 (0.94)	167 (6.57)	16.8
FSHCC	7 Day	146 (5.75)	21 (0.81)	167 (6.56)	14.4
FSHCC	50 Day	184 (7.23)	87 (3.44)	272 (10.7)	47.3
FSHCC	90 Day	186 (7.32)	81 (3.19)	267 (10.5)	43.5

layer thickness on both of these sections. Thickness of Sections 1, 3, and 5 are nominally 100 mm, 150 mm, and 200 mm, respectively. Comparison of the measured deflections (FSHCC) with respect to testing time shows that the deflection response increased somewhat between Day 7 and Day 50, similar to the trend observed for the North Tangent. This increase with time may be a result of the pavement temperature gradient at the time of testing and/or the beginning of micro- and macro-cracks from excessive shrinkage and curling.

Section 5 had the same surface thickness as the pavement sections on the North Tangent and showed similar increase in deflection variability with time as observed on the North Tangent.

9.5.1.2.2 Layer Moduli

PCC, FSHCC, and subgrade moduli were backcalculated for each test point using ELCON. For the purpose of the analyses, the pavement structure was assumed to be two layers. FSHCC moduli are plotted in Figure 9.22 and are somewhat consistent for Section 5, averaging approximately 38,000 MPa (5,500 ksi), but exhibit relatively large variability within Sections 1 and 3. This is not unexpected given that the reliability of backcalculated moduli from FWD measurements can typically be poor for thin sections. This is related to the measurement geometry, but can also be strongly influenced by construction thickness tolerances. In Section 1, core thicknesses range from 81 mm to 125 mm for a target thickness of 100 mm (4"). South Tangent layer moduli calculated from the deflection data are presented in Table 9.26.

The FSHCC moduli for Sections 1, 3, and 5 all show a fairly significant increase from Day 1 to Day 7. Calculated moduli for the three sections suggest a different response between the sections, as well as some difference from the North Tangent, although Section 5 appears comparable to the North Tangent results. As mentioned earlier, the effects of mix variations during construction need to be considered when interpreting the HWD results. Backcalculated subgrade moduli are shown in Figure 9.23. Inspection of this figure shows generally consistent subgrade response, with an average moduli of 240 MPa (35 ksi).

A comparison of PCC and FSHCC calculated surface moduli for the South Tangent shows a good relationship between the measured values. However, comparing PCC and FSHCC calculated subgrade moduli for the South Tangent suggests a poor relationship between the two values. Variability in the South Tangent subgrade moduli is similar to that of the North Tangent subgrade moduli presented in Table 9.22.

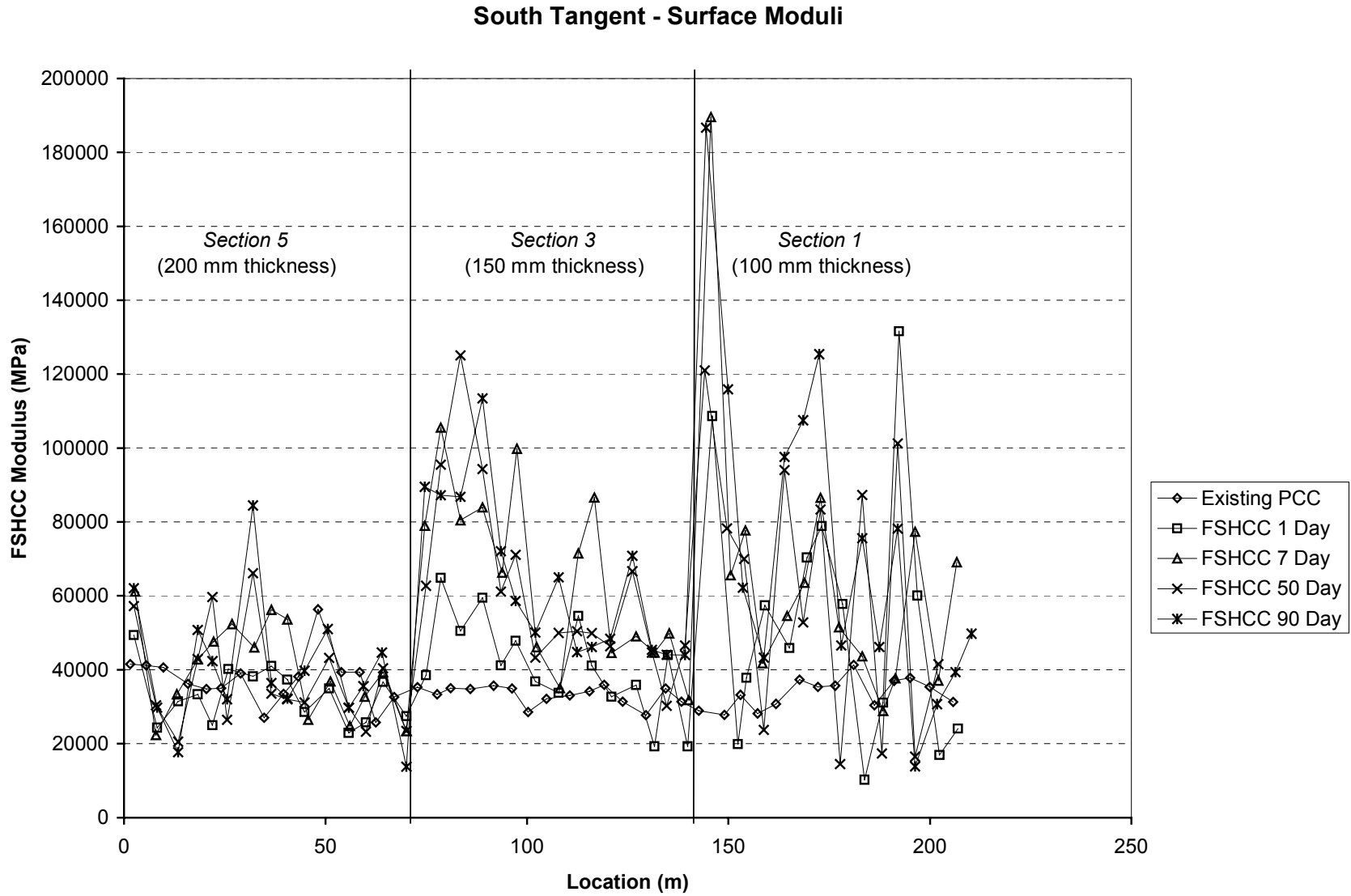


Figure 9.22. Surface Moduli (Backcalculated) for South Tangent.

South Tangent - Subgrade Moduli

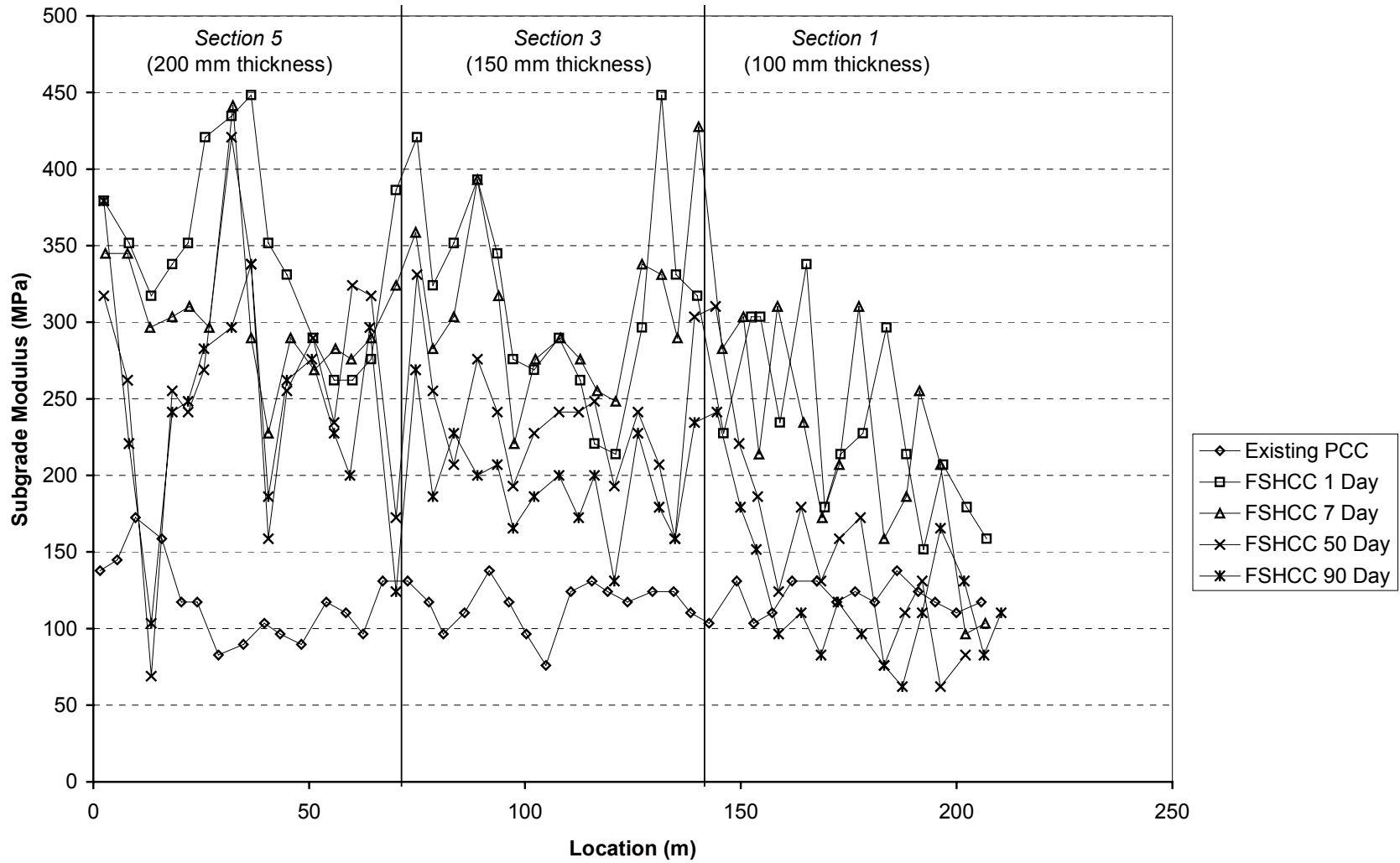


Figure 9.23. Subgrade Moduli (Backcalculated), South Tangent.

Table 9.26 South Tangent Layer Moduli Calculated from the Deflection Data.

Material	Age	PCC and FSHCC Moduli, MPa (ksi)			
		Average	Standard Deviation	84th Percentile	C.O.V., (Percent)
Old PCC	~30 Years	34751 (5039)	5227 (758)	29531 (4282)	15.0
Section 1					
FSHCC	1 Day	53607 (7773)	35255 (5112)	18352 (2661)	65.8
FSHCC	7 Days	66028 (9574)	39628 (5746)	26400 (3828)	60.0
FSHCC	50 Days	61662 (8941)	36241 (5255)	25421 (3686)	58.8
FSHCC	90 Days	74586 (10815)	45262 (6563)	29324 (4252)	60.7
Section 3					
FSHCC	1 Day	41317 (5991)	12972 (1881)	28345 (4110)	31.4
FSHCC	7 Day	64924 (9414)	23641 (3428)	41276 (5985)	36.4
FSHCC	50 Day	62517 (9065)	25090 (3638)	12060 (5427)	40.1
FSHCC	90 Day	64421 (9341)	21648 (3139)	42772 (6202)	33.6
Section 5					
FSHCC	1 Day	33103 (4800)	7531 (1092)	25572 (3708)	22.8
FSHCC	7 Day	39931 (5790)	12717(1844)	27214 (3946)	31.8
FSHCC	50 Day	37331 (5413)	14076 (2041)	23255 (3372)	37.7
FSHCC	90 Day	40152 (5822)	17483 (2535)	22669 (3287)	43.5

Table 9.27 South Tangent Subgrade Moduli Calculated from the HWD Deflection Data.

Material	Age	Subgrade Modulus, MPa (ksi)			
		Average	Standard Deviation	84th Percentile	C.O.V., (Percent)
Old PCC		117 (17)	21 (3)	97 (14)	17.6
Section 1					
	1 Day	234 (34)	55 (8)	172 (25)	23.5
	7 Days	221 (32)	69 (10)	145 (21)	31.3
	50 Days	152 (22)	69 (10)	83 (12)	45.5
	90 Days	124 (18)	48 (7)	76 (11)	38.9
Section 3					
	1 Day	317 (46)	69 (10)	248 (36)	21.7
	7 Days	310 (45)	55 (8)	255 (37)	17.8
	50 Days	234 (34)	41 (6)	193 (28)	17.6
	90 Days	193 (28)	34 (5)	158 (23)	17.9
Section 5					
	1 Day	345 (50)	62 (9)	290 (42)	18.0
	7 Days	303 (44)	48 (7)	255 (37)	15.9
	50 Days	262 (38)	83 (12)	179 (26)	31.6
	90 Days	248 (36)	76 (11)	172 (25)	30.6

The South Tangent subgrade moduli appear to be generally higher than those observed on the North Tangent. This condition may be related to stress sensitivity, but may also be due to differences in depth to bedrock between the sections. The difference in moduli could also be caused by the CTB on the North Tangent having an effect on the subgrade moduli results.

9.5.1.2.3 Joint Evaluation

The FSHCC joint evaluation analyses provides information in terms of calculated modulus of subgrade reaction (k) at the center and joint load transfer efficiency (L.T.E.), for both transverse and longitudinal joints, based on measured deflections. Average values for the calculated modulus of the subgrade reaction are shown in Figure 9.24. It should be noted that joint evaluation analysis results are typically highly dependent on the time of day at which the non-destructive testing was performed due to temperature effects. The L.T.E. information for the North Tangent is summarized in Table 9.28.

Figure 9.25 shows the L.T.E. across the transverse joints on the South Tangent. The L.T.E. for the South Tangent was quite variable. The variability could be a result of variation in slab thickness, slab temperature gradient, and underlying base support. The load transfer efficiency across the transverse joints on the South Tangent averaged approximately 75 percent after one day. By 90 days, the load transfer efficiency had decreased to approximately 50 percent. The low load transfer efficiency, both initially and after 90 days, is consistent with the thinness of the pavement, an aggregate base layer directly under the slab, drying shrinkage of the concrete, and most importantly, the absence of dowels at the joints. The L.T.E. at 90 days for the

South Tangent - Modulus of Subgrade Reaction

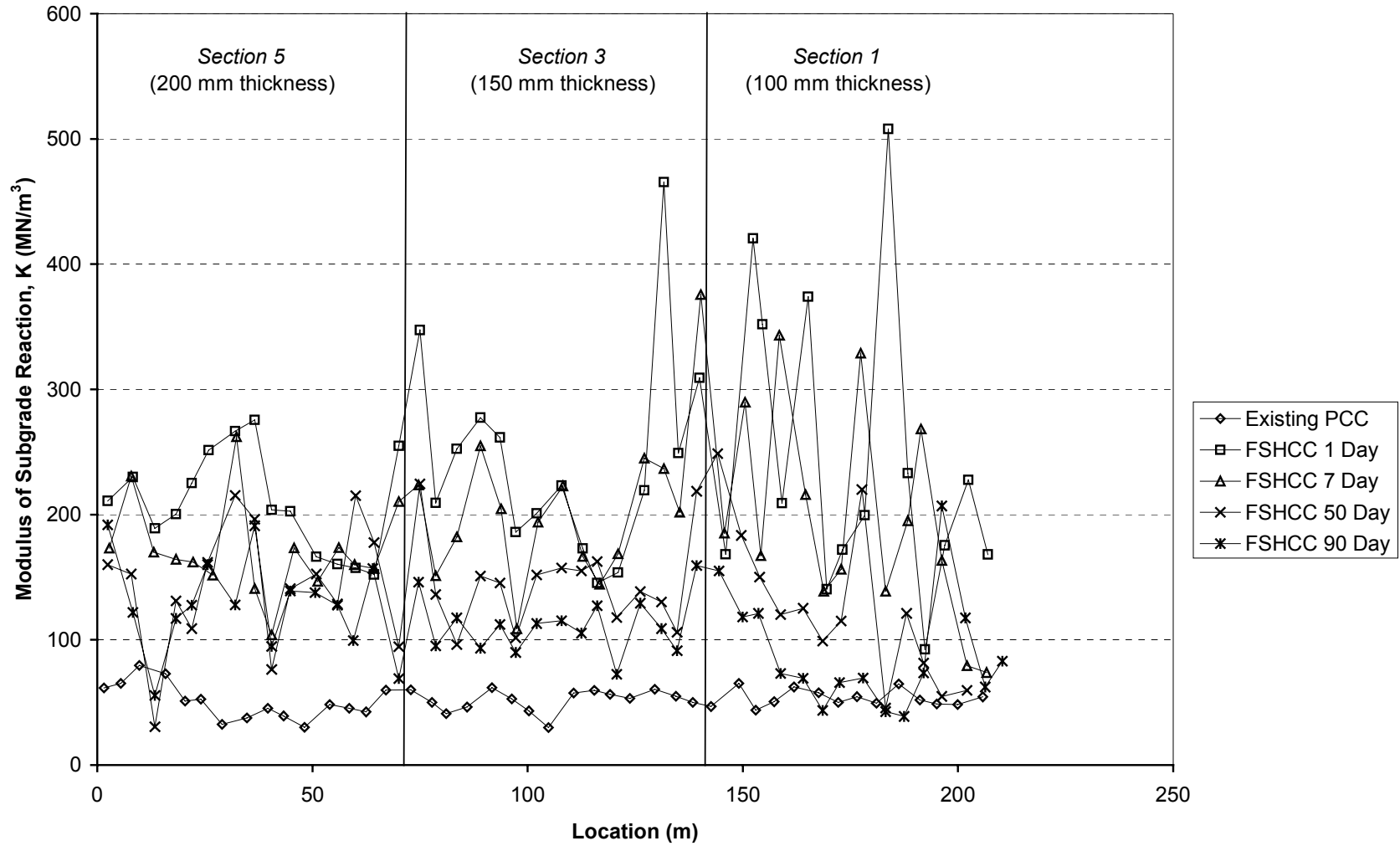


Figure 9.24. South Tangent Modulus of Subgrade Reaction.

South Tangent Transverse Joint Load Transfer Efficiency

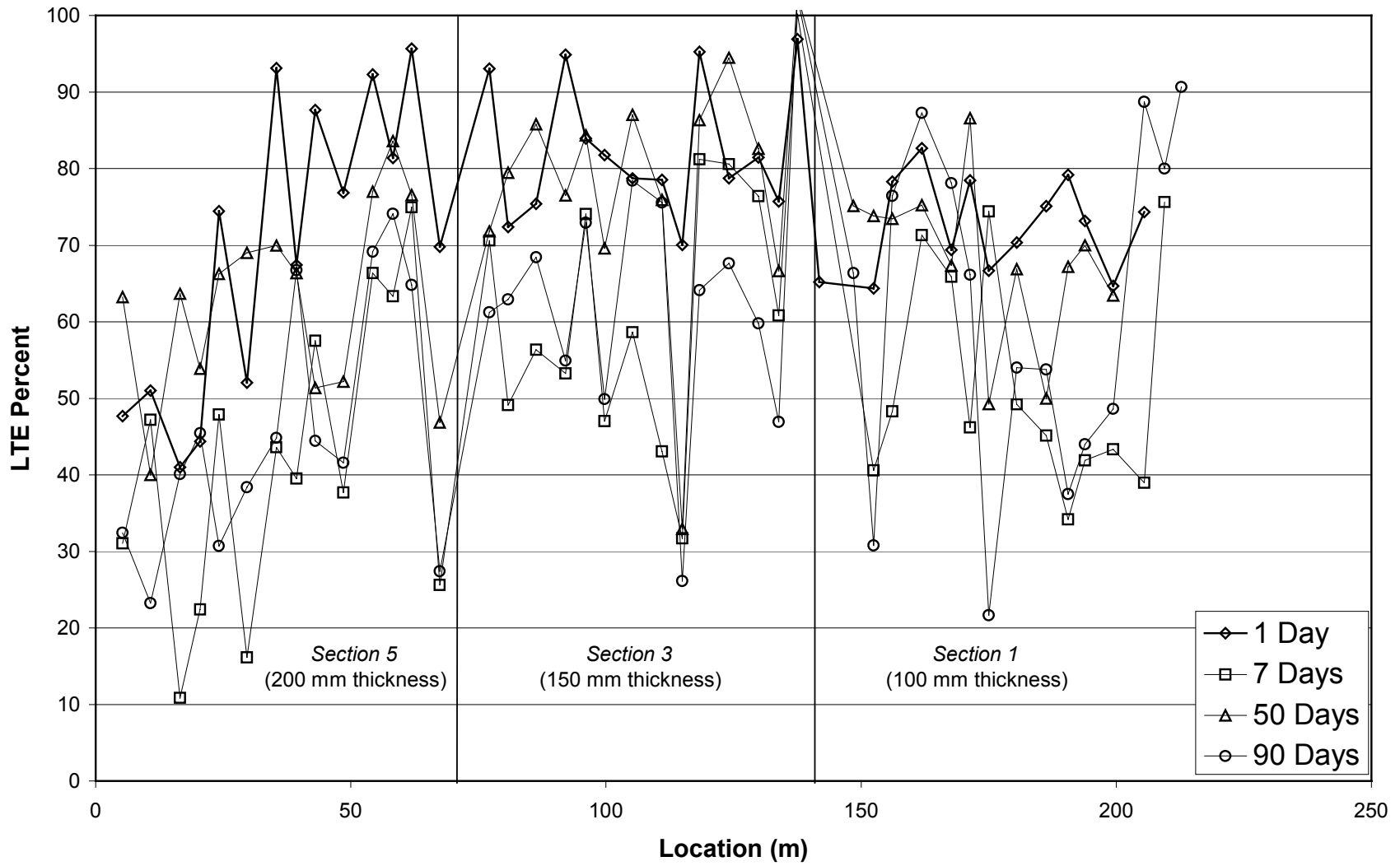


Figure 9.25. South Tangent Transverse Joint Load Transfer Efficiency.

Table 9.28 South Tangent Joint Load Transfer Efficiencies.

		Average Values of Joint Response	
		k_{center} , MN/m ³ (pci)	L.T.E., Percent Transverse
Old PCC ⁽¹⁾	~30 Years	52 (191)	No Test
Section 1			
FSHCC	1 Day	246 (904)	73
FSHCC	7 Days	196 (721)	52
FSHCC	50 Days	125 (460)	68
FSHCC	90 Days	89 (329)	40
Section 3			
FSHCC	1 Day	245 (901)	81
FSHCC	7 Days	205 (756)	63
FSHCC	50 Days	146 (538)	78
FSHCC	90 Days	112 (411)	64
Section 5			
FSHCC	1 Day	210 (772)	70
FSHCC	7 Days	172 (633)	42
FSHCC	50 Days	143 (525)	63
FSHCC	90 Days	128 (470)	46

1) No joint tests were taken on Route 14 existing PCC slabs.

South Tangent was similar to the L.T.E. measured on Section 7 of the North Tangent (200 mm without dowels).

9.5.2 Summary of HWD Results

Nondestructive testing of the Palmdale test sections with the HWD has demonstrated high variability in the all the pertinent pavement parameters. The subgrade modulus (k-value), concrete elastic moduli, and the load transfer efficiency (L.T.E.) across transverse and longitudinal joints all had high coefficients of variation. The main contributors to this variability in HWD test data were the variation in thickness of the slabs, variation in the FSHCC placed from each concrete truck, and the variation in support directly under the FSHCC. Further

complications to these variables are the high occurrence of transverse cracking on the Palmdale test sections. It is believed that this cracking was a result of drying shrinkage and curling. HWD results could have been affected by progressing microcracks not seen yet on the concrete surface.

The joint evaluation on the South and North tangent using the HWD results indicates that doweled transverse joints perform significantly better in terms of L.T.E. over time than do plain joints relying on aggregate interlock. Steel reinforcement bars used to tie adjacent concrete lanes did not significantly improve the L.T.E. across the joint, especially at the mid-slab edge. However, on slabs with tie bars there was a slight improvement in L.T.E. at the slab corner compared to untied longitudinal joints.

9.6 Field Core and Strength Testing

In order to verify the thickness and strength of all HVS test sections, coring and compressive strength testing was conducted. As shown in Appendix A, there are 4 HVS test sites in each test section, for a total of 24 potential HVS tests. A core was taken from each slab on which an HVS test was planned. The core was taken about 1 m from the non-loaded slab edge. The core diameters were nominally 100 mm for all test sections. Table 9.29 shows the location of each core and the measured core thickness. Note that the measured core thicknesses varied greatly from the target thicknesses. The average core thickness was 8 percent greater than the design thickness. This average thickness had a 10.5 percent standard deviation and a 137 percent coefficient of variation. This large variation indicates that the thickness of the constructed slabs could vary as much as 30 percent from the design thickness. This variation in core thickness was most likely the reason for the high variability found in all the HWD results.

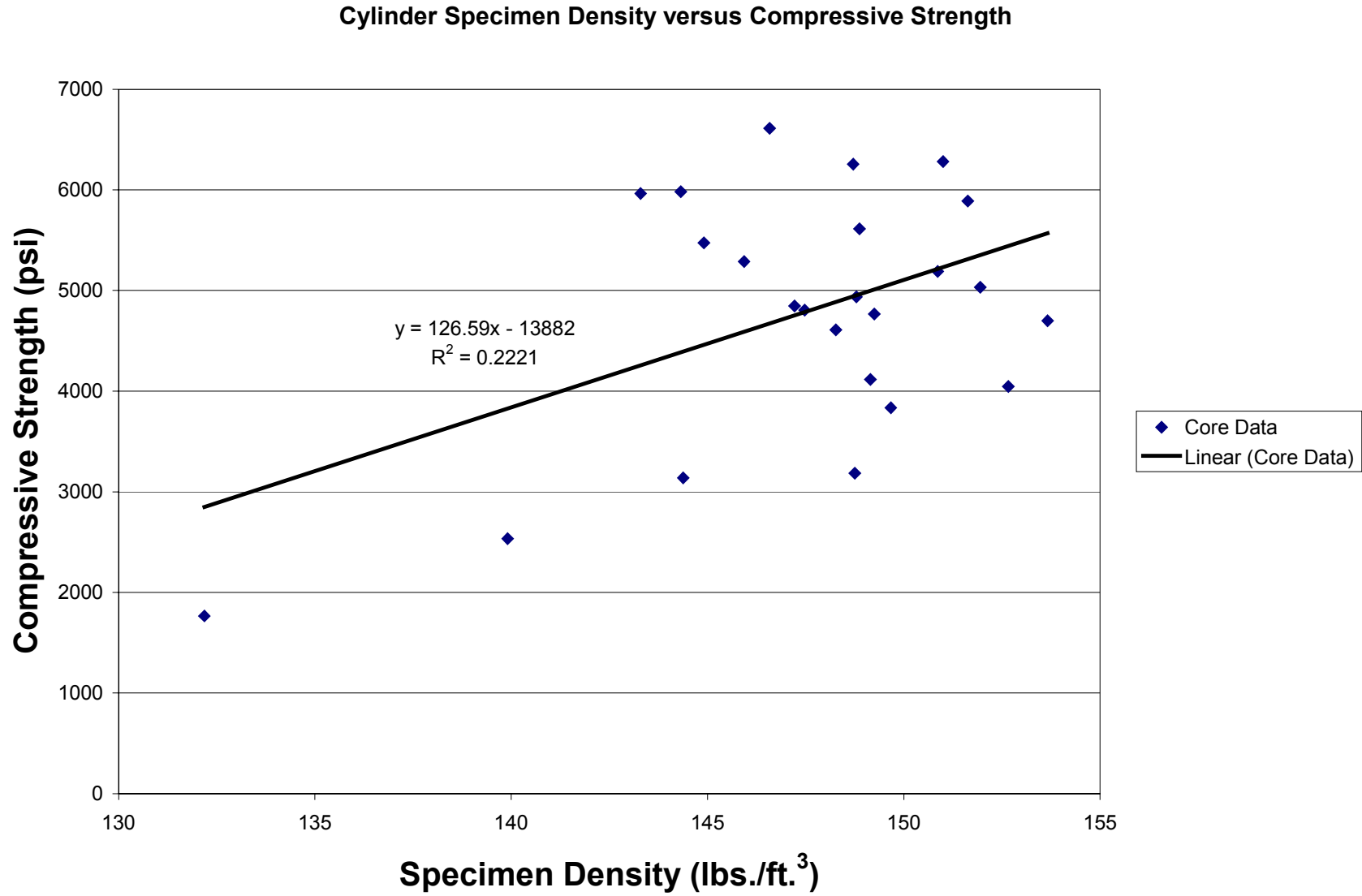


Figure 9.26. Cylinder Specimen Density versus Compressive Strength.

Table 9.29 Core Thickness and Compressive Strength for Palmdale HVS Sections

Core Number	Slab Number	Location	Core Dimensions		Design Thickness (in. [mm])	Thickness Deviation (Percent)	Density of Core (lbs./ft3 [g/cm3])	Corrected Compression Strength (psi [MPa])
			Diameter (in. [mm])	Length (in. [mm])				
1A-4	4	South 1-A	3.9 (99)	3.2 (81.25)	4 (101.6)	-20.0	145 (2.32)	5474 (37.74)
1B-8	8	South 1-B	3.94 (100)	4.33 (110)	4 (101.6)	8.3	150 (2.4)	3835 (26.44)
1C-12	12	South 1-C	3.91 (99.37)	4.9 (124.5)	4 (101.6)	22.5	148 (2.38)	4610 (31.78)
1D-14	14	South 1-D	3.92 (99.62)	4.47 (113.5)	4 (101.6)	11.7	149 (2.39)	4116 (28.37)
3A-17	17	South 3-A	3.88 (98.5)	5.93 (150.5)	6 (152.4)	-1.2	132 (2.12)	1767 (12.19)
3B-20	20	South 3-B	3.91 (99.37)	6.54 (166)	6 (152.4)	8.9	149 (2.38)	3186 (21.97)
3C-25	25	South 3-C	3.95 (100.37)	5.33 (135.5)	6 (152.4)	-11.1	147 (2.35)	6611 (45.58)
3D-28	28	South 3-D	3.95 (100.37)	7.87 (200)	6 (152.4)	31.2	149 (2.38)	4937 (34.04)
5A-32	32	South 5-A	3.93 (99.75)	7.72 (196)	8 (203.2)	-3.5	146 (2.34)	5288 (36.46)
5B-36	36	South 5-B	3.93 (99.75)	8.54 (217)	8 (203.2)	6.8	153 (2.45)	4046 (27.89)
5C-40	40	South 5-C	3.91 (99.25)	8.96 (227.5)	8 (203.2)	12.0	152 (2.43)	5034 (34.7)
5D-44	44	South 5-D	3.97 (100.75)	8.07 (205)	8 (203.2)	0.9	144 (2.31)	3140 (21.65)
7A-32	32	North 7-A	3.92 (99.62)	8.64 (219.5)	8 (203.2)	8.0	154 (2.46)	4700 (32.4)
7B-35	35	North 7-B	3.93 (99.75)	8.96 (227.5)	8 (203.2)	12.0	144 (2.31)	5983 (41.25)
7C-39	39	North 7-C	3.92 (99.62)	8.66 (220)	8 (203.2)	8.3	140 (2.24)	2534 (17.47)
7D-43	43	North 7-D	3.91 (99.25)	9.33 (237)	8 (203.2)	16.6	147 (2.36)	4806 (33.14)
9A-27	27	North 9-A	3.93 (99.75)	8.64 (219.5)	8 (203.2)	8.0	147 (2.36)	4847 (33.42)
9B-20	20	North 9-B	3.97 (100.87)	8.7 (221)	8 (203.2)	8.8	149 (2.38)	5613 (38.7)
9C-23	23	North 9-C	3.95 (100.37)	8.38 (212.75)	8 (203.2)	4.7	143 (2.3)	5964 (41.12)
9D-17	17	North 9-D	3.94 (100)	9.06 (230)	8 (203.2)	13.2	152 (2.43)	5888 (40.6)
11A-3	3	North 11-A	3.96 (100.5)	9.59 (243.5)	8 (203.2)	19.8	149 (2.39)	4766 (32.86)
11B-7	7	North 11-B	3.94 (100)	8.78 (223)	8 (203.2)	9.7	151 (2.42)	6281 (43.31)
11C-11	11	North 11-C	3.94 (100)	7.99 (203)	8 (203.2)	-0.1	151 (2.42)	5189 (35.77)
11D-14	14	North 11-D	3.92 (99.5)	8.66 (220)	8 (203.2)	8.3	149 (2.38)	6257 (43.14)
					<i>average</i>	<i>7.7</i>		
					<i>std. dev.</i>	<i>10.5</i>		
					<i>C.O.V.</i>	<i>137</i>		

Table 9.29 also shows the corrected compressive strength of the core and its density. The density of each core was measured to determine if core density would correlate to core strength. Figure 9.26 shows there was not a significant relationship between core density and compressive strength.

Early Age Concrete Properties

The presentation of early age concrete properties based on instrumentation data will be presented in a separate technical memorandum. This memorandum will look at the early age data taken from thermocouples, dynamic strain gages, length change gages, and dowel strain gages.

9.7 Initial Pavement Evaluation

Most sawed joints cracked before Pavement Research Center personnel left the construction site. An initial pavement survey did not reveal any environmentally induced surface cracks immediately after construction. There were several small corner cracks on the South Tangent, most likely due to construction equipment.

9.8 Long-Term Flexural and Compressive Strength Results

Beams and cylinders from Section 7 were sampled for long-term strength tests. Beam results showed no strength gain between 90 days and 575 days. The average strength for both 90 days and 575 days was 754 psi (5.20 MPa), as presented in Appendix C.

For three cylinders tested from Section 7, compressive strengths were found to have increased by only about 5 percent from 90 days [7007 psi (48.3 MPa)] to 625 days [7258 (50.08 MPa) psi (50.9 MPa)]. The results are presented in Appendix C.

10.0 CONCLUSION

Construction of the FSHCC test sections in Palmdale was completed in mid-June of 1998 with the successful installation of all instrumentation by PRC personnel. All gages survived the construction of the test sections with FSHCC with the exception of one thermocouple. The South Tangent concrete placement took two days while the North Tangent took three days.

Based on Caltrans beam strength (flexural) testing conducted on beams sampled from the Palmdale test sections, no beams tested met the strength requirements of 400 psi (2.76 MPa) at 8 hours set forth in the “Notice to Contractors and Special Provisions” (4). Furthermore, only 20 percent of the beams met the strength requirement of 600 psi (4.14 MPa) at 7 days. The average 90-day strength taken from PRC testing was 754 psi (5.20 MPa). Although the short-term strengths would not be acceptable in a project with trafficking 8 hours after construction, the 90-day strength (long-term) achieved at Palmdale is advantageous for long-life pavements. It should be emphasized that the strength results obtained from the PRC should not be used to determine whether the Palmdale special provision beam strength requirements were met. The PRC used a beam dimension and loading configuration other than the Caltrans standard test 523.

The FSHCC water-to-cement ratio at Palmdale was most likely the primary reason the 8-hour strength did not meet specification. Additionally, lower initial strengths may have been caused by other factors such as curing time, curing temperature, admixture variability, test type variability, cement variability, and dry mix batching. Another major issue to address in future projects that utilize FSHCC is the quick buildup of FSHCC material in the concrete trucks.

An attempt was made to correlate FSHCC beam and cylinder strength data taken from the Palmdale test site. The results showed that there was a correlation between beam and cylinder

strength data for the Palmdale FSHCC mix. The correlation between beam and cylinder strength was especially strong at 8 hours and 7 days of testing. At 90 days, there was a high variance in the data and no correlation could be established. Caution should be used when applying this correlation to other concrete mixes. Further laboratory testing is required to determine if this correlation is valid for other FSHCC mixes.

Cores taken from 24 slabs on the South and North Tangent demonstrated that the average thicknesses for the slabs was 8 percent greater than design. The coefficient of variation for the core thickness results was 137 percent. From the core results it can be concluded that there was a very high variability in thickness of the pavement from the target value.

HWD results at different pavement ages have shown that dowel bars at the transverse joints have a higher load transfer efficiency (L.T.E.) than do plain joints with aggregate interlock only. L.T.E. results across the longitudinal joints did not show a significant difference between tie bars and no tie bars, except for a slight improvement at the slab corner.

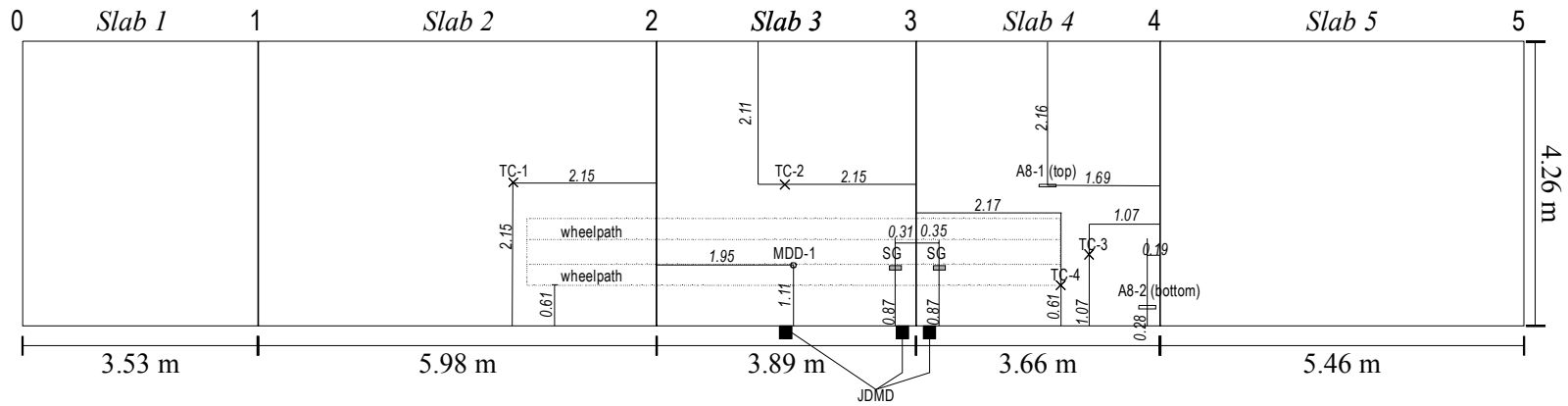
REFERENCES

1. Harvey, J., Roesler, J., Farver, J., and Liang, L., (1998), *Preliminary Evaluation of Proposed LLPRS Rigid Pavement Structures and Design Inputs*, Draft Report for California Department of Transportation, Pavement Research Center, 206 pp.
2. CAL/APT Contract Team. April, 1998. *Test Plan for CAL/APT Goal LLPRS—Rigid Phase III*. Report prepared for the California Department of Transportation. Pavement Research Center.
3. Smith, K. D., Wade, M. J., Peshkin, D. G., Khazanovich, L., Yu, H. T., and Darter, M. I., (1996), *Performance of Concrete Pavements Volume II – Evaluation of Inservice Concrete Pavements*, FHWA Contract No. DTFH61-91-C-00053, 330 pp.
4. Caltrans, “Notice to Contractors and Special Provisions for Construction on State Highway in Los Angeles County ...” Contract No. 07-180404, Sept. 1997.
5. *Standard Specifications*, State of California, Department of Transportation, Sacramento, CA, July 1995.
6. Laboratory testing at Caltrans indicates that test CT 523 yields results approximately five percent higher than those obtained from test ASTM C 78-94, personal conversation with Ric Maggenti of Translab.
7. Lindner, C. P. and Sprague, J. C. (1955), “Effect of Depth of Beam Upon the Modulus of Rupture of Plain Concrete,” *Proceedings, ASTM*, Vol. 55, p. 1062.
8. Kellerman, W. F. (1933), “Effect of Size of Specimen, Size of Aggregate, and Method of Loading Upon the Uniformity of Flexural Strength Tests,” *Public Roads*, Vol. 13, No. 11, January.
9. Tucker Jr., J (1941), “Statistical Theory of the Effect of Dimensions and of Method of Loading Upon the Modulus of Rupture of Beams,” *Proceedings, ASTM*, Vol. 41, p. 1072.
10. Walker, S. and Bloem, D. L. (1957b), “Studies of Flexural Strength of Concrete - Part 3: Effects of Variations in Testing Procedures,” *Proceedings, ASTM*, Vol. 57, pp. 1122-1139.
11. Erlin, Hime Associates, X-Ray Diffraction of Cement, July 1998.

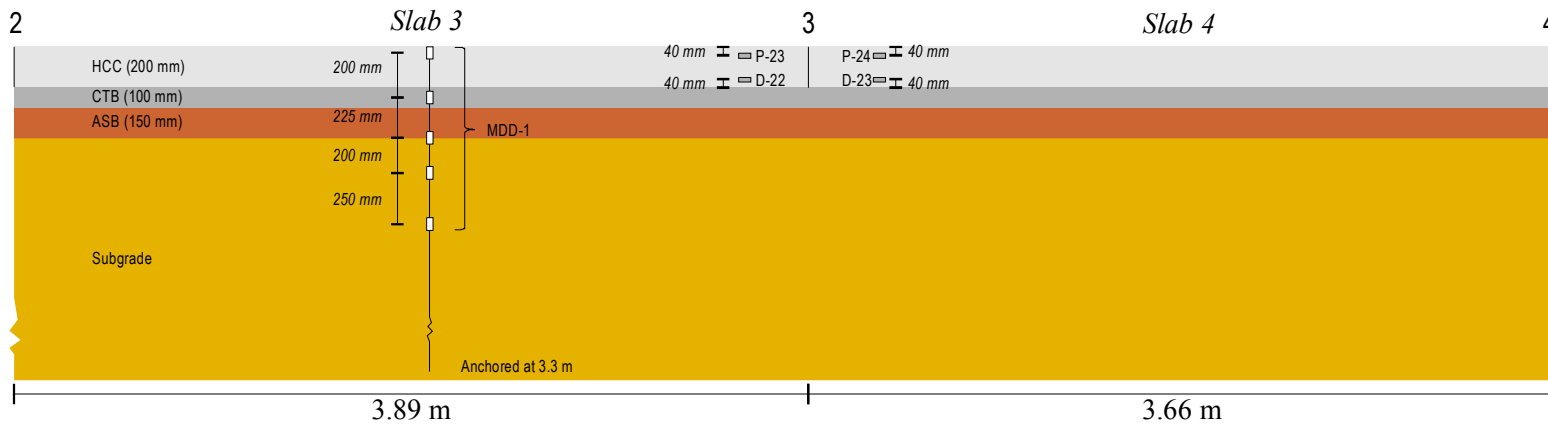
APPENDIX A: INSTRUMENTATION LOCATIONS FOR NORTH AND SOUTH TANGENTS

Section 11-A, North Tangent

Plan View of Test Area showing Instrument Locations (1:100 scale)

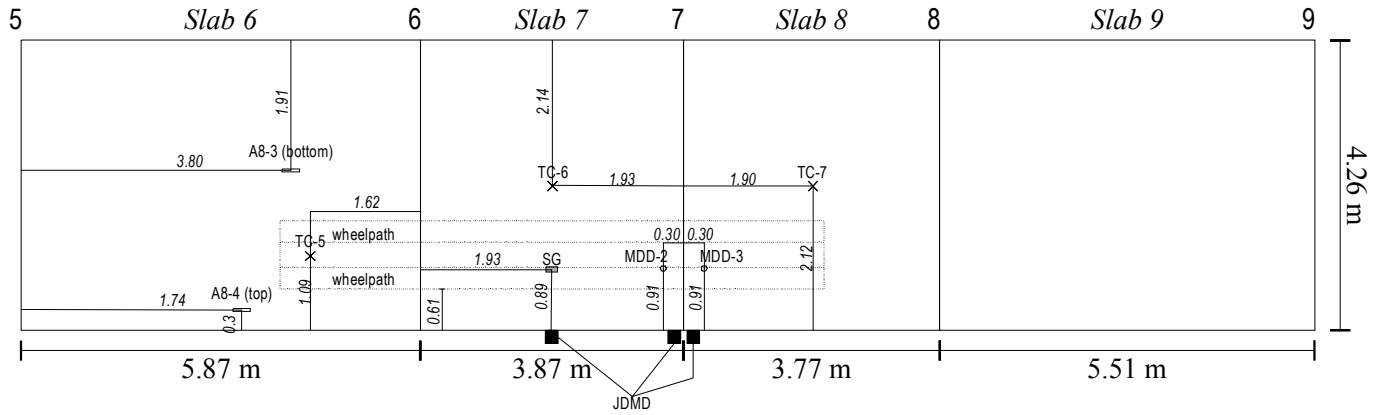


Cross-section View of Test Area (1:300 scale)

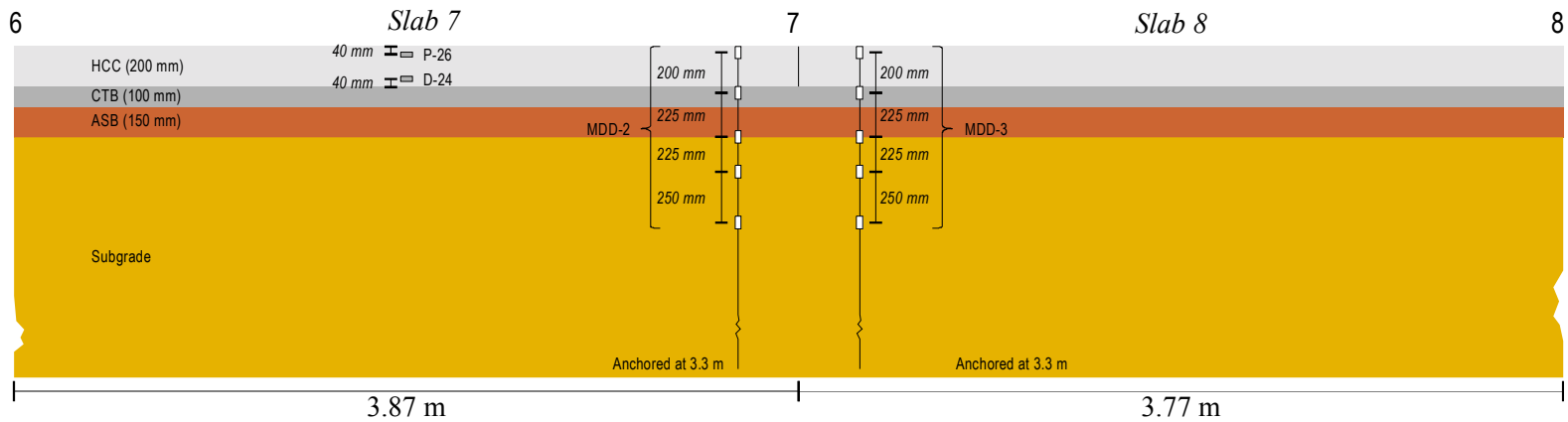


Section 11-B, North Tangent

Plan View of Test Area showing Instrument Locations (1:100 scale)

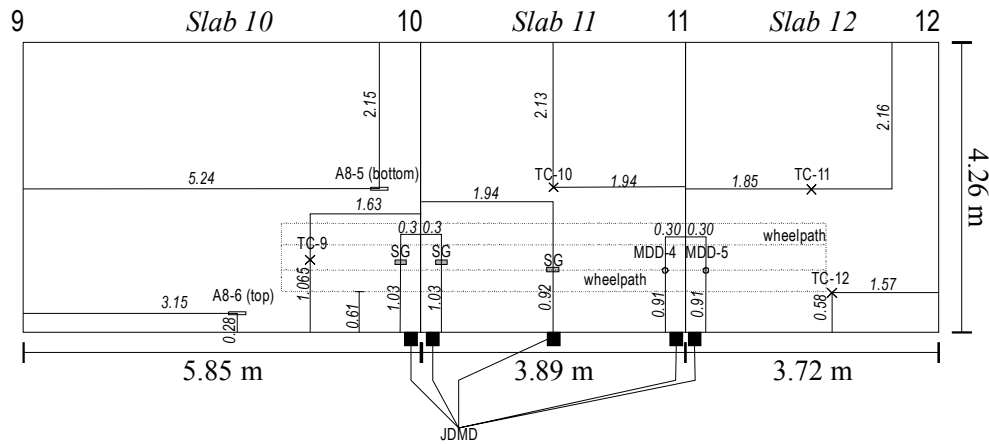


Cross-section View of Test Area (1:300 scale)

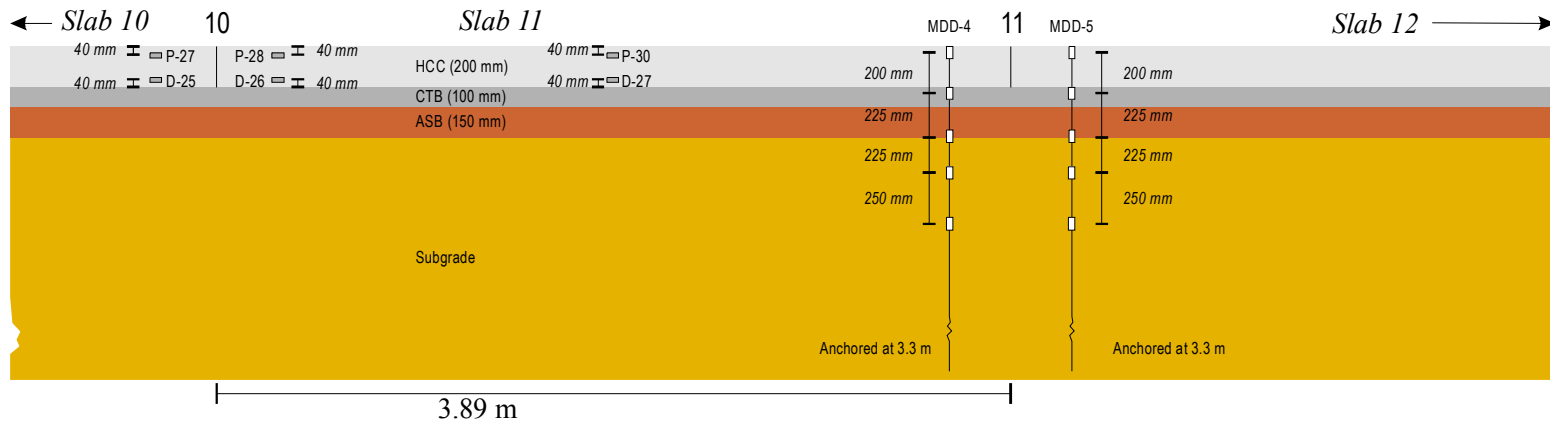


Section 11-C, North Tangent

Plan View of Test Area showing Instrument Locations (1:100 scale)

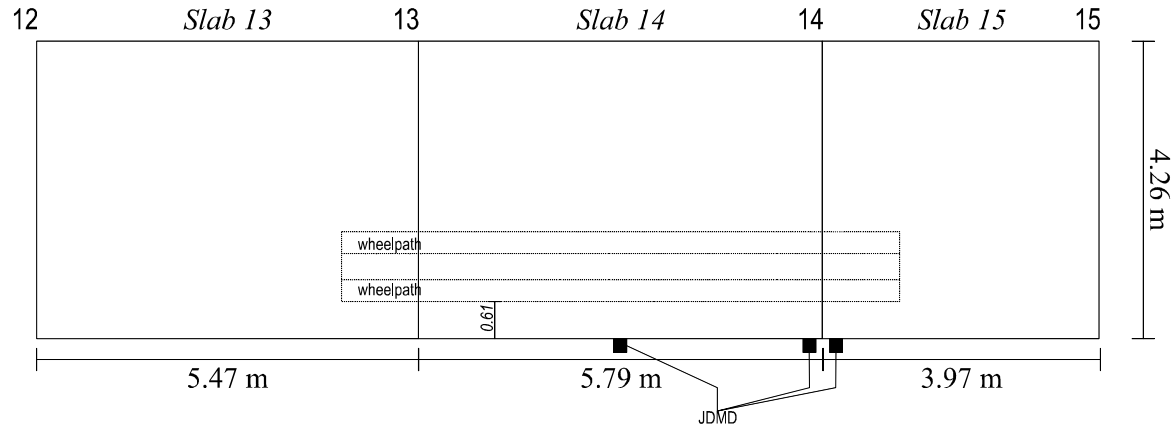


Cross-section View of Test Area (1:300 scale)

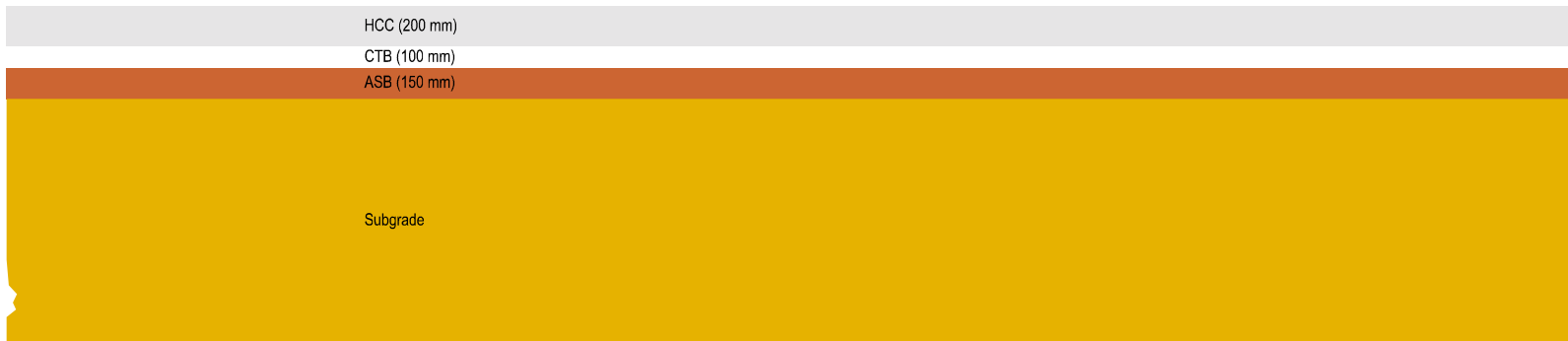


Section 11-D, North Tangent

Plan View of Test Area showing Instrument Locations (1:100 scale)

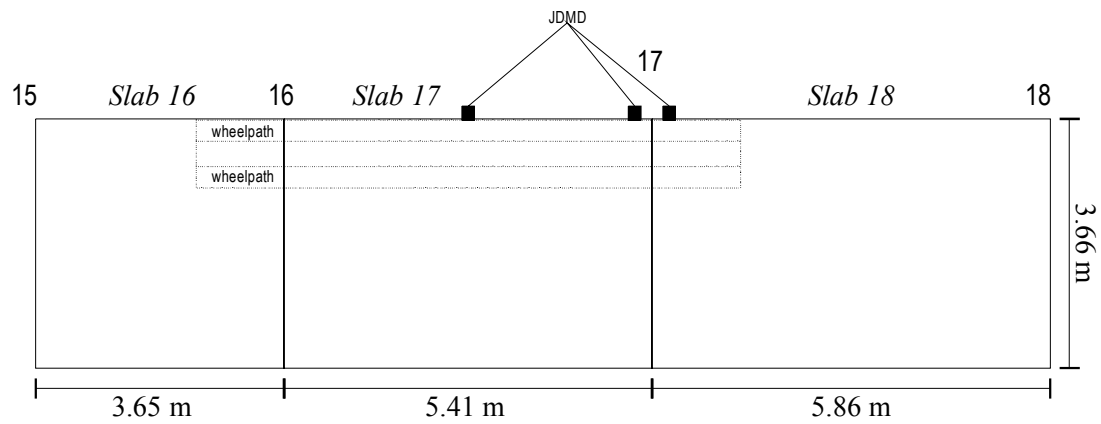


Cross-section View of Test Area (1:300 scale)

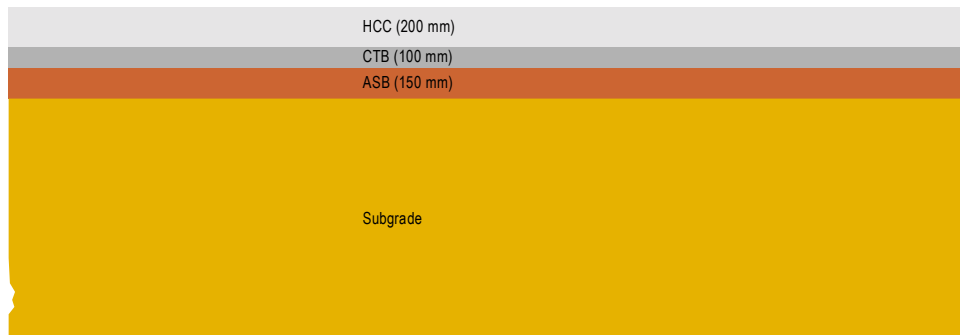


Section 9-D, North Tangent

Plan View of Test Area showing Instrument Locations (1:100 scale)

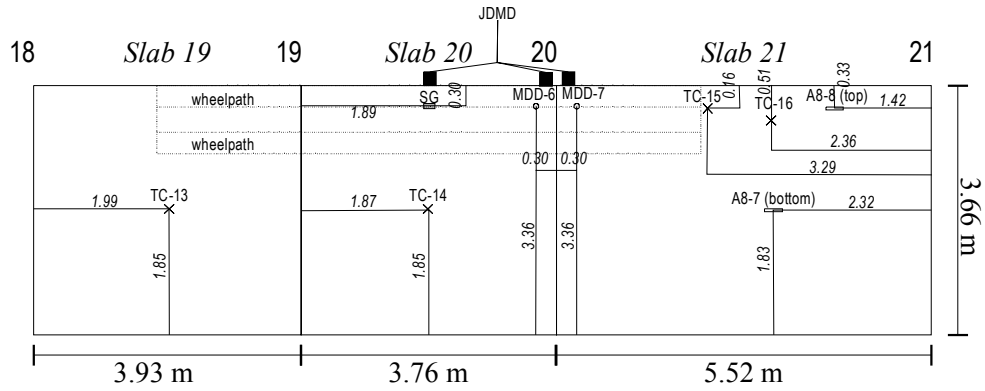


Cross-section View of Test Area (1:300 scale)

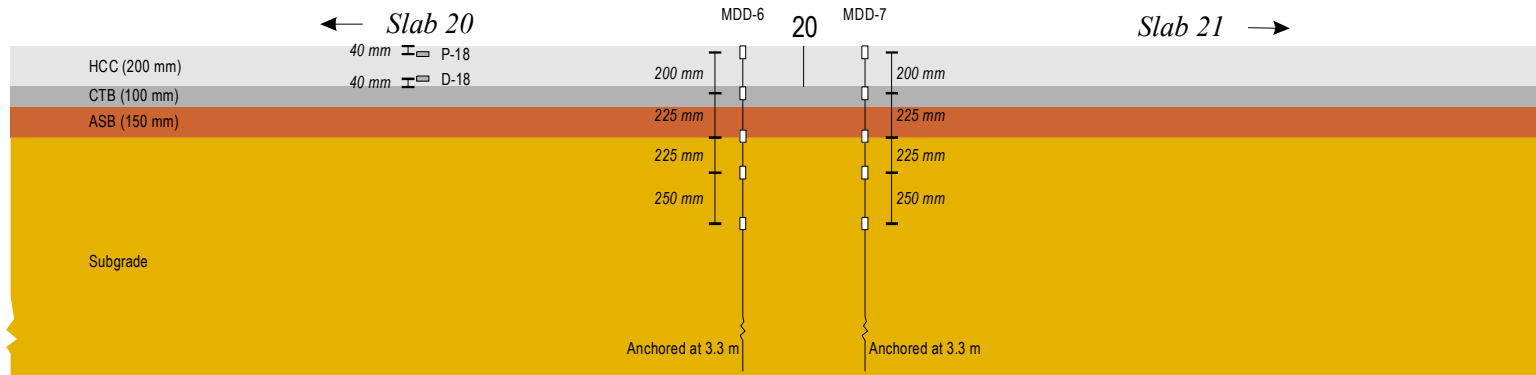


Section 9-B, North Tangent

Plan View of Test Area showing Instrument Locations (1:100 scale)

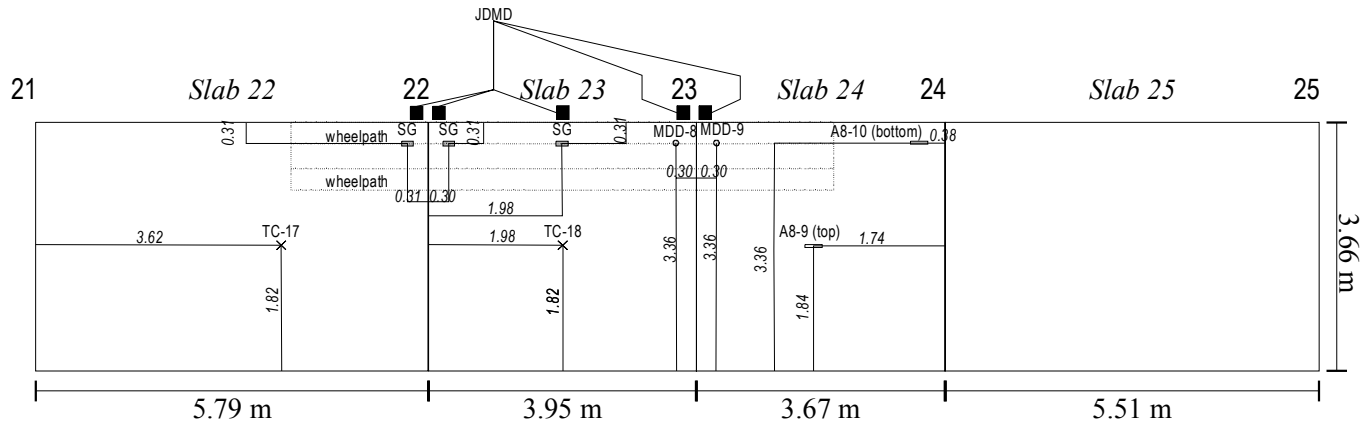


Cross-section View of Test Area (1:300 scale)

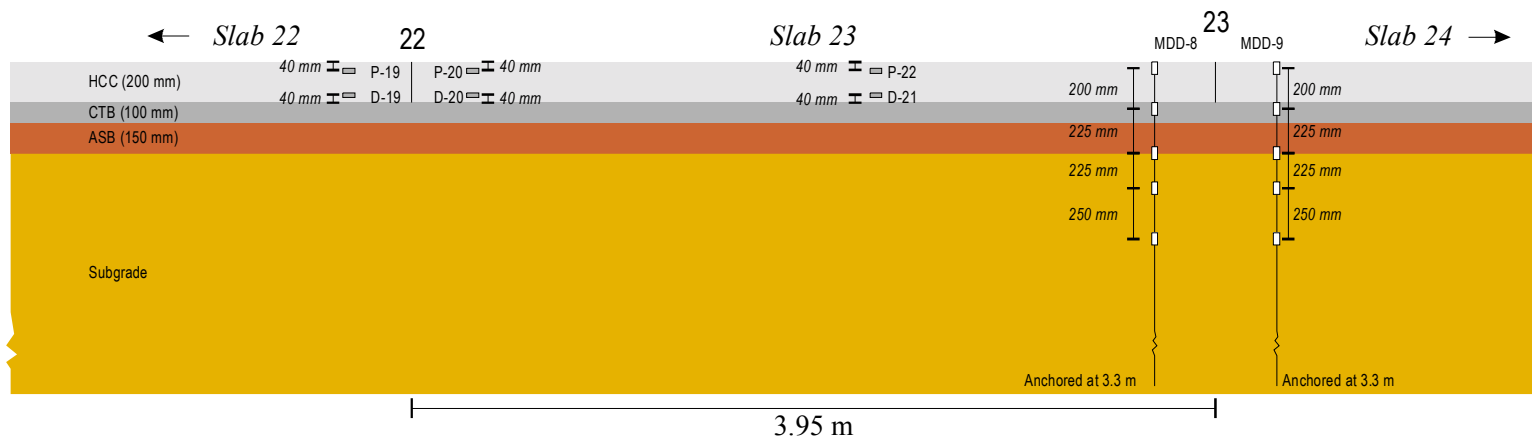


Section 9-C, North Tangent

Plan View of Test Area showing Instrument Locations (1:100 scale)

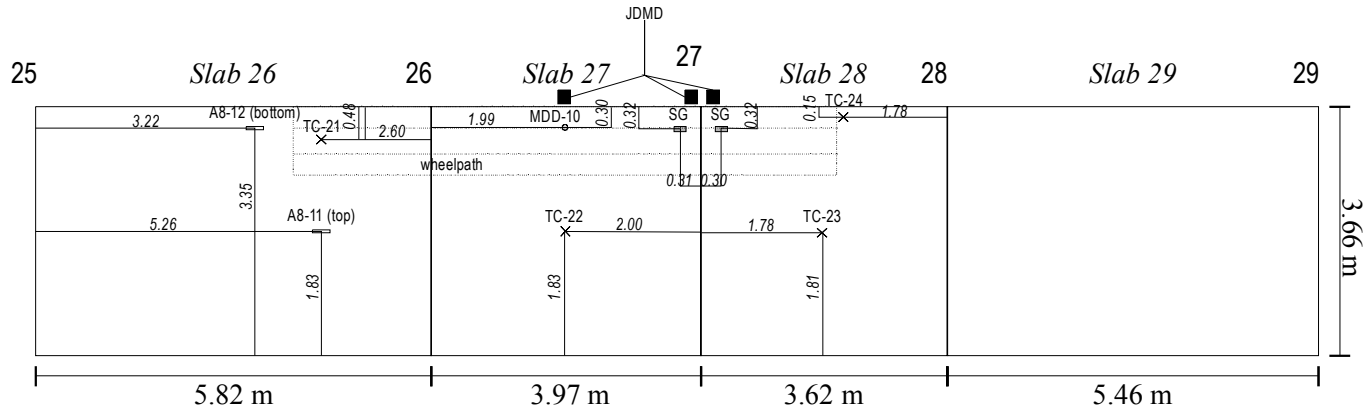


Cross-section View of Test Area (1:300 scale)

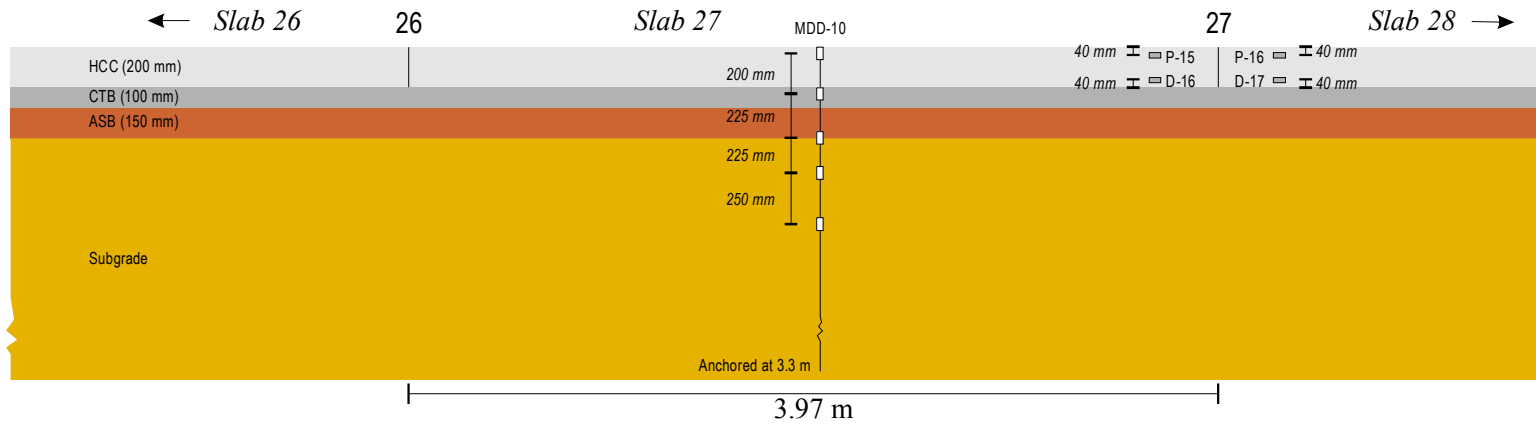


Section 9-A, North Tangent

Plan View of Test Area showing Instrument Locations (1:100 scale)

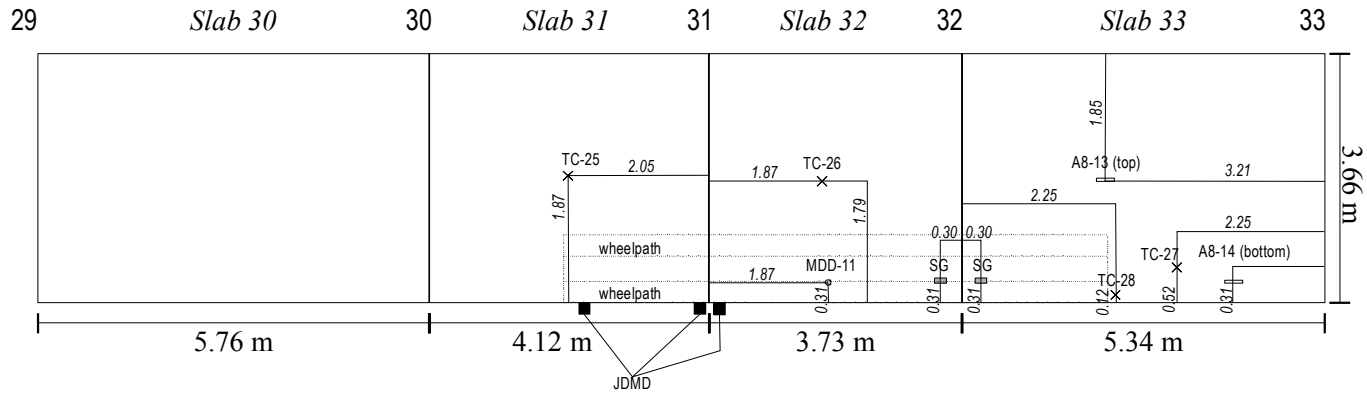


Cross-section View of Test Area (1:300 scale)

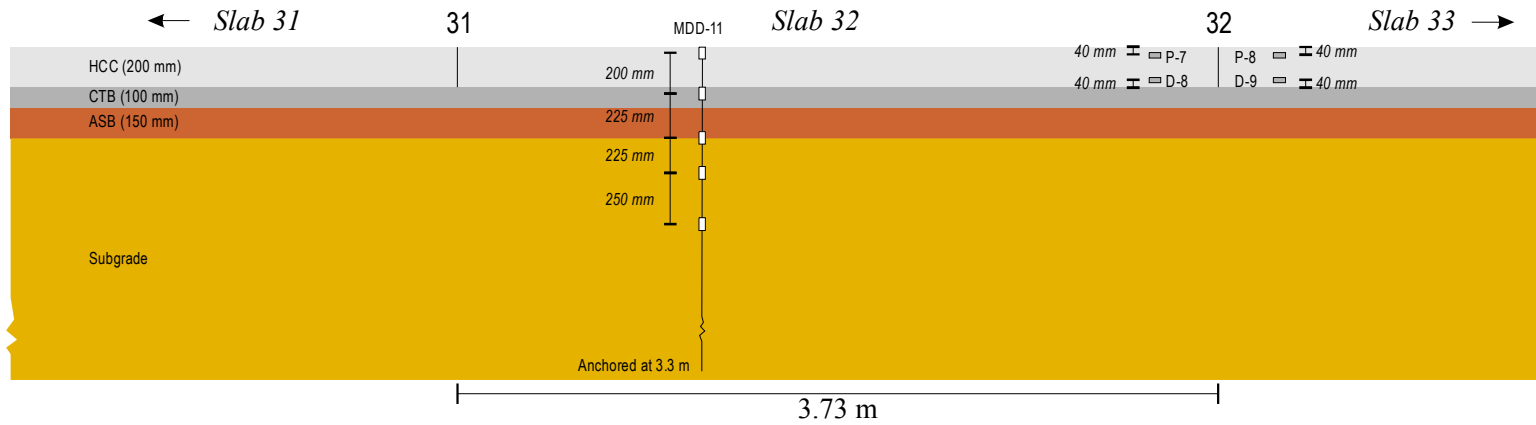


Section 7-A, North Tangent

Plan View of Test Area showing Instrument Locations (1:100 scale)

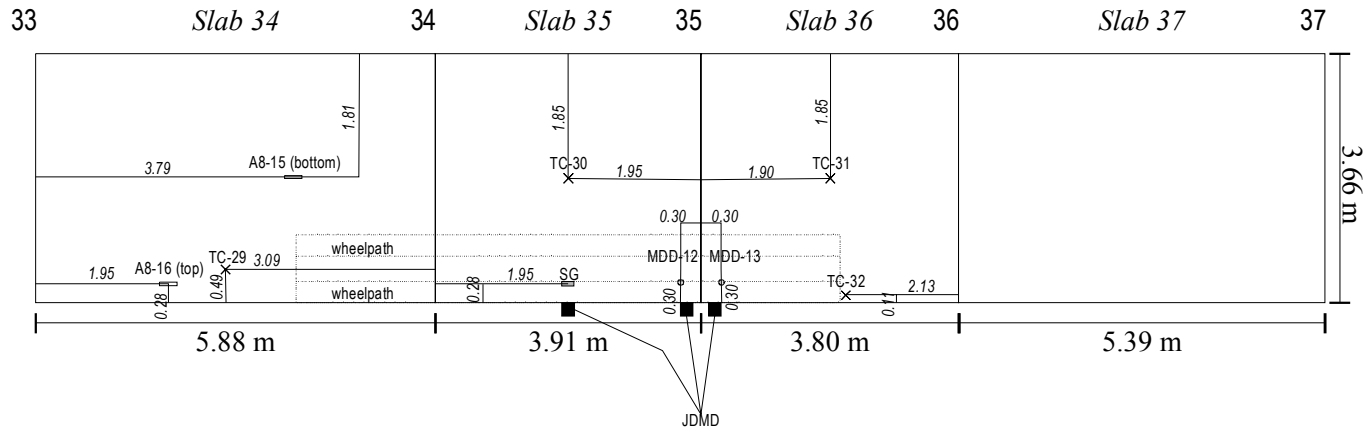


Cross-section View of Test Area (1:300 scale)

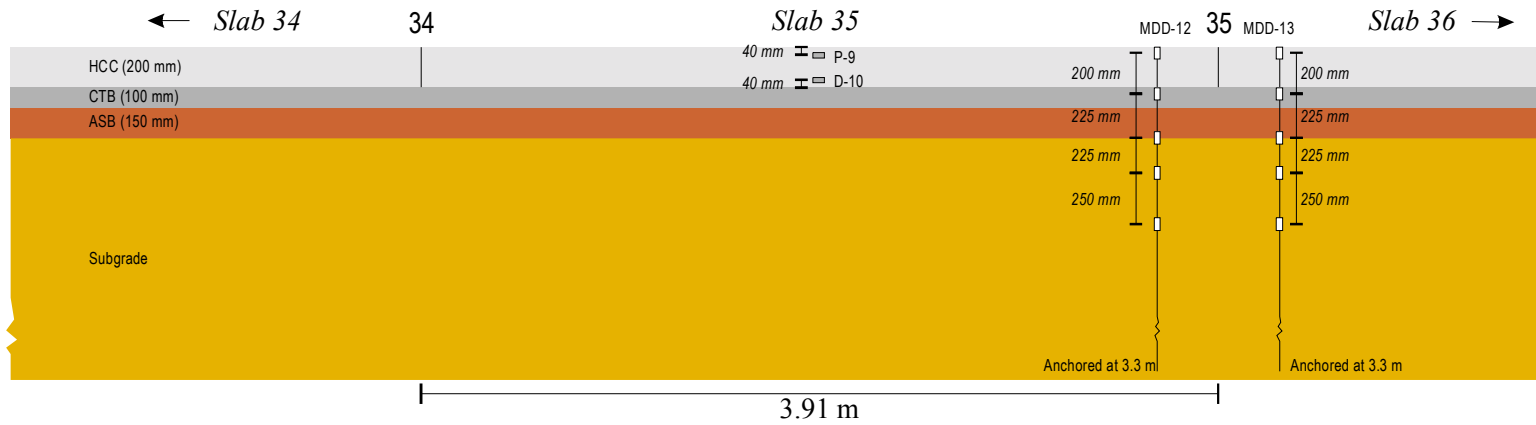


Section 7-B, North Tangent

Plan View of Test Area showing Instrument Locations (1:100 scale)

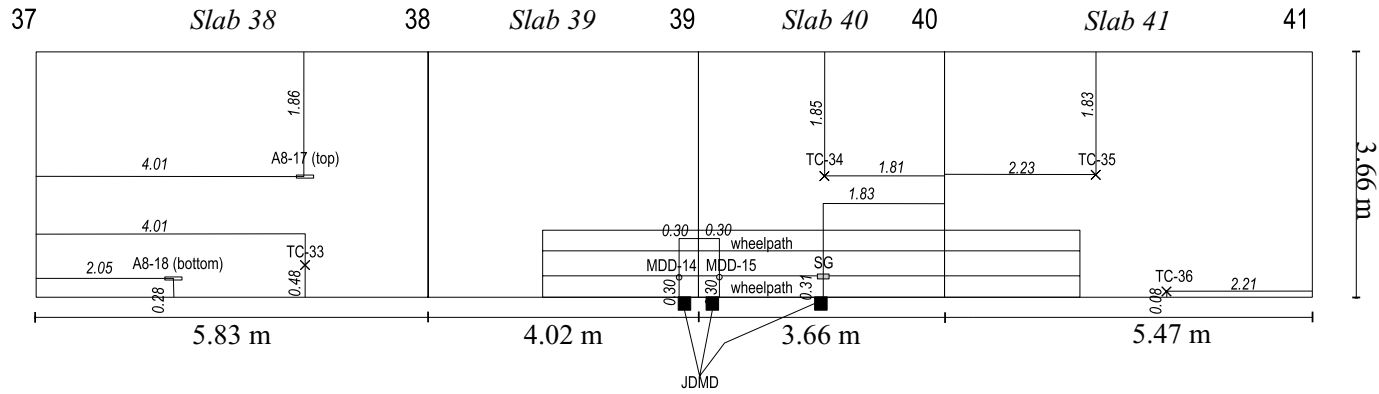


Cross-section View of Test Area (1:300 scale)

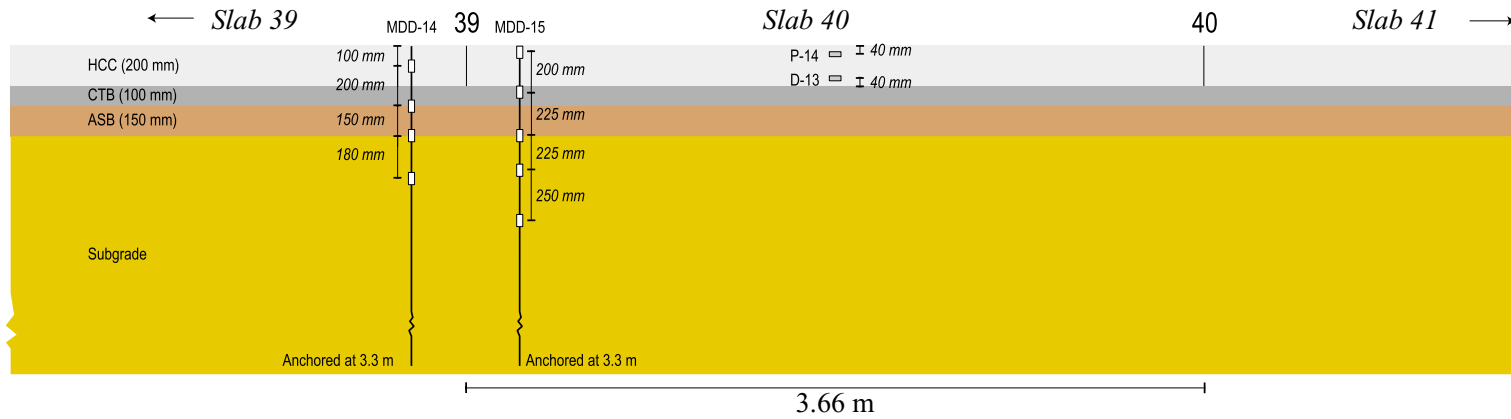


Section 7-C, North Tangent

Plan View of Test Area showing Instrument Locations (1:100 scale)

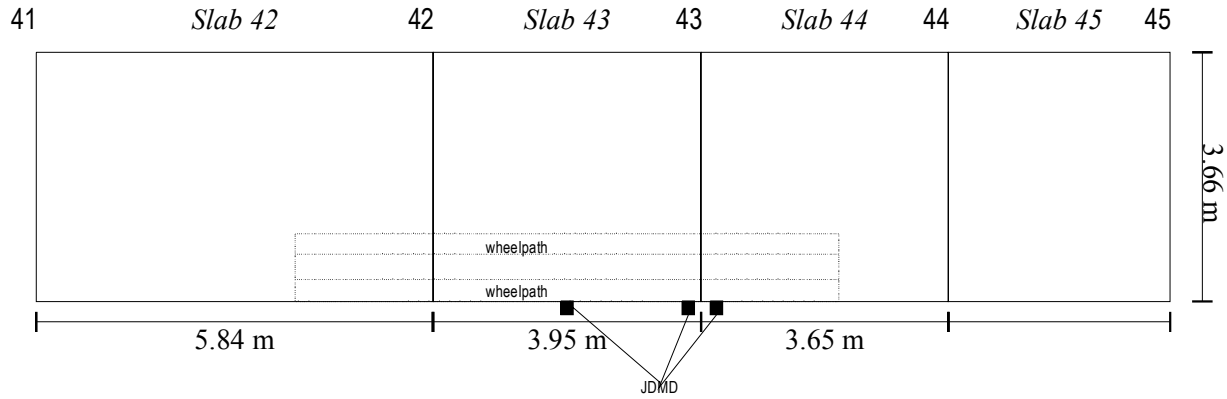


Cross-section View of Test Area (1:300 scale)



Section 7-D, North Tangent

Plan View of Test Area showing Instrument Locations (1:100 scale)

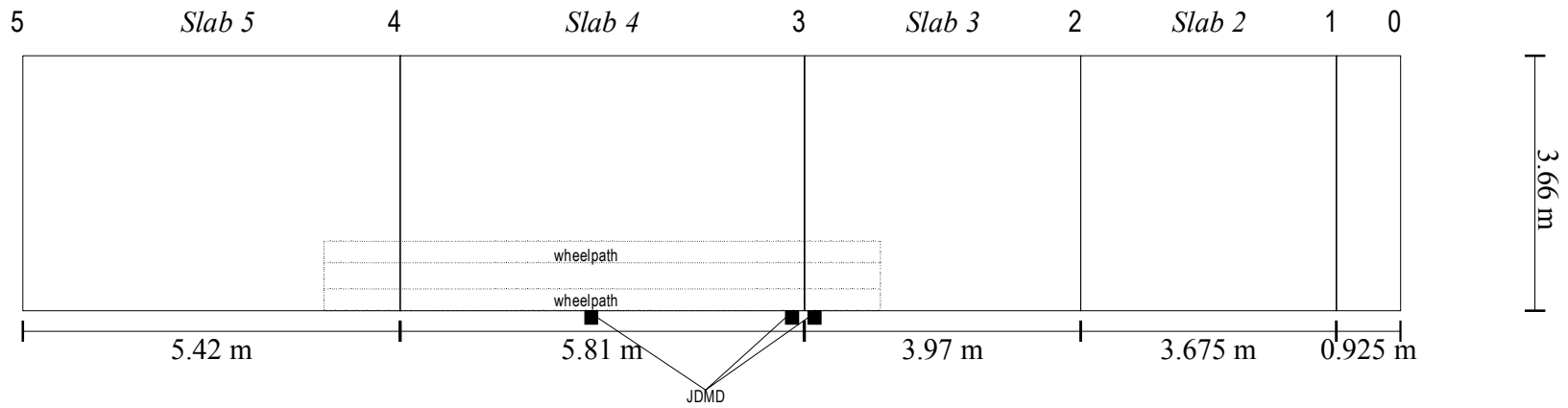


Cross-section View of Test Area (1:300 scale)



Section 1-A, South Tangent

Plan View of Test Area showing Instrument Locations (1:100 scale)

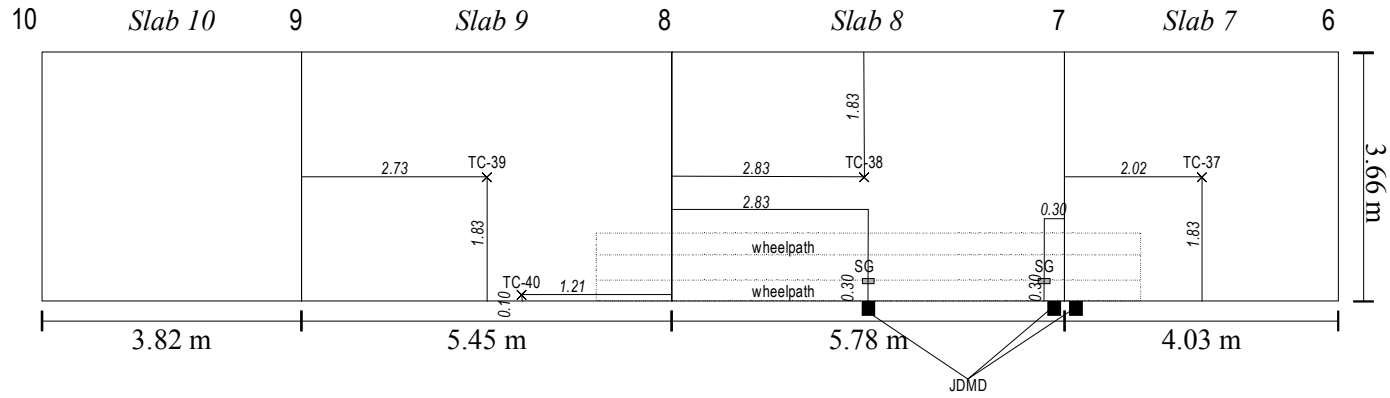


Cross-section View of Test Area (1:300 scale)

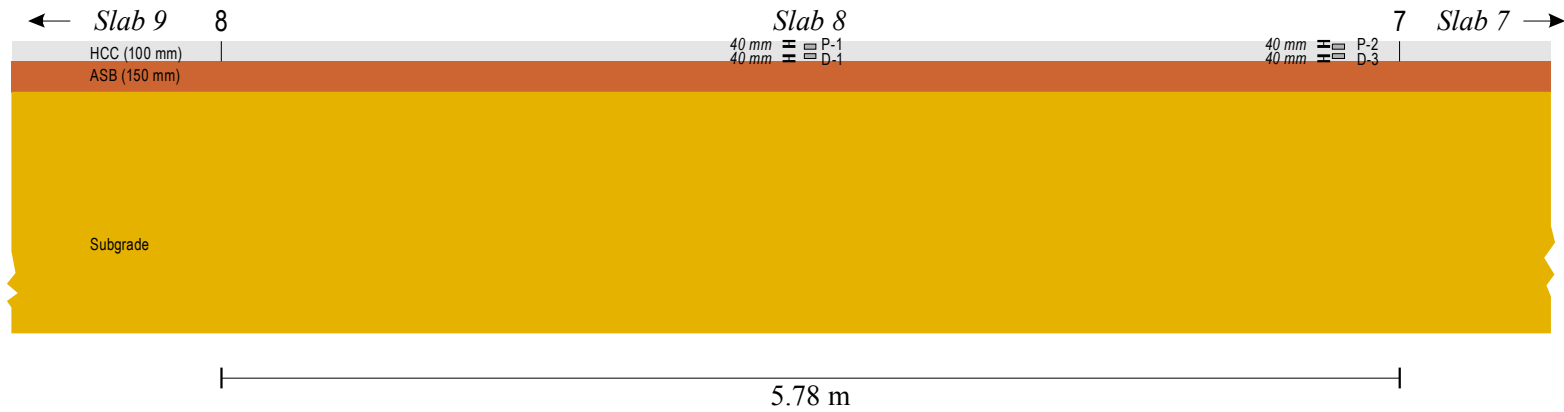


Section 1-B, South Tangent

Plan View of Test Area showing Instrument Locations (1:100 scale)

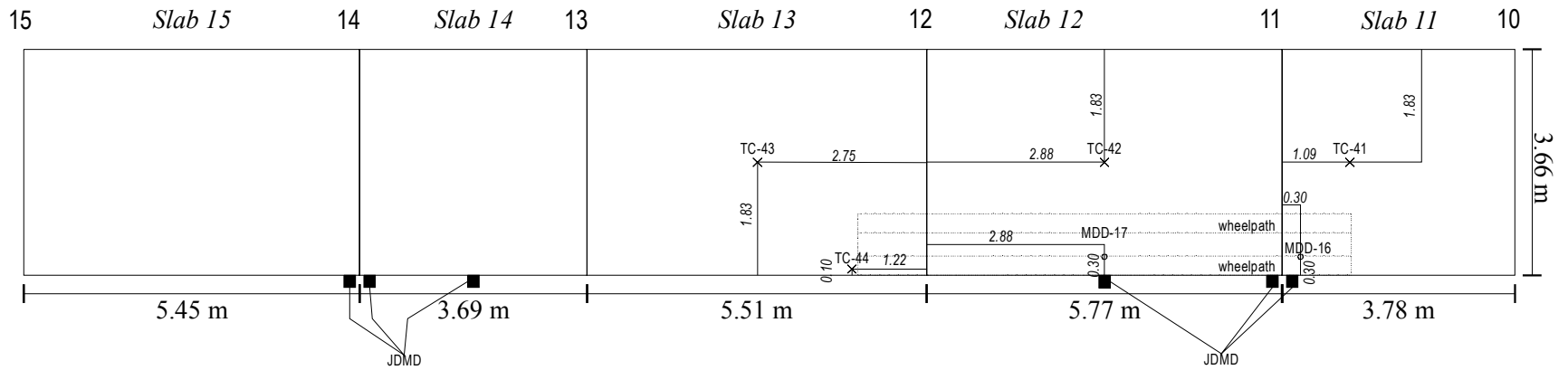


Cross-section View of Test Area (1:300 scale)

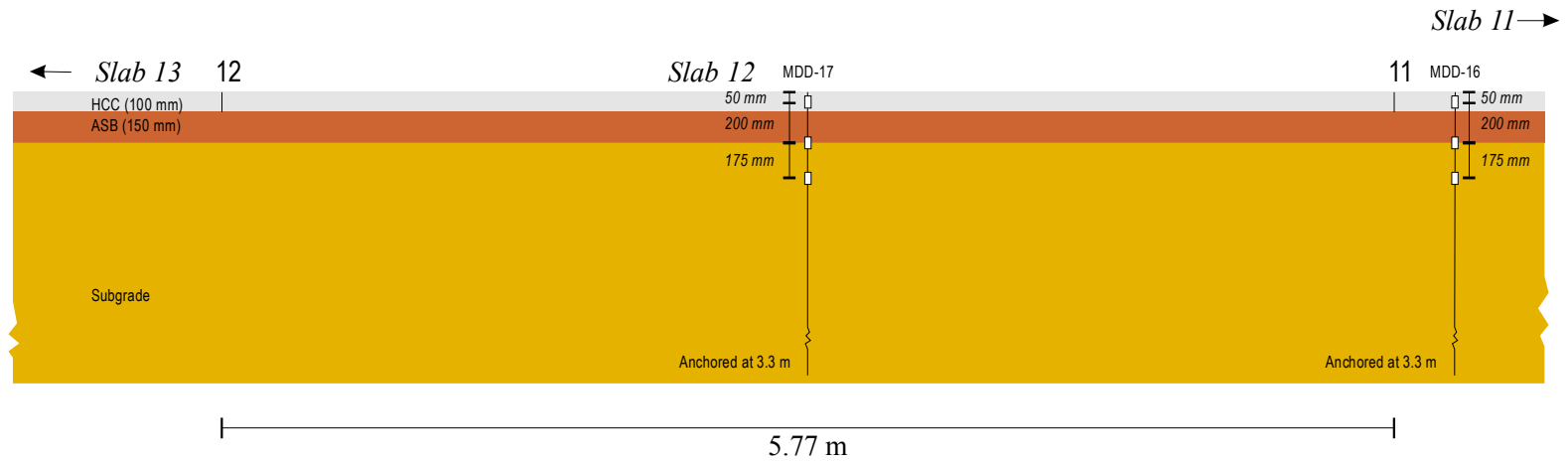


Section 1-C, South Tangent

Plan View of Test Area showing Instrument Locations (1:100 scale)

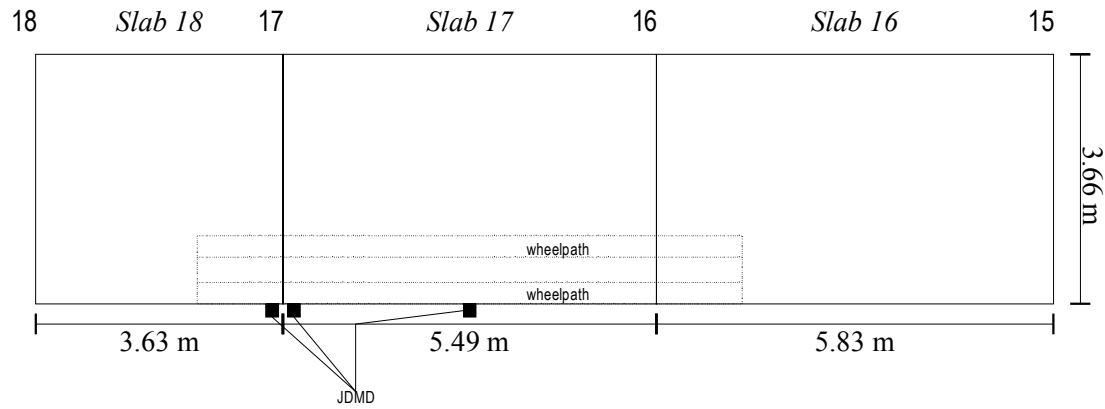


Cross-section View of Test Area (1:300 scale)

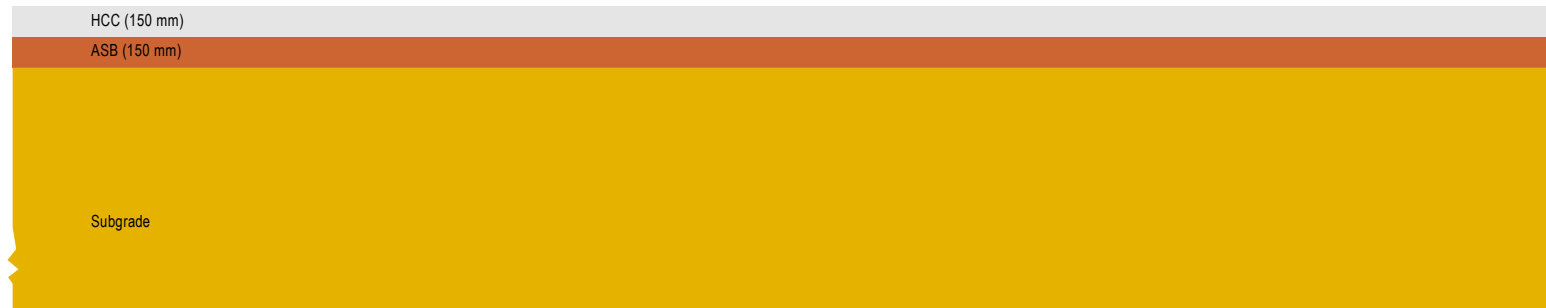


Section 3-A, South Tangent

Plan View of Test Area showing Instrument Locations (1:100 scale)

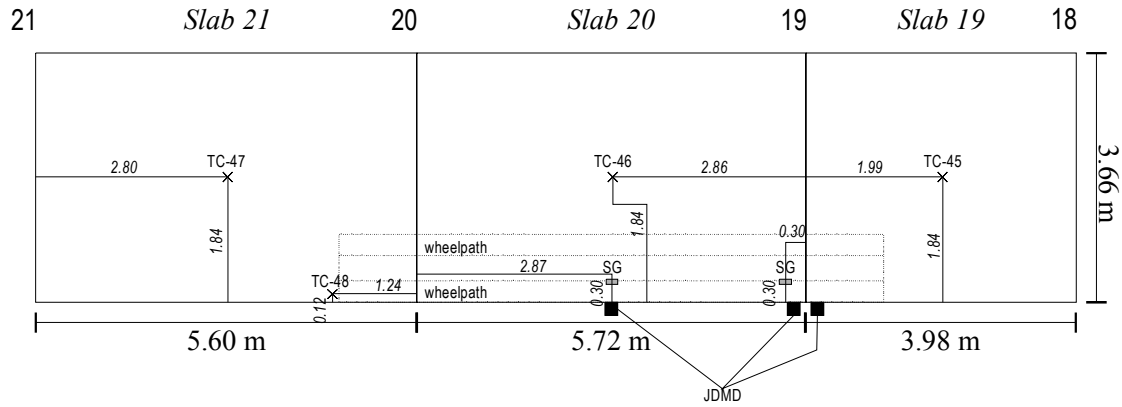


Cross-section View of Test Area (1:300 scale)

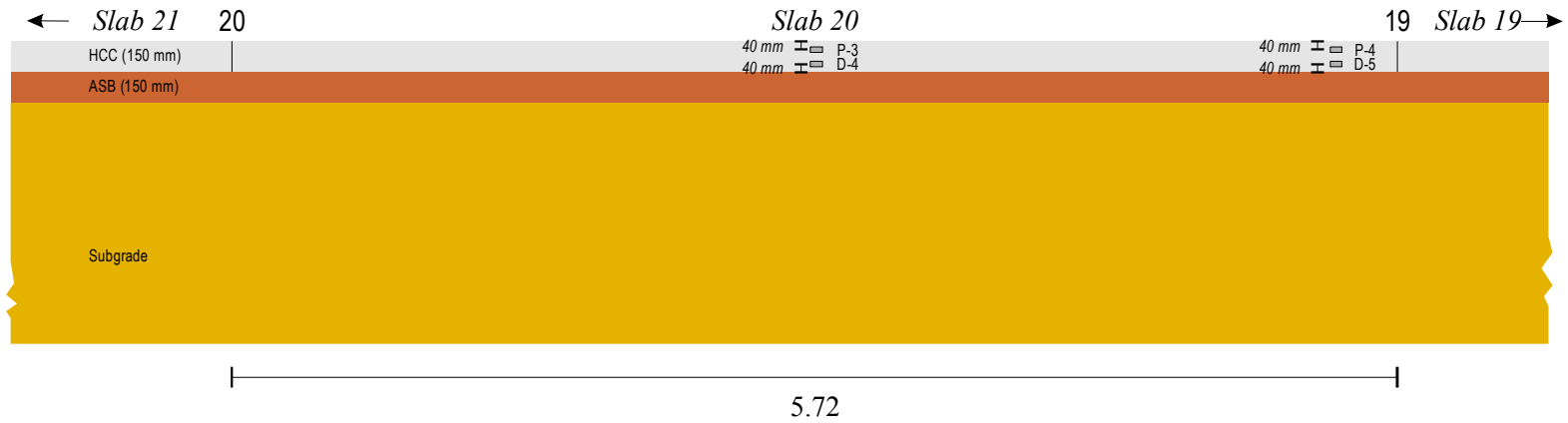


Section 3-B, South Tangent

Plan View of Test Area showing Instrument Locations (1:100 scale)

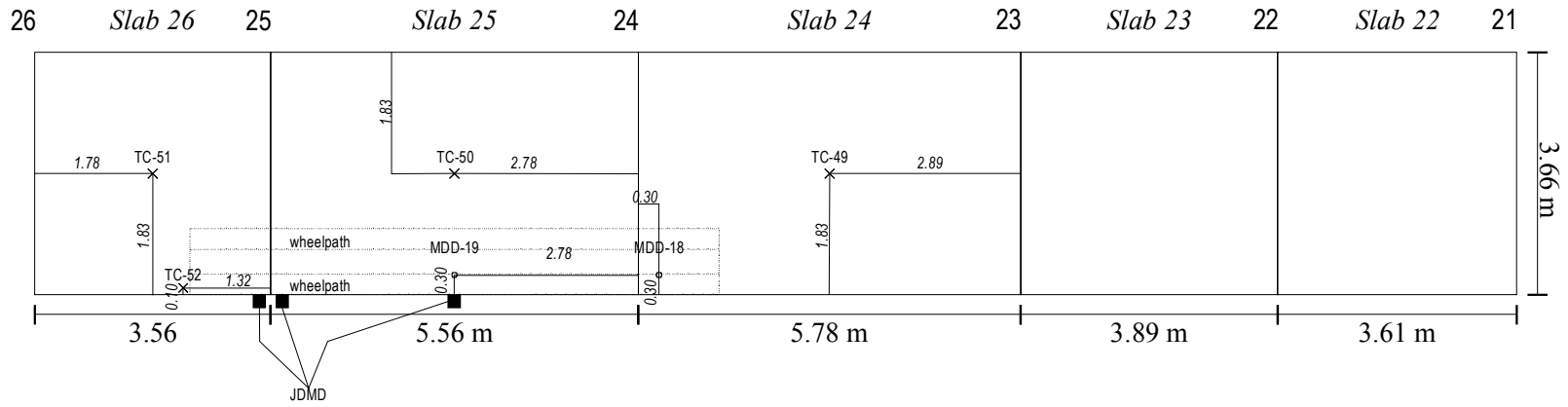


Cross-section View of Test Area (1:300 scale)

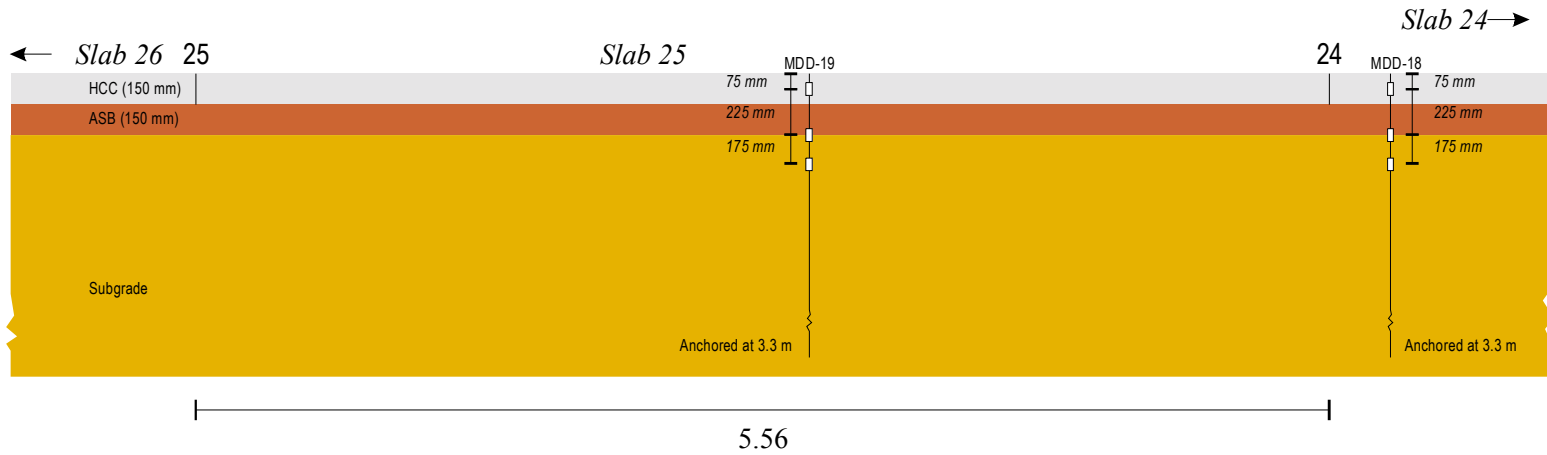


Section 3-C, South Tangent

Plan View of Test Area showing Instrument Locations (1:100 scale)

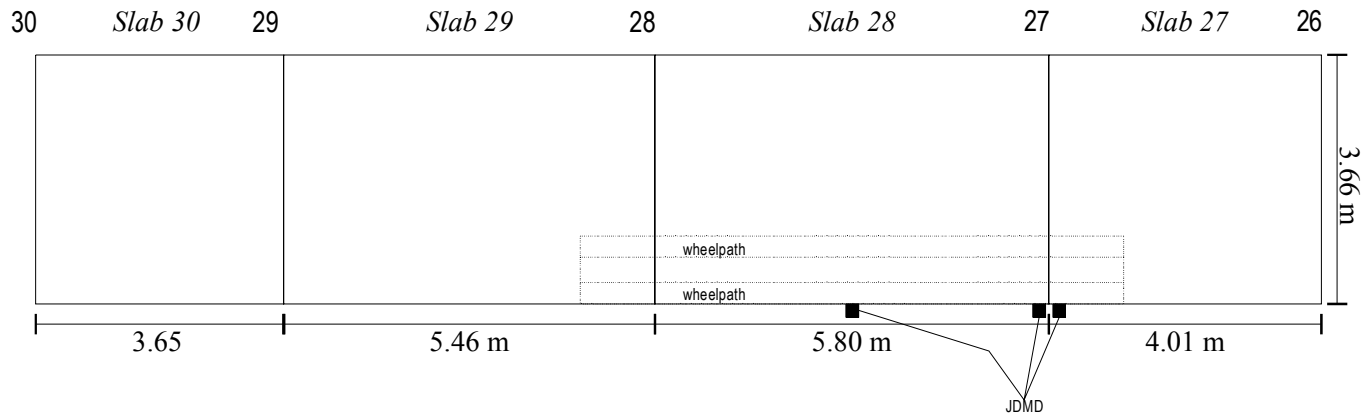


Cross-section View of Test Area (1:300 scale)

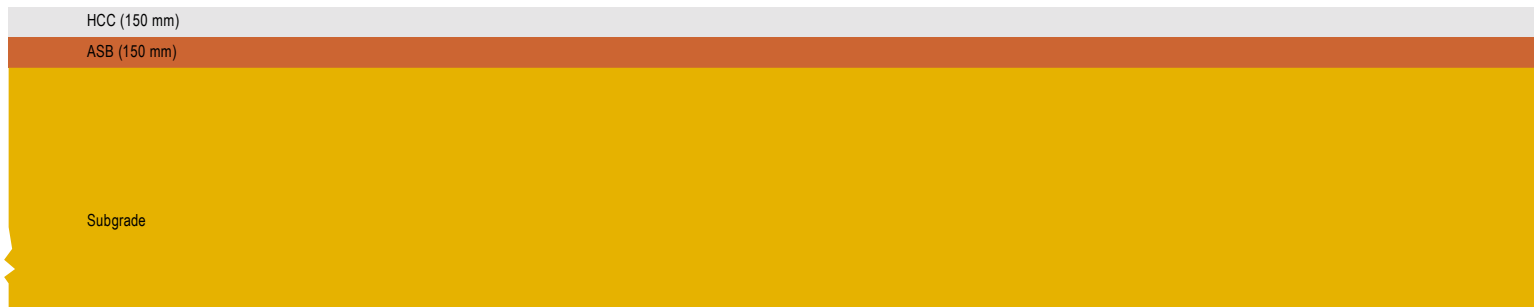


Section 3-D, South Tangent

Plan View of Test Area showing Instrument Locations (1:100 scale)

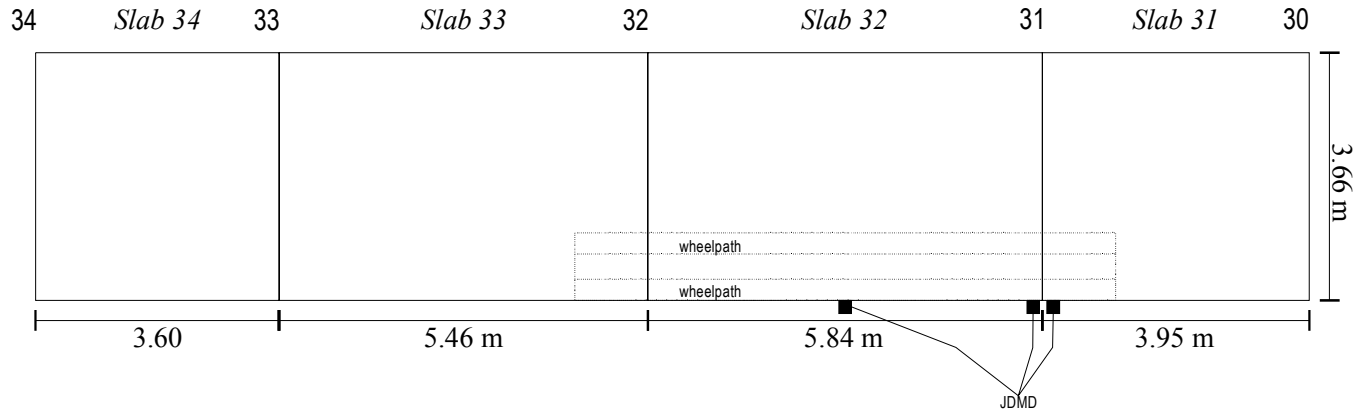


Cross-section View of Test Area (1:300 scale)



Section 5-A, South Tangent

Plan View of Test Area showing Instrument Locations (1:100 scale)

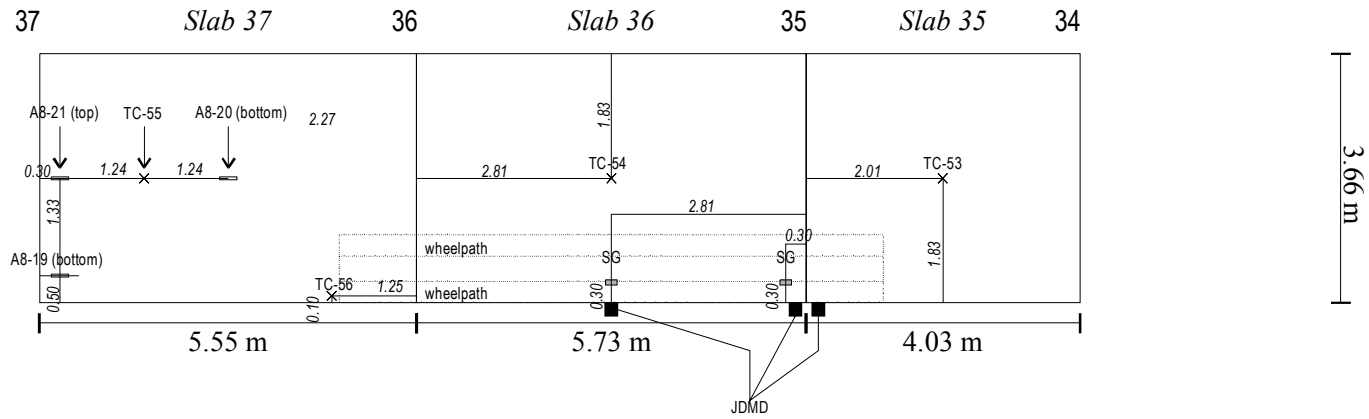


Cross-section View of Test Area (1:300 scale)

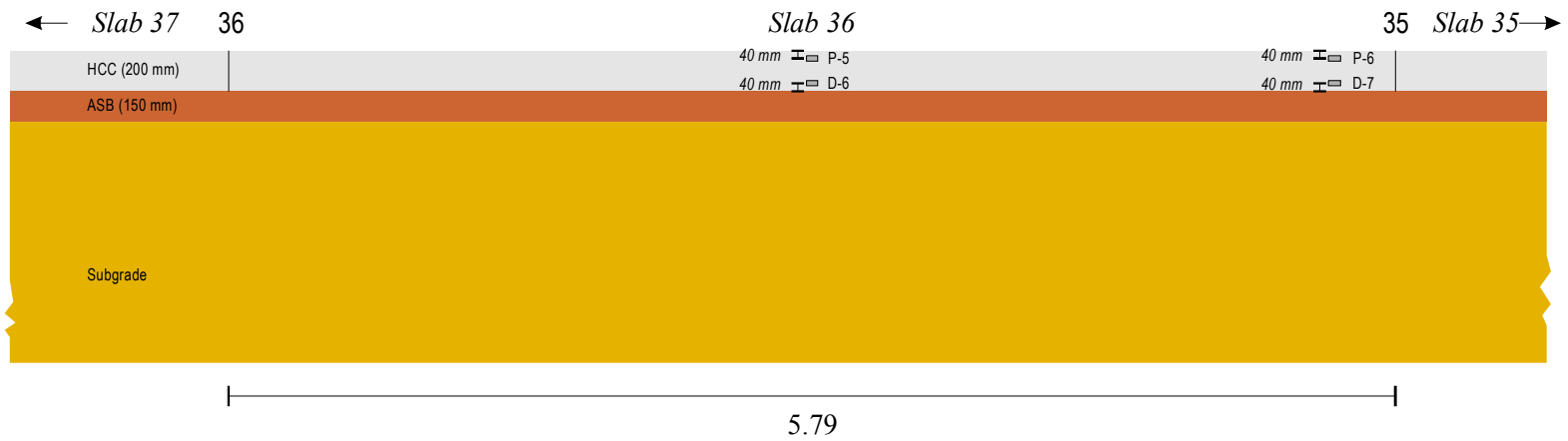


Section 5-B, South Tangent

Plan View of Test Area showing Instrument Locations (1:100 scale)

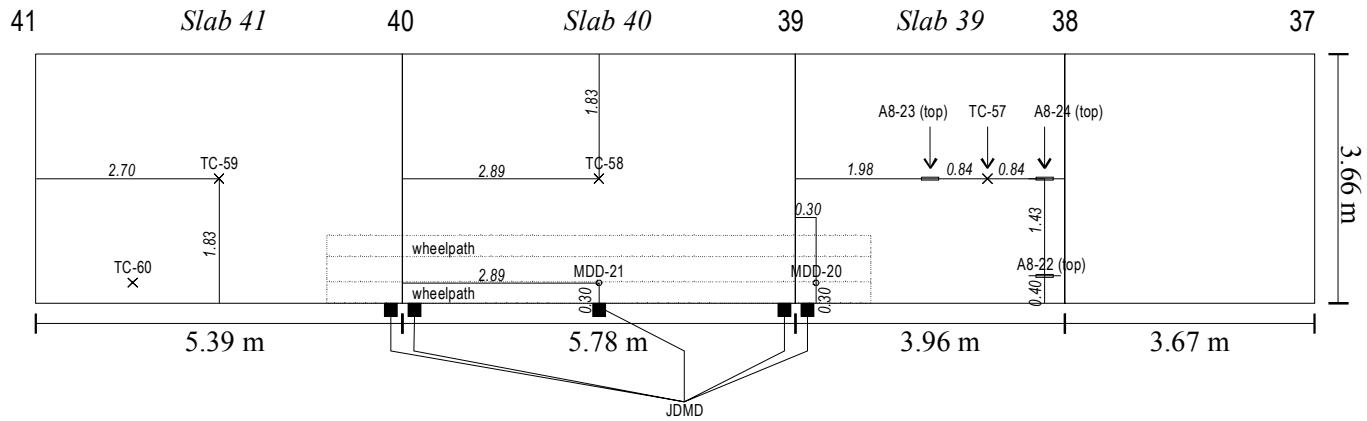


Cross-section View of Test Area (1:300 scale)

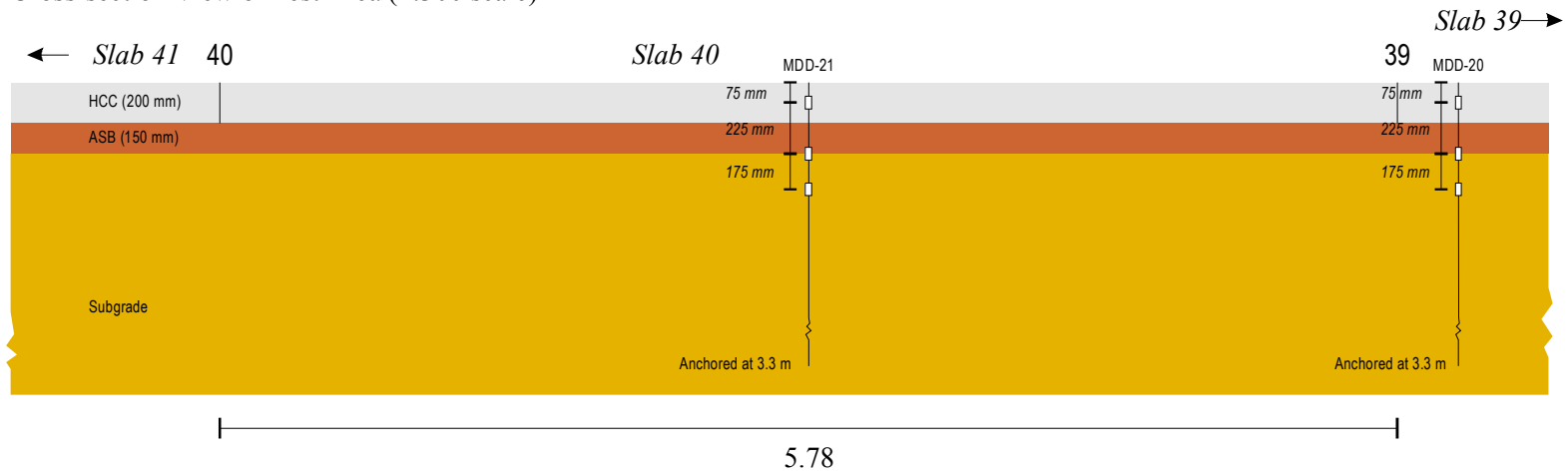


Section 5-C, South Tangent

Plan View of Test Area showing Instrument Locations (1:100 scale)

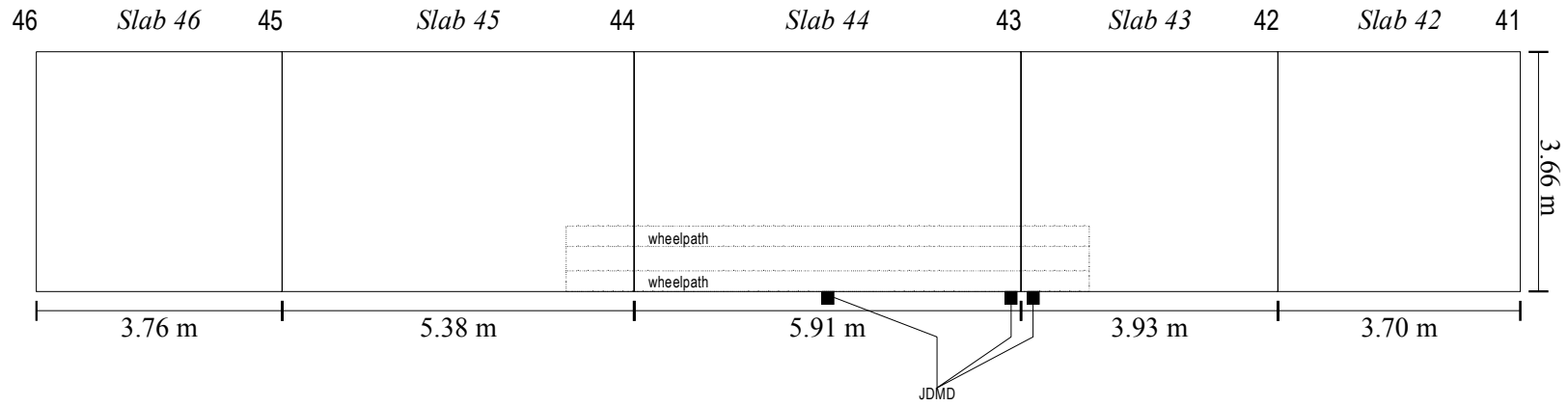


Cross-section View of Test Area (1:300 scale)



Section 5-D, South Tangent

Plan View of Test Area showing Instrument Locations (1:100 scale)



Cross-section View of Test Area (1:300 scale)



APPENDIX B: SITE PLAN FOR HVS TEST SECTIONS — PALMDALE, CA

APPENDIX C: LONG TERM BEAM AND CYLINDER RESULTS

Table C1 North Tangent Beams

Specimen	Specimen Age	M _R , psi (MPa)	Average, psi (MPa)	Standard Deviation	COV %
F7A7	575 Days	757 (5.22)	738 (5.09)	28	4
F7A8	575 Days	718 (4.95)			
F7C7	575 Days	736 (5.08)	770 (5.31)	48	6
F7C8	575 Days	804 (5.55)			

Table C2 Average Beam Strengths from Section 7.

Section 7: 8-hour Average Strength, psi (MPa)	Section 7: 7-day Average Strength, psi (MPa)	Section 7: 90-day Average Strength, psi (MPa)	Section 7: 575-day Average Strength, psi (MPa)
277 (1.91)	531 (3.66)	754 (5.20)	754 (5.20)

Table C3 North Tangent Cylinders

Specimen	Specimen Age	M _R , psi (MPa)	Average, psi (MPa)	Standard Deviation
C7A7	617 Days	7731	7731 (53.3)	N/A
C7C1	636 Days	6997	7022 (48.5)	35
C7C2	636 Days	7046		

Table C4 Average Cylinder Strengths from Section 7

Section 7: 8-hour Average Strength, psi (MPa)	Section 7: 7-day Average Strength, psi (MPa)	Section 7: 90-day Average Strength, psi (MPa)	Section 7: 636-day Average Strength, psi (MPa)
1800 (12.4)	4065 (28.3)	7007 (48.3)	7258 (50.1)